UNIVERSITEIT VAN AMSTERDAM

MASTER'S THESIS

Discrete gauge theories in two spatial dimensions

A Euclidean lattice approach

Author:
J.C. ROMERS

Supervisor:
Prof. dr. ir. F.A. BAIS

December 2007

Abstract

We study gauge theories in two spatial dimensions with a discrete gauge group on the lattice. It is well-established that the full symmetry of these theories is given by a Hopf algebra, the quantum double $D(H)$ of the gauge group H . The interactions in these theories are of a topological nature, and amount to nonabelian generalizations of the Aharanov-Bohm effect. The formalism of the quantum double allows one to study symmetry breaking of topologically ordered phases in gauge theories. In this setting one can go beyond the Higgs effect, where an electric sector has condensed, to situations where magnetic or dyonic sectors have nonzero expectation values in the vacuum.

We focus on magnetic condensates and study them using Euclidean lattice gauge theory. First we define the relevant actions for the theory, which contain one coupling constant for each class in the group. We then identify the different parts of the spectrum with different operators on the lattice. Pure charges and pure fluxes are identified with the Wilson and 't Hooft loops respectively. The spectrum of discrete gauge theories also contains dyonic excitations, carrying both magnetic and electric quantum numbers. For these excitations a new operator is constructed, the *dyonic loop*, which is a gauge invariant quantity that can be evaluated in the lattice path integral.

These operators are used to study a model system based on the gauge group $\overline{D_2}$. We construct part of the phase diagram for the pure gauge theory and locate the magnetic condensates. These are found at those regions in the phase diagram where the 't Hooft operator for the flux under consideration obtains a constant vacuum expectation value.

Our findings are that the spectrum of unconfined excitations after magnetic symmetry breaking corresponds to the result obtained by quantum double calculations.

Word of thanks

Allereerst wil ik beginnen met het bedanken van mijn begeleider, Sander Bais. Het onderwerp dat hij mij aangeboden heeft was zeer interessant en ik heb er flink mijn tanden in kunnen zetten. De soms urenlange discussies over het onderzoek vond ik zeer inspirerend en ook nog gezellig. Verder heb ik genoten van ons uitstapje naar de conferentie in Spanje, waar ik nog steeds leuke herinneringen aan heb.

Natuurlijk gaat er ook dank uit naar mijn ouders, die mij al een flinke tijd steunen in mijn student-zijn. Aan alles komt een einde, en ik denk dat zij het van harte met mij eens zijn dat het tijd wordt dat ik op eigen benen kom te staan.

Ook mijn vriendin Wendely mag niet ontbreken in dit lijstje. Dank je voor alle steun in deze drukke tijd, en alle lol die we toch samen hebben kunnen hebben. Ik zie er naar uit om de komende tijd wat dichter bij je in de buurt te zijn. Ook je familie, waarvan zelfs een delegatie op mijn praatje kwam, wil ik graag bedanken.

Tenslotte vanzelfsprekend al mijn vrienden. Hoewel ik geheel alleen op de Universiteit van Amsterdam was aangekomen, na mijn Bachelor aan de Technische Universiteit Delft, had ik al snel een groep mensen om me heen. Sander, Olaf en Reinier: het was mooi, en ik hoop dat we, waar we ook terecht komen, elkaar nog regelmatig zullen blijven zien. Ook mijn Delftse bestuur, waarmee ik nog vaak heb kunnen afspreken, wil ik bedanken: Cat, Stijn, Freek, Runo en Richard. Verder natuurlijk nog Remco: erg leuk dat je op mijn presentatie langsgekomen bent, en Niels, Jur, Roeland, Kevin en iedereen die ik vergeten ben.

Contents

Chapter 1

Introduction

In condensed matter systems, Landau's principle states that the different phases of a theory can be distinguished by studying what symmetries present in the Hamiltonian survive in the ground state. The Ising model for example loses its global $\mathbb{Z}_2$ symmetry once a ferromagnetic ground state, with all spins either up or down, has been realized. The BCS theory of superconductivity describes a nontrivial ground state filled with Cooper pairs that break the global U_1 gauge symmetry of the BCS Hamiltonian.

Also in the realm of high energy physics an important role is played by the concept of symmetry breaking. The most well-known example is that the masses of the W and Z bosons are accounted for by the breaking of the local $SU_2^W \times U_1^Y$ symmetry to U_1^{EM}. These three examples underline the relevance of symmetries and their breaking to theoretical physics.

Spontaneous symmetry breaking, global versus local

Essential in the discussion of symmetry breaking is the idea that certain excitations can form a (Bose) condensate thereby completely changing the physical properties of the system. The symmetry breaking mechanism in the Standard Model, for example, is due to a condensate of Higgs particles in the vacuum. The field describing these particles is a Lorentz scalar, which ensures trivial spin, and transforms nontrivially under part of the gauge group. In a ground state filled with these particles, the symmetry is lower than the symmetry of the action describing the fields of the theory.

The Higgs condensate is realized through a so-called "Mexican hat" potential describing its potential energy. The minimal energy configuration for such a potential is realized by a nonvanishing vacuum expectation value of the field. This mechanism, in which no symmetry-breaking terms are added to the action, but the theory dynamically generates a ground state with reduced symmetry, is called *spontaneous symmetry breaking*. This spontaneity is to be contrasted with the adding of (small) explicit symmetry breaking terms in the action, as happens for example in supersymmetric gauge theories attempting to describe the Standard Model.

Traditionally we distinguish global symmetries from local or gauge symmetries. The global symmetries lead to degeneracies in the spectrum of excitations described by the representation theory of the symmetry group. When they are broken, massless modes appear in the spectrum.

Local symmetries are more subtle in the sense that they are hidden: here, the symmetry is a redundancy in the labeling of vectors in the system's Hilbert space. They manifest themselves through the occurrence of massless vector particles. The breaking of local symmetries is usually

referred to as the Higgs effect and it manifests itself by generating a mass gap for some or all of the vector particles and possibly also through the appearance of topological excitations.

Topological excitations carry topological quantum numbers which are conserved not because of symmetry but because of topological arguments. However there are strong indications that there may be a hidden dual symmetry interchanging the role of ordinary and topological degrees of freedom.

In fact in two dimensions there are interesting models where this duality is taken care of by extending the (gauge) symmetry to a quantum group or Hopf algebra. Examples of such systems are Discrete Gauge Theories and fractional Quantum Hall systems. In these theories, the "electric", "magnetic" and "dyonic" charge sectors correspond to irreps of the quantum group describing the symmetry of the system.

Lattice gauge theories

In the lattice formulation of Yang-Mills theories, one replaces spacetime by a discrete set of points. Besides providing an automatic cutoff, this also opens up the possibility to apply the full machinery of calculational tools familiar from statistical mechanics, such as strong coupling expansions and Monte Carlo simulations. Furthermore, since the degrees of freedom in a lattice gauge theory take values in the gauge group, as opposed to the Lie algebra (as in the continuum), a lattice allows a direct formulation of a discrete gauge theory.

The actions used in a lattice gauge theory contain a set of free parameters, the coupling constants. By tuning these couplings, different ground state phases can be realized, which can be distinguished by the behaviour of order parameters. These order parameters have a one-to-one correspondence with the excitations of the theory, and tell us whether the excitations are free or confined.

This work

In this work, we present a lattice approach to discrete gauge theories in three spacetime dimensions. We study the formulation of actions and formulate order parameters corresponding to the electric, magnetic and dyonic excitations of the theory. By studying the behaviour of the magnetic order parameter, the 't Hooft loop, we identify the magnetic flux condensates. In these condensates, we study our set of operators and compare the results to what is known from the quantum group breaking formalism.

Chapter 2

Topological excitations

Both in statistical mechanics and in quantum field theories topological excitations play an important role. Topological excitations carry quantum numbers that are not conserved due to a symmetry present in the Hamiltonian or action, but because of topological considerations. Their occurence is not immediately evident from a glance at the action, although in many cases a dual formulation can be written down in which the role of the elementary excitations and the topological excitations is interchanged.

We will first discuss an example from statistical mechanics, the Ising model. After this our attention will focus on quantum field theories.

2.1 Statistical mechanics: two-dimensional Ising model

Statistical mechanics is a vast subject that concerns itself with all physical systems that have very many degrees of freedom and can thus not be described accurately by solving equations of motion for each individual particle. Important examples include the behaviour of particles that make up a gas and the properties of electrons in condensed matter systems (even leading to interesting phenomena such as superconductivity). Also a part of this branch of physics are the *lattice spin systems*, that go by names such as the *Ising model* and the *XY model*. Below we will discuss the Ising model. This discussion is based on [Einhorn et al. (1980)].

The Ising model was originally proposed as a model for a ferromagnet. It consists of a collection of sites with classical spins attached to them that can point either up or down. These spins experience two competing effects: on the one hand they want to have the same orientation as their neighbours (since it is a model of a magnet) and on the other hand, as a consequence of temperature, they each want to fluctuate in time. One can also add an external magnetic field, but that is not relevant for the present discussion.

In d dimensions, the model is described by the following Hamiltonian:

$$H = -\sum_{i,\hat{\mu}} \sigma_i \sigma_{i+\hat{\mu}} \tag{2.1}$$

Where i labels the sites, $\hat{\mu}$ is a unit vector running from 1 to d and σ_i represents the classical spin, which can take values $+1$ and -1.

2.1.1 Order and disorder

Physical intuition tells us there are probably two different phases the ground state of the system can be in. At low temperature, the interactions between neighbouring sites will dominate, and all the spins will align: $\sigma_i = +1$ or $\sigma_i = -1$ for all i. This is called the *ferromagnetic* or *ordered* phase.

As we let the temperature rise higher and higher, more spins will flip sign, until at infinite temperature, we arrive at the *disordered* phase. Here all of the σ_i take random values, and the order is lost. What happens in between can not be deduced from this simple analysis, but at least one gets a rough picture of what is going on.

2.1.2 Domain walls

Let us study the case $d = 2$ more closely, since that is where our interest lies. This case was solved exactly [Onsager (1944)], and from this we know there is a certain temperature at which there is a phase transition between the ordered and the disordered phase. We start with a system in the ordered phase. If we flip a collection of neighbouring spins, we introduce a *domain wall*: both inside and outside of the domain the spins are ordered, thus in a minimal energy configuration, but there is interaction energy between the pairs of spins that are antiparallel.

We can state this as follows: coming from the ordered phase, we introduce domain walls that carry an energy per unit length by flipping collections of spins. These domain walls live not on the original lattice, but on the *dual lattice*, the lattice that is obtained by shifting each lattice point by half a lattice spacing. Up to a flip of all of the spins, the description of configurations in terms of domain walls is related uniquely to a description in terms of spin values. These domain walls are our first example of a *topological excitation*.

2.1.3 Phase transition

From the Onsager solution, or, more straightforward, from the duality transformation [Kramers and Wannier (1941)], we know the exact temperature at which the transition from order to disorder takes place. This happens at $\beta = \frac{1}{2}\log(1+\sqrt{2})$, and it is interesting to see how well we can do using our description of the model in terms of topological excitations.

The domain walls carry some energy per unit length. The ordered phase thus corresponds to a situation where they form small closed loops, whereas the disordered phase corresponds to a high abundance of domain walls of arbitrary size: the jargon is that in the latter phase the topological excitations have *condensed*. Thus there exists a temperature $T = \frac{1}{\beta}$ where the domain wall length L that minimizes the free energy F goes from $L = 0$ to $L = \infty$. To find this temperature we use a so-called *energy-entropy argument*.

The cost in energy for making a domain wall one unit larger is two units of energy, since the $\sigma_i\sigma_{i+\hat{\mu}}$ term in the Hamiltonian goes from $+1$ to -1. To estimate the number of ways in which this extension can happen, we suppose that the walls perform a selfavoiding random walk. For a wall of length L there are thus 3^L possible configurations. Our expression for the free energy then becomes:

$$
\begin{aligned}
F &= E - TS && (2.2)\\
&= 2L - \frac{1}{\beta}\log 3^L && (2.3)\\
&= L(2 - \frac{\log 3}{\beta}) && (2.4)
\end{aligned}
$$

From 2.4 we can see that as $\beta \to \infty$ the second (entropy) term can be neglected, and $L = 0$ minimizes the free energy. As we raise the temperature however, the entropy comes into play, and we need to minimize the free energy with respect to the length L. This gives us a critical temperature of $\beta = \frac{1}{2}\log 3 \approx 0.55$, which is quite near the exact value $\beta = \frac{1}{2}\log(1+\sqrt{2}) \approx 0.44$. This simple short calculation shows that the topological excitation point of view of phases can be a valuable tool, not only qualitatively, but also quantitatively.

2.2 Gauge theories

We now turn to the study of that which is the main subject of this thesis, namely topological excitations in gauge theories. These objects roughly fall into two classes, *instantons* ['t Hooft (1976)] and *solitons* [Coleman (1975)].

Instantons are solutions to the Euclidean Yang-Mills equations with finite action, and are therefore localized in both space and time. They can be used as classical starting points around which we can perform quantum perturbations and allow one to describe tunneling in the path integral formulation of quantum mechanics and quantum field theory.

For our purposes, solitons are more important. These are solutions to the Euclidean Yang-Mills equations with finite energy, instead of finite action. They are therefore localized in space, and thus behave as particles.

We will show that these phenomena have everything to do with the topology of the gauge group and the manifold the theory is defined on. This discussion is based on [Bais (1981)].

2.2.1 Topology and gauge fields

Classes of solutions in Yang-Mills theory

Let us consider a Yang-Mills theory with compact gauge group G and a Higgs field ϕ which breaks the symmetry spontaneously due to its potential $V(\phi)$:

$$
S = \int d^d x \left\{ -\frac{1}{4} F^a_{\mu\nu} F^{a\mu\nu} - \frac{1}{2} D_\mu \phi D^\mu \phi - V(\phi) \right\} \tag{2.5}
$$

We will study the possibility of topologically nontrivial solutions in a Euclidean spacetime $M = \mathbb{R}^d$. To obtain a solution with finite action, we demand the terms of equation (2.5) to vanish seperately at infinity. For the Higgs field this means:

$$
\frac{\partial V}{\partial \phi}|_{x \in \partial M} = 0 \tag{2.6}
$$

Say we have a particular solution ϕ_0 that minimizes the potential. Then, because of the symmetry in (2.5), any $\phi = g\phi_0$ is a minimum of V for all elements $g \in G$. Now suppose the symmetry is not

completely broken, because the field ϕ does not transform under a faithful representation of G. Then there exist a residual symmetry group H, given by the stabilizer of ϕ_0:

$$H = \{h | h \in G, h\phi_0 = \phi_0\} \tag{2.7}$$

This allows us to split each element in G into a group product of an element in the coset G/H and an element in H:

$$g = kh,\ h \in H,\ k \in G/H \tag{2.8}$$

The manifold of vacua is therefore not the full group V, but the coset space G/H:

$$g\phi_0 = k\phi_0 \simeq G/H \tag{2.9}$$

And, since ϕ need not be a constant function at the boundary of spacetime ∂M:

$$\phi(\partial M) = k(\partial M)\,\phi_0 \tag{2.10}$$

We can construct a map from the boundary of space to the vacuum manifold:

$$k(\partial M) : \partial M \to G/H \tag{2.11}$$

The boundary of the spacetime manifold in d dimensions can be thought of as a hypersphere S_X^{d-1}, where the X has been added to emphasize this concerns spacetime, as opposed to group space. The maps k in equation (2.11) fall into different topological classes that cannot be continuously deformed in one another. They are therefore labeled by the elements of the homotopy group of the vacuum manifold of order $(d-1)$, $\pi_{d-1}(G/H)$.

This observation tells us what possible pointlike topological defects are possible in the theory. For example, in $\mathbb{R}^4$ the boundary of spacetime is topologically equivalent to the three-sphere S^3. From homotopy theory it is known that $\pi_3(S^3) = \mathbb{Z}$. This means that the instantons, as the pointlike topologically nontrivial solutions are called, are here labeled by an integer.

Higher dimensional topological defects

So far we have discussed instantons, the case where the topological defect is localized at a point in spacetime. We can also have higher dimensional cases. Consider for example the case of a monopole in the three spatial dimensions of $\mathbb{R}^4$. This is an example of a soliton, since it corresponds to a particle-like excitation. Although in space this is a pointlike object, in spacetime it becomes a one-dimensional worldline.

To classify such objects, we need to consider different homotopy groups than the previously given π_{d-1}. If d is the dimension of spacetime, and D is the dimension of the topological defect in spacetime, the relevant homotopy group becomes:

$$\pi_{d-D-1}(G/H) \tag{2.12}$$

In which we consistently use a spacetime point of view, so for example in $\mathbb{R}^4$ an instanton is a point, a monopole is linelike since it moves through space and time and a fluxtube sweeps out an area in spacetime - thus being a two-dimensional object. Some of the more common topological excitations in gauge theories are collected in table 2.1.

d	D	Homotopy group	Name
3	0	$\pi_2(G/H)$	Instanton
3	1	$\pi_1(G/H)$	Fluxtube
4	0	$\pi_3(G/H)$	Instanton
4	1	$\pi_2(G/H)$	Monopole
4	2	$\pi_1(G/H)$	Fluxtube

Table 2.1: Names and relevant homotopy groups for some topological excitations in gauge theories. The dimensionality of spacetime is d, the dimensionality of the defect in spacetime is D and the vacuum manifold is G/H.

Fluxes in discrete gauge theories in two spatial dimensions

As yet we have not said anything on how to determine $\pi_n(G/H)$. The relevant tool here is the so-called *exact sequence*, which relates homotopy groups of different order and of different topologies with one another. A more elaborate discussion can be found in among others [Bais (1981)]. We will only discuss the results for $d = 3$ and H a discrete group.

To obtain a discrete gauge theory, we start with a continuous symmetry group G, and break this to a discrete and in general non-abelian group H by the Higgs mechanism. We are interested in the solitons in $d = 3$, the fluxes, which according to table 2.1 are given by the elements of $\pi_1(G/H)$.

How do we determine the elements of this homotopy group? Here the exact sequence comes into play:

$$0 \simeq \pi_1(H) \to \pi_1(G) \to \pi_1(G/H) \to \pi_0(H) \to \pi_0(G) \simeq 0 \tag{2.13}$$

Where the first isomorphism is true because H is discrete and the last one because G is continuous. If G is simply connected, then $\pi_1(G) \simeq 0$ and we have the result:

$$\pi_1(G/H) \simeq \pi_0(H) \simeq H \tag{2.14}$$

Where the last isomorphism holds because H is discrete and π_0 just labels its elements.

The stable fluxes of a discrete H gauge theory are thus in one-to-one correspondence with the elements of the group H. This means that they carry charges that can fuse according to the group multiplication of H.

One final remark needs to be made in case G is not a simply connected group. If $\overline{G}$ is the universal covering group of G and $\overline{H}$ is the lift of H into $\overline{G}$, we have $\overline{G}/\overline{H} \simeq G/H$. Since this holds, the following also holds:

$$\pi_1(G/H) \simeq \pi_1(\bar{(}G)/\bar{(}H)) \tag{2.15}$$

In the case of a non-simply connected original group G, the fluxes are thus labeled by the lift $\overline{H}$ of the discrete group into the universal covering group of the continuous group.

Chapter 3

Topological interactions

In the quantum field theory picture of nature, the basic building blocks of the world around us roughly fall into two classes: the particles that make up matter, the fermions, and the particles that mediate forces of interactions, the gauge bosons. Underlying each force is a gauge symmetry, whose gauge field carries the force-mediating particles: *e.g.* for the strong nuclear force the symmetry is SU_3 and the excitations of the gauge field are called gluons, for electromagnetism there is a U_1 symmetry and the excitations are the photons.

So far, so good: forces mediated by particles provide an intuitive picture of what is going on, particularly when one uses Feynman diagrams. However, this is not the whole story. In the late fifties it was pointed out [Aharonov and Bohm (1959)] that in a quantum theory the topology of the space has to be taken into account because subtle observable interference effects can arise, which we call topological interactions.

3.1 The Aharonov-Bohm effect

Quantum electrodynamics is the simplest case of a Yang-Mills theory, where the gauge group is abelian, namely U_1. Imposing a local symmetry on the Dirac action requires the introduction of a new field, the A_μ gauge field. This field acts as a potential for the electric and magnetic fields. However, the $\boldsymbol{E}$ and $\boldsymbol{B}$ fields are not affected by a gauge transformation, whereas the A_μ field, by its very nature, transforms. It is therefore common usage to refer to the latter as an *unphysical* field, whereas the former describe the real physical degrees of freedom. They are related as follows after fixing the gauge to only allow time-independent transformations:

$$A_\mu = \left(\phi, \boldsymbol{A}\right) \tag{3.1}$$

$$\boldsymbol{E} = \nabla\phi \tag{3.2}$$

$$\boldsymbol{B} = \nabla \times \boldsymbol{A} \tag{3.3}$$

That this is not a correct picture can be understood by the following gedankenexperiment. Put a very long solenoid somewhere in space, for example along the z-axis. This will create some magnetic field inside the solenoid, but outside of it, there are no so-called physical fields. The configu-

ration is thus as follows inside the solenoid:

$$\boldsymbol{E} = \boldsymbol{0} \tag{3.4}$$
$$\boldsymbol{B} = B\boldsymbol{z} \tag{3.5}$$
$$\boldsymbol{A} = \left(-\frac{By}{2}, \frac{Bx}{2}, 0\right) \tag{3.6}$$

Where we use $\boldsymbol{z}$ for a unit vector in the z-direction, B for the magnitude of the magnetic field and x, y and z for ordinary Cartesian coordinates. Outside the solenoid, the following situation is realized:

$$\boldsymbol{E} = \boldsymbol{0} \tag{3.7}$$
$$\boldsymbol{B} = \boldsymbol{0} \tag{3.8}$$
$$\boldsymbol{A} = \left(-\frac{BR^2 y}{2r^2}, \frac{BR^2 x}{2r^2}, 0\right) \tag{3.9}$$

In which R is the radius of the solenoid and r is the distance from the center of the solenoid.

Now consider an interference experiment with two electrons and the solenoid. One part of the electron wavefunction will travel underneath the solenoid and the other part will go over it. The two parts will interfere with a phase difference that is observable.

The phase acquired by an electron moving in the background of a gauge field can be determined by minimal substitution, or alternatively, by interpreting the gauge field as a connection. We will do the latter, and find for the phase θ acquired after parallel transport along a path C:

$$\theta(C) = \frac{-e}{\hbar}\int_C \boldsymbol{A}\cdot d\boldsymbol{r} \tag{3.10}$$

The phase difference between the two paths is then, using Stokes' theorem:

$$\Delta\theta = \theta(C_1) - \theta(C_2) = \int_{C_1 \cup -C_2} \boldsymbol{A}\cdot d\boldsymbol{r} \tag{3.11}$$
$$= \frac{e}{\hbar}\oint_{C_1\cup -C_2} \boldsymbol{A}\cdot d\boldsymbol{r} \tag{3.12}$$
$$= \frac{e}{\hbar}\int_S \nabla\times\boldsymbol{A}\cdot d\boldsymbol{s} \tag{3.13}$$
$$= \frac{e}{\hbar}\int_S \boldsymbol{B}\cdot d\boldsymbol{s} = \frac{e}{\hbar}\Phi \tag{3.14}$$

Where $C_1 \cup -C_2$ denotes the path obtained by first traversing C_1, and then C_2 in opposite direction. S is the surface spanned by this curve and Φ the total magnetic flux piercing S, which in this situation is of course equal to the magnetic flux created by the solenoid.

Thus: the electrons pass only through parts of space where the electric and magnetic fields are zero, but there is a physically observable effect. This effect only depends on the number of turns taken around the flux, i.e. it is a function of the topology of the path.

3.2 Confinement in planar gauge theories through condensation of fluxes

To understand the relationship between topological interactions and confinement of charges in (2+1) dimensions, we will discuss the arguments given in ['t Hooft (1978)]. The situation in the

non-abelian discrete gauge theory setting is richer than here, but to understand the physical cause of the confinement mechanism, this discussion may be of value.

We consider an SU_N theory in two spatial dimensions, where the confinement mechanism for charges is due to the condensation of central $\mathbb{Z}_N$ vortices or fluxes. It is shown that a pair of external charges put into the gauge theory draws a string in the vacuum when pulled apart. This string carries a finite amount of energy per unit length, and therefore the particles cannot propagate freely in space, but will be confined to very small distances.

3.2.1 Setting the stage: soliton operators

Consider a SU_N gauge theory in (2+1) dimensions, with a Higgs field that breaks the symmetry to the center $\mathbb{Z}_N$. The group $\mathbb{Z}_N$ can be parametrized as $e^{2\pi i n/N}$, where n is an integer and 1_N is the N-dimensional unit matrix.

This theory contains stable solitons which look like vortices in the gauge field. Let us try to construct a set of operators $\phi(x)$ that create or annihilate solitons at a point x.

We denote the state of the fields vector field A and the Higgs field H by a ket $|A_i(\boldsymbol{x}), H(\boldsymbol{x})>$ such that the eigenvalues of the vector field and Higgs field operators are $A_i(\boldsymbol{x})$ and $H(\boldsymbol{x})$ respectively.

Let R be a region in the plane, where there may or may not be a soliton present. This region is surrounded by another region B, where the fields have zero energy density. In the latter region, we have for the Higgs field:

$$< H^2(\boldsymbol{x}) >= F \tag{3.15}$$

for some constant F. We can always gauge transform H in this region to have a constant value H_0 by some transformation $\Omega(\boldsymbol{x})$:

$$\Omega(\boldsymbol{x}) H(\boldsymbol{x}) = H_0 \tag{3.16}$$

Since the Higgs field is invariant under $\mathbb{Z}_N$, we can only determine $\Omega(\boldsymbol{x})$ up to factors of $\mathbb{Z}_N$. If we follow a closed contour in B parametrized by an angle $\theta \in [0, 2\pi]$, thus enclosing the region R too, we obtain the following equality:

$$\Omega(2\pi) = e^{2\pi i n/N} \Omega(0) \tag{3.17}$$

with n an integer ranging from 0 to $N-1$. If $n \neq 0$, the Higgs field has to vanish somewhere within the region R to maintain continuous gauge fields in the entire region. This configuration thus carries net energy, and we say a soliton is present.

With this information we can construct the alluded operator $\phi(\boldsymbol{x})$ that creates or annihilates a soliton. Let us denote a special case of the gauge transformation in (3.17) by $\Omega^{[x_0]}(\theta)$:

$$\Omega^{[x_0]}(2\pi) = e^{2\pi i/N} \Omega^{[x_0]}(0) \tag{3.18}$$

For a curve enclosing the point $\boldsymbol{x_0}$ parametrized by θ and going round it in the counterclockwise direction.

We now define $\phi(\boldsymbol{x})$ by the following relation:

$$\phi(\boldsymbol{x_0}) |A_i(\boldsymbol{x}), H(\boldsymbol{x})>= |A_i^{\Omega^{[x_0]}}(\boldsymbol{x}), H^{\Omega^{[x_0]}}(\boldsymbol{x})> \tag{3.19}$$

Where the gauge field and Higgs field on the right side of the equality have been gauge transformed by the special gauge transformation (3.18). From the definition, it is clear that $\phi(\boldsymbol{x})$ annihilates one unit of solitonic $\mathbb{Z}_N$ charge, whereas $\phi^\dagger(\boldsymbol{x})$ creates one unit. Since this charge is defined modulo N, we could just as well say that ϕ creates an antisoliton that $\phi^\dagger$ can annihilate.

3.2.2 Breaking the topological symmetry

The field $\phi(\boldsymbol{x})$ transforms as a scalar under Lorentz transformations. We can argue this from the fact that the only quantity characterizing the field is the number of units of topological charge at different points in space. Since the latter notion is topological in nature, it will transform trivially under coordinate transformations.

This observation enables us to write down a low-energy effective action for the soliton field. If we include an N-soliton interaction term in the standard action for a scalar field, the ϕ^4 action, we obtain the following expression for the Euclidean low-energy effective action for the solitons:

$$\mathscr{L}(\phi,\phi^*) = -\partial_\mu\phi^*\partial_\mu\phi - M^2\phi^*\phi - \frac{\lambda_1}{N!}\left(\phi^N + (\phi^*)^N\right) - \frac{\lambda_2}{2}(\phi^*\phi)^2 \tag{3.20}$$

This Lagrangian possesses a global $\mathbb{Z}_N$ invariance:

$$\phi \;\mapsto\; e^{2\pi i n/N}\phi \tag{3.21}$$

$$\phi^* \;\mapsto\; e^{-2\pi i n/N}\phi^* \tag{3.22}$$

for n ranging from 0 to $N-1$.

We can study what happens when this global symmetry is broken spontaneously. We had assumed that in the original theory, the gauge bosons had become massive due to the Higgs field. The soliton mass is thus caused by the Higgs field having a nonzero vacuum expectation value. If we now switch off the Higgs field, by flipping the sign of its mass term in the action for example, it is imaginable that the M^2 term in equation (3.20) also changes sign. This will lead to a Mexican hat potential for the soliton field, and realizes a dual Higgs effect: the effective field theory describing the solitonic excitations in the gauge field obtains a nonzero vacuum expectation value.

We can walk through the manifold of inequivalent vacua by multiplication with elements of $\mathbb{Z}_N$. This gives us N different vacuum states, of which one is realized:

$$|\phi_1> = e^{2\pi i n/N}|\phi_2> = \cdots = e^{2\pi i(N-1)/N}|\phi_N> \tag{3.23}$$

Like the original theory, this theory too can have topological defects. A region of space where the realized vacuum $|\phi_n>$ is seperated from a region where the vacuum is $|\phi_m>$ by a domain wall carrying $n-m$ units of topological charge. These walls carry energy per unit length, since the ϕ field cannot be in a potential minimum along the wall - otherwise it would be discontinuous. A natural way to picture these defects is by comparing them to islands of misaligned spins in a $\mathbb{Z}_N$-spin model [Einhorn et al. (1980)] from statistical mechanics, which is illustrated in figure 3.1.

These walls have a property that will turn out to be useful. Several walls can come together at a given point in space and end there. The total topological charge of these walls will have to be zero, so a possible situation is that N walls of unit charge end at the same point.

3.2.3 Introducing charges, confinement

Let us study the behaviour of charged particles in this newly realized phase. To gauge-invariantly introduce charges, we require the Wilson line operator $A(C)$ along a curve C with endpoints $\boldsymbol{x_1}$ and $\boldsymbol{x_2}$:

$$A(C,\boldsymbol{x_1},\boldsymbol{x_2}) = \mathrm{P}e^{ig\int_C A_k dx^k} \tag{3.24}$$

Which transforms as follows under a gauge transformation $\Omega(\boldsymbol{x})$:

$$A^\Omega(C,\boldsymbol{x_1},\boldsymbol{x_2}) = \Omega(\boldsymbol{x_1})A(C,\boldsymbol{x_1},\boldsymbol{x_2})\Omega^\dagger(\boldsymbol{x_2}) \tag{3.25}$$

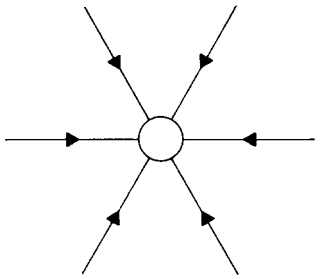

Figure 3.1: A vortex in the case $N = 6$ with six domain walls carrying unit topological charge ending on it.

And thus allows us to create the gauge-invariant combination

$$\overline{\psi}(\boldsymbol{x_1})A(C,\boldsymbol{x_1},\boldsymbol{x_2})\psi(\boldsymbol{x_2}) \tag{3.26}$$

for charged fields transforming as follows:

$$\psi(\boldsymbol{x}) \quad \mapsto \quad \Omega(\boldsymbol{x})\psi(\boldsymbol{x}) \tag{3.27}$$
$$\overline{\psi}(\boldsymbol{x}) \quad \mapsto \quad \overline{\psi}(\boldsymbol{x})\Omega^{\dagger}(\boldsymbol{x}) \tag{3.28}$$

However, for showing the effect the novel vacuum has on the introduction of charges in the theory, we need not introduce matter fields, the operator (3.24) suffices. Consider the latter operator after closing the curve C and tracing the obtained matrix element:

$$A(C) = \mathrm{Tr}A(C,\boldsymbol{x_1},\boldsymbol{x_1}) \tag{3.29}$$

Now we consider a special contour C, namely one that encloses a point $\boldsymbol{x_0}$ where the operator $\phi(\boldsymbol{x_0})$ has acted. From equation (3.17) we deduce that the value of A for such a contour has shifted by a factor of $e^{2\pi/N}$, leading to the following commutation relation between the A and ϕ operators:

$$A(C)\phi(\boldsymbol{x_0}) = \phi(\boldsymbol{x_0})A(C)e^{2\pi i/N} \tag{3.30}$$

Let us study this relation in two different bases for the Hilbert space of the theory. First we use a basis where $A(C)$ is a diagonal operator. Relation (3.30) states that if ϕ acts before A, the eigenvalue of the latter operator is shifted by $e^{2\pi i/N}$. Physically, we say that ϕ creates a unit of magnetic flux, and that A creates a loop of electric flux measuring the amount of magnetic flux inside.

However, in the Hilbert space basis where ϕ is a diagonal operator, a different picture arises. Consider the manifold of vacua given in equation (3.23). If $A(C)$ acts, the eigenvalue of the ϕ operator inside the contour C shifts by $e^{2\pi i/N}$, thus transforming the vacuum inside the contour to another state.

The latter point of view shows that in the vacuum where the soliton operator has obtained a vacuum expectation value, the operator creating a loop of electric flux actually creates a domain wall between two inequivalent vacua. This wall, as stated before, carries energy per unit length.

Therefore, the expression (3.26), which inserts two charges into the theory, creates a line of electric flux between them that carries energy. Seperating charges is thus costly, and the particles of the theory will remain confined. In this theory, there still are unconfined excitations, but they are combinations of elementary excitations.

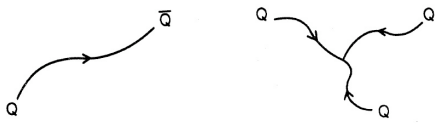

Figure 3.2: A mesonic composite $Q\overline{Q}$ and a baryonic composite QQQ, with the Wilson lines connecting them.

On the one hand, there are the mesonic excitations. These are simply particle-antiparticle pairs created by (3.26) with a very short Wilson line connecting them. While the individual charges at the ends of the line are confined, the combination can propagate freely.

On the other hand, we can have baryonic composites. These are those combinations of N charges that have all of their electric flux lines end on a single point. These composites are also, as a whole, unconfined. A graphical interpretation of these composites is given in figure 3.2.

Comparison with discrete gauge theories

The arguments given above show that for an SU_N gauge theory in two spatial dimensions broken to a $\mathbb{Z}_N$ gauge theory by the Higgs effect, there is the possibility of realizing a phase where the original Higgs effect is replaced by a "dual Higgs" effect that causes topological excitations to obtain a vacuum expectation value. Charges put into this phase are linearly confined.

In nonabelian discrete gauge theories, similar mechanisms are at work. The residual gauge symmetry in the above theory after applying the Higgs effect was abelian, allowing a relatively straightforward labeling of vacua (3.23) and leading to a commutation relation (3.30). When there exist nonabelian fluxes in the theory, the manifold of possible vacua becomes much less transparent than in the above situation and it is impossible to write down commutation relations of the type (3.30).

To rigorously study the different possible vacua and their response to external charges in a nonabelian discrete gauge theory, more mathematical machinery is required than in the above example. The notion of a group has to be extended to a braided Hopf algebra, which allows a nonabelian generalization of expression (3.30) in terms of braid operators.

Furthermore, since the representation theory of the Hopf algebra in question, the quantum double $D(H)$ of a discrete group H, treats the electric sectors (the charges of the theory) on equal footing with the magnetic sectors (the topological excitations of the theory), a transparent picture of the electric-magnetic duality for these theories can be established.

Chapter 4

Hopf symmetry and its breaking

The excitations in gauge theories fall into two classes, which we call electric and magnetic. The electric excitations are the fields that transform nontrivially under the gauge group, either put into the theory as external charges or by explicitly introducing extra dynamical terms in the action. An example is the particle-antiparticle pair put into the $\mathbb{Z}_N$ gauge theory by use of the operator in equation (3.26).

The magnetic class of excitations are the topologically nontrivial solutions to the gauge field equations. As has been discussed in section 2.2, there exists a great many of such solutions, but we will apply the notion "magnetic" solely the solitonic excitations. In planar physics, see table 2.1, these are the fluxes.

4.1 Electric and magnetic symmetries

In what follows, we will discuss the way in which both the electric and magnetic excitations of a discrete gauge theory transform under gauge transformations, followed by a part on more exotic excitations, the dyons, which carry both magnetic and electric charge. After this, the mathematical framework of the *quantum double* [Drinfeld (1988)], in which these notions stick together, will be built up [Bais et al. (1992)].

In this discussion, spacetime is continuous. This restricts the gauge freedom: if we want the map defining a gauge transformation to be smooth and continuous, it has to be a constant in the case of a discrete group. Therefore only global gauge transformations are allowed in what follows.

The discrete group under consideration is denoted H, group elements are $g, h \in H$, and a Hilbert space formalism with Dirac notation is used for the fields. Matrix indices are suppressed.

4.1.1 Electric charges

The electric excitations of a theory are described by some field $|v^\alpha(\boldsymbol{x})>$. Here α is an index labeling the representation under which the field transforms when acted upon by a gauge transformation. The field takes values in the vector space V_α associated with the representation α and may take different values at different spatial locations $\boldsymbol{x}$. However, for convenience, we will drop this index.

Let us perform a gauge transformation by an element $g \in H$:

$$|v^\alpha> \mapsto D_\alpha(g)|v^\alpha> \tag{4.1}$$

Where $D_\alpha(g)$ is the matrix representing g in representation α. This works well for single particle states. If we want to describe the action of the gauge group on multiparticle states, we have to

make use of the direct product representation. An n-particle state is given by the direct product of single particle Hilbert space vectors:

$$|v^\alpha > \otimes |v^\beta > \otimes |v^\gamma > \cdots \tag{4.2}$$

This product is in general not irreducible anymore, even is the original representations α, β , $\cdots$ were. To simplify the gauge action on the combination, we can use the Clebsch-Gordan decomposition:

$$|v^\alpha > \otimes |v^\beta > = \bigotimes_\xi N_\xi^{\alpha\beta} |v^\xi > \tag{4.3}$$

Where $N_\xi^{\alpha\beta}$ is commonly called the multiplicity of the ξ irrep in the product of α and β. It is given here for a product between two representations, but it can be generalized to n-particle states by repeated application.

4.1.2 Magnetic charges

We have seen that electric charges are labeled by the representations of the group. Since any representation can be decomposed into irreps, the fundamental electric particles are labeled by the irreps of the group H.

We now wish to construct a similar labeling for the magnetic sectors of the theory. In section 2.2.1, we saw that by using homotopy arguments, the magnetic sectors could be associated with group elements. In a non-abelian setting however, the identification of one group element with one magnetic particle species is not correct. Let us therefore study this problem in detail in a more physical setting than before.

Realizing a discrete gauge theory

To gain insight as to how the magnetic sectors of a discrete gauge theory are labeled, consider how we can realize a discrete gauge theory to begin with. Let us start with a G gauge theory, where G is a simply connected continuous group, for example SU_2. By using the Higgs mechanism, this theory can be transformed into a H gauge theory, with H a discrete group. For this end, we require a scalar field in some representation of G invariant under the subgroup H.

By letting the mass of the Higgs field go to infinity, the only excitations present in the gauge-Higgs system above are the magnetic fluxes. Parallel transport can be realized by the untraced Wilson line operator along some curve C:

$$\mathrm{P}\exp(ig\int_C \boldsymbol{A}\cdot d\boldsymbol{x}) \tag{4.4}$$

This object will in principle take values in the full gauge group G. Let us use this object to take the Higgs field at a certain point x, transport it along C, and close C such that we end up at the same point x again, We desire the Higgs field to be single valued, so operator (4.4) should act trivially upon it. Since the Higgs field has invariance under the discrete subgroup H, we see that for all closed curves C, the untraced Wilson loop takes values in H. Therefore, magnetic fluxes are labeled by group elements of H, as a Wilson loop operator measures the magnetic flux within the loop.

However, in the non-abelian case, this is not the complete story. Let us consider charges introduced in the theory that are not H invariant and their transport around a flux. First we work

in a gauge where the flux is labeled by $g \in H$. If we parallel transport a charge in representation α around it, the topological interaction between them works as follows:

$$|v^\alpha > \mapsto D_\alpha(g)|v^\alpha > \tag{4.5}$$

Let us compare this event to another situation, where we first perform a global gauge transformation by the group element h. This transformation has two effects: it acts on the internal space of the α charge with the element h and it will change the flux to some unknown value g'. The parallel transport equivalent to equation (4.5) is now given by:

$$D_\alpha(h)|v^\alpha > \mapsto D_\alpha(g')D_\alpha(h)|v^\alpha > = D_\alpha(g'h)|v^\alpha > \tag{4.6}$$

After this parallel transport, let us transform back to the original gauge by performing a transformation with element h^{-1}. The effect of parallel transport is now as follows:

$$|v^\alpha > \mapsto D_\alpha(h^{-1}g'h)|v^\alpha > \tag{4.7}$$

Since we work in the same gauge as in equation (4.5), the result should be the same. Therefore we arrive at the following equality:

$$g' = hgh^{-1} \tag{4.8}$$

This is the transformation law for a flux labeled by a group element g under a gauge transformation h. The gauge invariant notion for the magnetic sectors of the theory is thus not given by individual group elements, but by the conjugacy classes of H.

However, although the above effect is inherently quantum mechanical, it still is not a complete treatment of the full quantum theory. We have neglected the fact that these fluxes might be in a superposition of classical states. To make this more clear in our notation and also pave the way for the quantum double treatment, from now on we will also denote fluxes as kets in a vector space. The vector space of interest here is the group algebra $\mathbb{C}H$, the space of formal linear combinations of group elements:

$$\mathbb{C}H = \left\{ \sum_i c_i|g_i > | c_i \in \mathbb{C}, |g_i > \in H \right\} \tag{4.9}$$

Concluding what we have learned so far: the electric sectors of the theory are labeled by the irreducible representations α and the magnetic sectors are labeled by the conjugacy classes A. Now let us study how the fluxes interact.

Interactions between fluxes and flux metamorphosis

Consider the situation where two fluxes in states g_1 and g_2 are next to each other, the former left of the latter. An electric charge transported around the two will be acted upon bu the product of the two:

$$|v^\alpha > \mapsto D_\alpha(g_1 g_2)|v^\alpha > \tag{4.10}$$

Let us now define a counterclockwise interchange, or *braid*, operator for this pair. What is the effect of such an interchange on the internal space of the fluxes, that moves g_2 to the left of g_1, in a counterclockwise manner?

Let us gauge the system such that the flux starting as g_1 remains unchanged and g_2 transforms in g_2'. We know that an electric charge at a large distance having topological interactions with the

pair should not feel any effect of the interchange, leading to the following equality:

$$g_1 g_2 = g_2' g_1 \tag{4.11}$$
$$g_2' = g_1 g_2 g_1^{-1} \tag{4.12}$$

This class of topological interactions between magnetic fluxes, called *flux metamorphosis* [Bais (1980)] appear only when there are nonabelian magnetic sectors present, otherwise the conjugation in equation (4.12) are trivial.

In terms of the braid operator $\mathscr{R}$ acting on the two-particle Hilbert space of the two pure fluxes we can formulate this as follows:

$$\mathscr{R} : \mathbb{C}H \otimes \mathbb{C}H \rightarrow \mathbb{C}H \otimes \mathbb{C}H \tag{4.13}$$
$$\mathscr{R}|g_1> |g_2> = |g_1 g_2 g_1^{-1}> |g_1> \tag{4.14}$$

As a corrolary we can also derive the action of moving a flux around another flux, back to its original location, called a *monodromy*:

$$\mathscr{R}^2 |g_1> |g_2> = |(g_1 g_2) g_1 (g_1 g_2)^{-1}> |g_1 g_2 g_1^{-1}> \tag{4.15}$$

The product of the two fluxes after the monodromy is still $g_1 g_2$, as should be the case.

Determining unknown flux

The interactions between fluxes can be used to determine the magnetic charge of an unknown flux. The group elements form an orthonormal basis for the group algebra $\mathbb{C}H$ in the sense $< g_i | g_j > = \delta_{ij}$, which allows us to determine the flux of an unknown magnetic excitation $|h>$ by performing a series of interference experiments. We do this by calculating the following matrix element:

$$< h| < g_i|\mathscr{R}|g_i> |h> = < g_i | h g_i h^{-1} >< h|(g_i h) h (g_i h)^{-1} > \tag{4.16}$$
$$= \delta_{g_i, h g_i h^{-1}} \delta_{h, (g_i h) h (g_i h)^{-1}} \tag{4.17}$$

By repeating this experiment for all fluxes g_i, we obtain a set of matrix elements unique for the flux h, allowing this flux to be uniquely established.

4.1.3 Dyonic sectors

Discrete gauge theories also carry dyons in their spectrum, sectors with both magnetic and electric quantum numbers [Bais et al. (1992)]. Let us start out with a magnetic flux, and try to attach some electric charge to it. Say we first try to attach a representation α of the full discrete group H to a given flux in a conjugacy class A. The ket describing this dyonic state is given by:

$$|g, v^\alpha> = |g> \otimes |v^\alpha> \in \mathbb{C}H \otimes V_\alpha \tag{4.18}$$

Where v^α is a vector in the carrier space V_α of the representation α and g lives in the group algebra $\mathbb{C}H$. Let us try to probe this sector using test excitations to find out which electric representation is present, in an experiment akin to equation (4.16). We arrive at the following matrix element:

$$< g, v^\alpha| < g_i|\mathscr{R}|g_i> |g, v^\alpha> = < g, v^\alpha | g_i g g_i^{-1}, D_\alpha(g_i) v^\alpha >< g_i|(g_i g) g_i (g_i g)^{-1} > \tag{4.19}$$
$$= < v^\alpha | D_\alpha(g_i) v^\alpha > \delta_{g, g_i g g_i^{-1}} \tag{4.20}$$

The delta function in this expression restricts the set of group elements we can use to calculate nonzero matrix elements to the group elements that commute with g. The physical origin of this is clear: if we probe the long-distance electric charge of a dyonic sector with a flux not commuting with the magnetic charge on the dyon, the internal flux state of the dyon ends up orthogonal to its original orientation.

The above means that not all charges can unambiguously be attached to a given flux. Only charges forming a representation of the centralizer ${}^gN$, the set of elements in H commuting with g, can be implemented in a consistent manner.

4.2 Unified framework: quantum double

Let us recall what we have seen so far. Electric sectors are labeled by irreducible representations α of the gauge group and the internal space of an electric excitation is the carrier space of its representation V_α. Magnetic sectors are labeled by the conjugacy classes A of the gauge group. Since a magnetic excitation can be in a linear superposition of classical fluxes, its internal space is the group algebra $\mathbb{C}H$. The dyonic sectors are labeled by both electric and magnetic quantum numbers, but its electric representations are restricted to those of the centralizer ${}^gN$ of the flux g.

We will now construct all of the above in a more unified framework. We denote a general state in a discrete gauge theory as

$$|h, v^\alpha >\in V_\alpha^A \tag{4.21}$$

Where we have defined the combined Hilbert space V_α^A for general discrete gauge theory sectors labeled by a class A and a centralizer charge α. Let us define two operators that can work on the internal states of particles. The first operator, P_g, projects out the flux g as follows:

$$P_g|h, v^\alpha >= \delta_{g,h}|h, v^\alpha > \tag{4.22}$$

The second operator, which we denote by g, performs a global gauge transformation:

$$g|h, v^\alpha >= |ghg^{-1}, D_\alpha(g)v^\alpha > \tag{4.23}$$

These operators do not commute, and realize the following algebra:

$$P_g P_{g'} = \delta_{g,g'} P_g \tag{4.24}$$

$$hP_g = P_{hgh^{-1}} h \tag{4.25}$$

The set of combined flux projections and gauge transformations $\{P_g h\}_{g,h\in H}$ generates the quantum double $D(H)$, a Hopf algebra. We will give all the definitions of Hopf algebra operations in what follows, but first we will construct irreducible representations and see they correspond directly to the electric, magnetic and dyonic sectors of a discrete gauge theory.

4.2.1 Constructing irreps

We now turn to finding the irreducible representations for this Hopf algebra: this allows us to label all of the sectors in the spectrum. The representation theory of the quantum double $D(H)$ of a finite group H was first worked out in [Roche et al. (1990)] but here we follow the discussion presented in [de Wild Propitius and Bais (1995)].

Let A be a conjugacy class in H. We will label the elements within A as follows:

$$\{{}^Ah_1, {}^Ah_2, \cdots, {}^Ah_k\} \in A \tag{4.26}$$

For a class A of order k. In general, the centralizers for the different group elements within a conjugacy class are different, but they are isomorphic to one another. Let ${}^A N \subset H$ be the centralizer for the first group element in the conjugacy class A, ${}^A h_1$.

The set ${}^A X$ relates the different group elements within a conjugacy class to the first:

$$ {}^A X = \left\{ {}^A x_1, {}^A x_2, \cdots, {}^A x_k | {}^A h_i = {}^A x_i^A h_1^A x_i^{-1} \right\} \tag{4.27} $$

This still leaves a lot of freedom, but we fix our convention such that ${}^A x_1 = e$. The centralizer ${}^A N$, being a group, will have different irreps, which we label by α. The vector space for a representation α is spanned by a basis ${}^\alpha v_j$. The total Hilbert space that combines magnetic and electric degrees of freedom, V_α^A, is then spanned by the following set of vectors:

$$ \left\{ |{}^A h_i, {}^\alpha v_j > \right\} \tag{4.28} $$

Where i runs over the elements of the conjugacy class, $i = 1, 2, \cdots, \dim A$ and j runs over the basis vectors of the carrier space of α, $j = 1, 2, \cdots, \dim \alpha$.

To see that this basis is a natural one to act on with our flux measurements and gauge transformations, consider an irreducible representation Π_α^A of some combined projection and gauge transformation $P_h g$:

$$ \Pi_\alpha^A (P_h g) | {}^A h_i, {}^\alpha v_j > = \delta_{h, g^A h_i g^{-1}} | g^A h_i g^{-1}, \sum_m D_\alpha (\tilde{g})_{mj}^\alpha v_m > \tag{4.29} $$

Where the element $\tilde{g}$ is the part of the gauge transformation g that commutes with the flux ${}^A h_1$, defined as follows:

$$ \tilde{g} = {}^A x_k^{-1} g^A x_i \tag{4.30} $$

With ${}^A x_k$ implicitly defined by ${}^A h_k = g^A h_i g^{-1}$. This indeed commutes with the element ${}^A h_1$:

$$ {}^A h_k = g^A x_i^A h_1^A x_i^{-1} g^{-1} \rightarrow {}^A h_1^A x_k^{-1} = {}^A x_k^{-1} g^A x_i^A h_1^A x_i^{-1} g^{-1} \tag{4.31} $$

So

$$ \begin{aligned} {}^A h_1 \tilde{g} &= {}^A h_1^A x_k^{-1} g^A x_i \\ &= {}^A x_k^{-1} g^A x_i^A h_1^A x_i^{-1} g^{-1} g x_i \\ &= {}^A x_k^{-1} g x_i h_1 = \tilde{g}^A h_1 \end{aligned} $$

We will make use of this relation in defining the dyonic operators on the lattice, and give a concrete example by constructing a map Θ from the full group to the normalizer subgroup:

$$ \begin{aligned} \Theta : (A \times H) &\rightarrow {}^A N \\ (h, g) &\mapsto \tilde{g} \end{aligned} \tag{4.32} $$

This map has one property that we later on require for gauge invariance of our dyonic operators. From equation (4.30) we can see that conjugation of h or g amounts to multiplication of the ${}^A x_i$. Combined with the definition of ${}^A h_k$, this results in the following property of the map Θ:

$$ \Theta(h, kgk^{-1}) = \Theta(k^{-1} hk, g) \tag{4.33} $$

4.2.2 Ribbon element

By viewing a dyon as a combination of a magnetic flux and an electric charge with some spatial seperation between the two, we can define an operator that signals the spin of the excitation. Since spin is the eigenvalue of a state belonging to the operator that rotates the state by 2π, the following operator, called the ribbon element c, will do the job:

$$c = \sum_{g \in H} P_g g \tag{4.34}$$

It is a central element in $D(H)$ and hence can be used to label its irreps. Letting c work on a given state leads to the following relation:

$$\Pi^A_\alpha \left(\sum_g P_g g \right) |^A h_i, ^\alpha v_j > = |^A h_i, \sum_m D_\alpha (^A h_1)^\alpha_{mj} v_m > \tag{4.35}$$

And since the element $^A h_1$ commutes with all elements in the centralizer $^A N$ the operator c, by Schur's lemma, needs to be proportional to the unit matrix:

$$D_\alpha (^A h_1) = e^{2\pi i s_{(A,\alpha)}} 1_\alpha \tag{4.36}$$

Where we have defined the topological spin s of each sector of $D(H)$.

4.2.3 Coproduct

We can also use the Hopf algebra language to act on multiparticle states. The coproduct Δ, the coalgebraic dual to multiplication, is the natural object for this purpose:

$$\Delta : D(H) \to D(H) \otimes D(H) \tag{4.37}$$

Which satisfies a property called *coassociativity*:

$$(\Delta \otimes \mathrm{id}) \circ \Delta = (\mathrm{id} \otimes \Delta) \circ \Delta \tag{4.38}$$

Where id is the identity map. Given the flux projectors P_h and gauge transformations g, the concrete construction is as follows:

$$\Delta(P_h g) = \sum_{h' h'' = h} P_{h'} g \otimes P_{h''} g \tag{4.39}$$

The constraint in this sum means we project out all combinations of fluxes that carry total flux h and implement a gauge transformation by the group element g on both excitations.

In the case of $D(H)$ with H an abelian group, the coproduct also satisfies cocommutativity. We first define τ, the flip operator:

$$\tau : D(H) \otimes D(H) \quad \to \quad D(H) \otimes D(H) \tag{4.40}$$

$$P_h g \otimes P_{h'} g' \quad \mapsto \quad P_{h'} g' \otimes P_h g \tag{4.41}$$

Then cocommutativity amounts to $\Delta = \tau \circ \Delta$.

On the representation level the comultiplication leads to the definition of the tensor product or fusion rules of states.

4.2.4 Counit

In an algebra, there exists the unit element that makes multiplication act as the identity map. In our Hopf algebra, the element doing the same for comultiplication is the *counit*:

$$\epsilon : D(H) \to \mathbb{C} \tag{4.42}$$

In such a way that:

$$(\epsilon \otimes \mathrm{id}) \circ \Delta = \mathrm{id} = (\mathrm{id} \otimes \epsilon) \circ \Delta \tag{4.43}$$

Which, on the representation level, is precisely what is expected from the vacuum irrep. Fusing a given irrep with the vacuum sector, be it from the right or the left, should keep a state invariant:

$$\Pi_1^e \otimes \Pi_\alpha^A \simeq \Pi_\alpha^A \simeq \Pi_\alpha^A \otimes \Pi_1^e \tag{4.44}$$

4.2.5 Fusion

The direct product of two irreducible representations of a group is in general not irreducible anymore. It decomposes into a direct sum of irreps, with multiplicities given by the Clebsch-Gordan coefficients. For direct products of irreps of a Hopf algebra, there is an analogous decomposition:

$$\Pi_\alpha^A \otimes \Pi_\beta^B = \bigotimes_{C,\gamma} N_{\alpha\beta C}^{AB\gamma} \Pi_\gamma^C \tag{4.45}$$

Where the coefficients can be calculated from the Verlinde formula, see [**?**]. This relation describes the possible channels Π_γ^C two particles Π_α^A and Π_β^B can fuse into. Alternatively, one can use it to work out the different decay channels for a single particle state that can be regarded as a composite of Π_α^A and Π_β^B.

4.2.6 Braiding and the universal R-matrix

In the scattering experiments described by equation (4.16), we already alluded to the braid operator $\mathscr{R}$. We will now explicitly present a construction. Acting on a two-particle state, we want the right particle to be acted upon by the flux of the left particle and then have their positions interchanged. It is useful to decompose the braid operator into into the latter part, which is the flip operator τ and the former part, called the *universal R-matrix*:

$$R = \sum_h (P_h, e) \otimes (1, h) \in D(H) \otimes D(H) \tag{4.46}$$

The first term projects out the flux of the first particle, which is then implemented on the second. Combining this with the representation functions and the flip operator gives us the braid operator:

$$\mathscr{R}_{\alpha\beta}^{AB} = \tau \circ (\Pi_\alpha^A \otimes \Pi_\beta^B)(R) \tag{4.47}$$

Quasi-cocommutativity

It can be checked that the braiding operator and the coproduct commute, which is expected from physical considerations, since the local interchange of two particles cannot affect the long-range properties of the pair:

$$\Delta(P_h g)\mathscr{R} = \mathscr{R}\Delta(P_h g) \tag{4.48}$$

This is a consequence of the relation:

$$(\tau \circ \Delta(P_h g))R = R\Delta(P_h g) \tag{4.49}$$

Quasi-triangularity

Given two particles, the effect of braiding the second around the first and then letting the first decay should equal letting the decay process take place first and then braiding the second particle around the decay products.

By using explicit matrix notation, we can specify the action of the R-matrix on three-particle states. Let us first write the universal R-matrix as follows: $R = \sum_k R_l^k \otimes R_r^k$. Now, for actions on three-particle states, we define R_{ij}, the triple product with R_l^k on position i, R_r^k on position j and 1 on the other position. For example:

$$\begin{aligned} R_{23} &= \sum_k 1 \otimes R_l^k \otimes R_r^k \\ R_{31} &= \sum_k R_r^k \otimes 1 \otimes R_l^k \end{aligned}$$

The physical condition described above is then formulated as the quasi-triangularity conditions, illustrated in figure 4.1:

$$(\Delta \otimes \mathrm{id})R = R_{13}R_{23} \tag{4.50}$$

$$(\mathrm{id} \otimes \Delta)R = R_{13}R_{12} \tag{4.51}$$

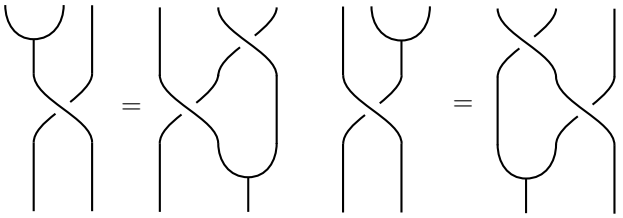

(a) $(\Delta \otimes \mathrm{id})R = R_{13}R_{23}$ (b) $(\mathrm{id} \otimes \Delta)R = R_{13}R_{12}$

Figure 4.1: Quasi-triangularity conditions.

Yang-Baxter equation

The final property that should be satisfied by the universal R-matrix is the *Yang-Baxter equation*. Physically, it represents a consistency relation to make braiding operations on three-particle states well-defined, which is represented graphically in figure 4.2. The algebraic expression, which can be proven from equations (4.48), (4.50) and (4.51), is as follows:

$$R_{12}R_{13}R_{23} = R_{23}R_{13}R_{12} \tag{4.52}$$

4.3 Symmetry breaking

A systems with a gauge symmetry in the Hamiltonian or action need not have the same symmetry present in its ground state. This is called symmetry breaking. For gauge systems transforming under a group, the symmetry breaking is realized by condensing a scalar field in the vacuum, transforming nontrivially under this group. We know this as the Higgs effect. In our present setting, this would equal breaking the electric part of the quantum double symmetry.

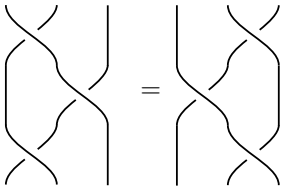

Figure 4.2: Yang-Baxter equation.

Since the quantum double formalism treats the electric and magnetic sectors of the theory on equal footing, we can also study the effect of magnetic condensates, a situation for which no general formalism has yet been developed in the case of gauge systems transforming under a Lie group.

The more general result of what follows is:

- Electric condensates lead to confinement of magnetic charges.
- Gauge-invariant magnetic condensates lead to confinement of electric charges.
- Non-gauge invariant magnetic condensates and dyonic condensates lead to a combination of both electric and magnetic confinement.

Two complementary pictures are available to study what happens when a quantum double symmetry gets broken by a vacuum vector $|\phi>$ transforming nontrivially under (part of) the group. On the one hand, one can study the set of operations from the original symmetry algebra leaving the vacuum invariant [Bais et al. (2003)]. After having worked out the residual symmetry structure, one can again look for representations, throw away the confined excitations, and identify the broken theory with a low-energy effective theory.

On the other hand, one can take a representation-theoretic perspective to begin with [Bais and Slingerland (2007)]. After identifying the representation the condensate vector $|\phi>$ transforms under with the vacuum sector, a new set of fusion rules can be worked out. By demanding these fusion rules to be consistent as well as commutative and associative, a residual spectrum of quantum double representations can be established.

We will give the recipe to work out the symmetry breaking using the second approach in detail. Here, we will only give a general result that has been obtained by using this approach for the situation of a gauge-invariant magnetic condensate.

4.3.1 Representation view on breaking

In the introduction to this section, we have already alluded to the fact that taking the representation-theoretic perspective on symmetry breaking lets us abandon the algebra and give center stage to the representations labels and their fusion rules.

The fundamental idea is that some sector Π_α^A of the unbroken theory gets identified with the vacuum sector Π_1^e in the broken theory. This identification will break the original set of fusion rules, since any given representation should fuse trivially with the vacuum. In general however, one can make the fusion rules consistent again by identifying representations of the original theory with a new set of representations describing the spectrum of the broken theory.

To achieve consistency, there are three rules at our disposal that can be applied in the identification process:

- $\Pi^B_\beta \to \Pi^e_1$: Representations other than the condensed sector Π^A_α might become identified with the vacuum. In the broken theory, the excitations labeled by these sector thus disappear completely from the spectrum. In physical terms, one could say that for these excitations, it is possible to fuse with the vacuum sector into the vacuum sector.

- $\Pi^B_\beta, \Pi^C_\gamma \to \Pi^D_\delta$: A number of sectors from the original theory become indistinguishable from each other in the broken theory. This means that in the broken theory, these sectors have to be given the same label. A physical picture for this situation is that fusion with the vacuum sector allows these excitations to be changed into each other.

- $\Pi^B_\beta \to \Pi^C_\gamma + \Pi^D_\delta$: Irreducible representations from the original theory might become reducible in the broken phase. We call this *branching* of representations. Physically, this corresponds to an excitation being fundamental in the unbroken phase and decaying into two or more components in the broken theory.

One can argue that the first two of these are the same, but their physical pictures are so different we decided to treat them separately. In general one can also have combinations of these rules.

In the identification process, the dimensionality of the representations one is working with has to be constantly kept in mind: on both sides of the "identification arrow", the dimensionalities of the representations have to be equal. This immediately poses a problem when condensing a multidimensional representation, since when Π^A_α is, for example, two dimensional, the identification

$$\Pi^A_\alpha \to \Pi^e_1 \tag{4.53}$$

does not obey the above dimensionality rule. A way out of this is to apply the branching rule, and writing down:

$$\Pi^A_\alpha \to \Pi^e_1 + \Pi^B_\beta \tag{4.54}$$

Where Π^B_β is some *a priori* unknown irrep of the quantum double $D(H)$, which is dictated by consistency. In principle there might be different Π^B_β that do the job, which would indicate different broken phases can be realized after condensation of Π^A_α. We have however not encountered these.

The new fusion rules have to be free of inconsistencies, and obey commutativity and associativity. After constructing such a set of fusion rules, there might still be excitations in the spectrum that are confined by the vacuum sector. A representation Π^B_β in the broken theory will be confined when a representation in the unbroken theory that braids nontrivially with the new vacuum sector Π^A_α gets identified with Π^B_β. The set of representation labels of the broken theory, without these confined sectors, should also have a closed fusion algebra, otherwise two unconfined excitations could, after fusing, become confined.

The unconfined set of representations can in general be identified with the representation theory of the quantum double $D(\tilde{H})$ of another group $\tilde{H}$, smaller than the original group H. This identification gives us a low-energy effective theory.

General recipe for breaking

With the above rules at our disposal, we can now give the general recipe to work out the effective theory for a system with broken quantum double symmetry:

1. Work out the full representation theory of the quantum double of the full, original gauge group H. This gives a set of representations $\{\Pi^A_\alpha\}$.

2. Determine all the fusion rules between the representations.

3. Determine the representation Π_α^A that is to be condensed to achieve the desired symmetry breaking.

4. Identify Π_α^A with the vacuum sector Π_1^e. If Π_α^A is a multidimensional representation, it will branch into the vacuum plus some other set of representation, so in general the identification will be $\Pi_\alpha^A \to \Pi_1^e + \sum_{B,\beta} \Pi_\beta^B$.

5. Plug this identification into the original fusion rules, and start identifying representations until the fusion rules are self-consistent again. For this, we have to use the three identification rules given above.

6. The above step will give a new set of representations $\{\Pi_{\alpha'}^{A'}\}$. This set contains the full spectrum of the broken theory, but includes confined sectors.

7. For each sector in the set $\{\Pi_{\alpha'}^{A'}\}$, check whether it is confined or not. To do this, first check which sectors of the original theory are identified with which sectors of the broken theory. For a representation to be unconfined in the broken theory, each sector it is identified with in the original theory has to braid trivially with the condensed representation Π_α^A.

8. The previous step generates a new set of representations $\{\Pi_{\alpha''}^{A''}\}$. Check whether the fusion rules for the representations in this set close on the set. If not, a mistake has been made and the construction is not self-consistent.

9. Identify the representations contained in $\{\Pi_{\alpha''}^{A''}\}$ with the representation theory of the quantum double $D(\tilde{H})$ of some discrete group $\tilde{H}$. This quantum double describes the low-energy effective theory of the broken phase.

We will use this recipe to calculate the effective theories of a $D(\overline{D_2})$ system, with condensed representations corresponding to the gauge-invariant magnetic sectors in the final chapter.

4.3.2 Algebraic view on breaking

As has been alluded to earlier, it is also possible to study the topological symmetry breaking in discrete gauge theories by studying the algebraic structure of the theory. This approach has been worked out in [Bais et al. (2003)], and has for example been applied to the situation of discrete gauge symmetries in condensed matter theory [Bais and Mathy (2007)]. We will briefly discuss the general idea, after which we present the results for gauge invariant magnetic condensates.

In this view on breaking, one starts out again with a vector describing the condensate ground state

$$|\phi> \in V_\alpha^A \tag{4.55}$$

The first step in this procedure is similar to the stability group method one applies when determining the residual symmetry group in electric symmetry breaking by the Higgs effect. We determine the set of elements $P_g h \in D(H)$ that leave the condensate vector invariant

$$\Pi_\alpha^A(P_g h)|\phi> = |\phi> \tag{4.56}$$

This set of operations defines a new algebra, since the product of two operations leaving the condensate invariant will also leave it invariant. However, in general this is not a Hopf algebra, and we

do need the coproduct to act on multiparticle states, so we take of this set the maximal sub-Hopf algebra: the *residual symmetry algebra* $\mathscr{T}$.

After having determined this residual symmetry algebra, one can again look for representations: these will label the different sectors of the broken theory. We expect that not all of these will have trivial braiding with the condensate, which means we will have to remove some of them to find the low-energy effective theory.

Having removed these sectors from the theory, one is left with the representations of the *unconfined symmetry algebra* $\mathscr{U}$. Finding the group $\tilde{H}$ of which the quantum double $D(\tilde{H})$ corresponding to this algebra is the last step in the formulation of the effective theory for the broken phase.

Result for gauge invariant magnetic condensates

Within this viewpoint of quantum double symmetry breaking, it is possible to calculate a general result for the symmetry algebra of the broken phase in the case of a gauge invariant magnetic condensate. We will be dealing with these condensates later on, and although we will approach the symmetry breaking from the representation side, this result will serve as a good check for our results.

Consider a magnetic sector Π_1^A. In the carrier space V_α^A of this representation there is exactly one vector invariant under all gauge transformations:

$$|\phi>=\sum_{g\in A}|g> \tag{4.57}$$

This state is called the *gauge invariant magnetic condensate*, and is equivalent to identifying Π_1^A with the vacuum sector Π_1^e when studying this problem using representations.

Consider now K: the smallest subgroup of H that contains the elements of the class A. It follows that K is normal, so that the coset H/K is also a group. The result [Bais et al. (2003)] is now that the residual symmetry algebra $\mathscr{T}$ and unconfined symmetry algebra $\mathscr{U}$ are given by

$$\mathscr{T} = F(H/K)\otimes\mathbb{C}H \tag{4.58}$$

$$\mathscr{U} = D(H/K) \tag{4.59}$$

Chapter 5

Lattice gauge theory

Quantum field theory in its perturbative formulation has been extremely successful as a theory: it provides the framework for the standard model, what many would call the cornerstone of modern physics, and has also led to great successes in condensed matter theory. As a physical theory however, it has a few serious shortcomings: some conceptual in nature, some more technical. Most of these problems can be overcome by a collection of mathematical tricks known as *regularization*.

Many of these problems can be overcome by replacing continuous spacetime by a lattice of discrete points. As we venture into the land of lattice gauge theories, we will often note which problems of continuum gauge theory are solved, and sometimes sadly so, which new problems are introduced. This discussion can be found in many textbooks on the subject, such as [Smit (2002)] and [Itzykson and Drouffe (1989)]. It is however amusing to see that many of the original articles on the subject, for example the original [Wilson (1974)] and a series of review articles [Balian et al. (1974)], [Balian et al. (1975a)] and [Balian et al. (1975b)], are still very readable today. The forthcoming discussion is mainly based on the latter articles, and we shall use their notation.

Note that we use a three-dimensional spacetime all throughout this thesis, unless noted otherwise, and although our interests lie in the application of discrete gauge groups, most of the information presented here will be for a general group H.

5.1 Formulation of field theory on the lattice

5.1.1 Path integral and Wick rotation

For a scalar field ϕ in the continuum in three spacetime dimensions, the path integral is defined as follows:

$$S(\phi) = \int dx_0 d^2x \left(\frac{1}{2} \left[(\partial_0 \phi)^2 - (\nabla \phi)^2 \right] - V(\phi) \right) \tag{5.1}$$

$$Z = \int D\phi e^{iS(\phi)} \tag{5.2}$$

To proceed to the lattice formulation, it will be necessary to perform a Wick rotation to imaginary time, leaving Minkowski space for Euclidean space. For this purpose, let us temporarily introduce the variable x_3:

$$x_3 = ix_0 \tag{5.3}$$

$$S^E(\phi) = i \int dx_3 d^2x \left(\frac{1}{2} \left[(\partial_0 \phi)^2 + (\nabla \phi)^2 \right] + V(\phi) \right) \tag{5.4}$$

Where S^E is the Euclidean action. Since we will not be leaving the Euclidean formulation from now on, we can let our indices run from 0 to 2 again and drop the superscript on the action. The Euclidean formulation of the path integral is then:

$$S(\phi) = \int d^3x \left(\frac{1}{2} (\partial\phi)^2 + V(\phi) \right) \tag{5.5}$$

$$Z = \int D\phi e^{-S(\phi)} \tag{5.6}$$

Where $\partial\phi$ now lives in a Euclidean space:

$$(\partial\phi)^2 = (\partial_0\phi)^2 + (\partial_1\phi)^2 + (\partial_2\phi)^2 \tag{5.7}$$

Which is our starting point for the formulation of field theories on the lattice.

5.1.2 Introduction of the lattice

Let us continue this discussion by replacing continuum spacetime by a set of points. Introducing unit vectors n_i, integers x_i and a length scale a, the lattice spacing, we can write any point in spacetime as:

$$x = \sum_{i=0}^{2} x_i n_i a \tag{5.8}$$

Let us stick to the most straightforward case and pick a cubic lattice, where $n_i \cdot n_j = \delta_{ij}$, and denote the position dependence of the fields as follows:

$$\phi_i = \phi(x(x_i)) \tag{5.9}$$

so we can label the sites of the lattice by Roman letters $i, j, k, \cdots$ from now on.

5.1.3 Scalar action

The theory described by equation (5.6) still requires a well-defined action on the lattice. In principle, any action that reproduces the kinetic term in equation (5.5) will suffice. Here we will give an example of such an action. Consider the following lattice action:

$$S(\phi) = -\sum_{\{i,j\}} \frac{1}{ag} \cos\left(a^{-\frac{1}{2}} (\phi_i - \phi_j) \right) \tag{5.10}$$

Where the sum is over sets of neighbouring lattice points $\{i, j\}$, and g plays the role of a coupling constant. To see that this action produces the correct continuum limit, we perform a first order Taylor expansion:

$$\begin{aligned} S(\phi) &= -\sum_{\{i,j\}} \frac{1}{ag} \cos\left[a^{\frac{1}{2}} \left(\frac{\phi_i - \phi_j}{a} \right) \right] \\ &\approx -\sum_{\{i,j\}} \frac{1}{ag} \left[1 - \frac{1}{2} a \left(\frac{\phi_i - \phi_j}{a} \right)^2 \right] \\ &\to \int d^3x \frac{1}{2g} (\partial\phi)^2 + \text{const} \end{aligned}$$

Which is the kinetic term in the continuum action (5.5), up to an irrelevant constant. Expanding the square in the second line above, gives two types of terms, typical in any lattice action.

The first class are the local terms, which contain only the value of the field at a certain point i, for example:

$$\sum_i \phi_i \phi_i \tag{5.11}$$

In addition to this, there are also nonlocal terms, containing products of fields at different locations, such as:

$$\sum_{\{i,j\}} \phi_i \phi_j \tag{5.12}$$

We will see in the next section that the nonlocal terms require the introduction of a lattice gauge field.

5.1.4 Gauge fields

We will now study the effect of adding charge to the fields in our theory. This is done by letting the field ϕ live in the representation space of a symmetry group H. We will show that after making the symmetry local, it is necessary to introduce an extra group-valued gauge field on the links of the lattice to be able to compare the values of the fields at different points.

Global versus local transformations

Consider a field ϕ_i^α on the lattice, like in the previous discussion, with the addition that this field now forms a representation α of some group H. A global gauge transformation with group element g

$$\phi_i^\alpha \mapsto D_\alpha(g)\phi_i^\alpha \tag{5.13}$$

leaves the action invariant, if we change the local terms (5.11) and nonlocal terms (5.12) to products of representations α and conjugate representations α^*. Noting the conjugate representations work as follows

$$D_{\alpha^*}(g) = D_\alpha(g^{-1}) \tag{5.14}$$

We have

$$\phi_i^{\alpha^*}\phi_i^\alpha \quad \mapsto \quad \phi_i^{\alpha^*} D_\alpha(g^{-1}) D_\alpha(g)\phi_i^\alpha = \phi_i^{\alpha^*}\phi_i^\alpha \tag{5.15}$$

$$\phi_i^{\alpha^*}\phi_j^\alpha \quad \mapsto \quad \phi_i^{\alpha^*} D_\alpha(g^{-1}) D_\alpha(g)\phi_j^\alpha = \phi_i^{\alpha^*}\phi_j^\alpha \tag{5.16}$$

Since the group element working on site i equals the group element working on site j.

Let us now study group transformations g_i differing from site to site:

$$\phi_i^\alpha \mapsto D_\alpha(g_i)\phi_i^\alpha \tag{5.17}$$

The local terms (5.11) are clearly invariant, but the nonlocal terms are not. To be able to construct a gauge-invariant action nevertheless, we require the introduction of a lattice gauge field. This field U_{ij} takes values in the gauge group, and lives on the links ij connecting the sites i and j. The orientation is important:

$$U_{ji} = U_{ij}^{-1} \tag{5.18}$$

By imposing the following transformation rule under local gauge transformations for this field, we are able to construct locally gauge-invariant actions:

$$U_{ij} \mapsto g_i U_{ij} g_j^{-1} \tag{5.19}$$

The gauge invariant actions will now have their nonlocal terms $\phi_i^{\alpha^*}\phi_j^{\alpha}$ replaced by the product $\phi_i^{\alpha^*} D_\alpha(U_{ij})\phi_j^{\alpha}$. This combination is manifestly gauge invariant:

$$\phi_i^{\alpha^*} D_\alpha(U_{ij})\phi_j^{\alpha} \mapsto \phi_i^{\alpha^*} D_\alpha(g_i^{-1}) D_\alpha(g_i U_{ij} g_j^{-1}) D_\alpha(g)\phi_j^{\alpha} = \phi_i^{\alpha^*} D_\alpha(U_{ij})\phi_j^{\alpha} \tag{5.20}$$

The meaning of the gauge field becomes clear: the group element U_{ij} allows us to parallel transport the field at position i towards j and compare the field values at that location.

Gauge field dynamics

So far, the gauge field U_{ij} acts only as a bookkeeping device: it allows us to compare the field values at different locations after having allowed for local gauge transformations. By adding a term to the action, we can give the gauge field physical degrees of freedom. This situation is similar to the continuum case, where the gauge field A_μ has no physics before adding an $F_{\mu\nu}F^{\mu\nu}$ term to the action.

Gauge invariance is a necessity to for the gauge field action. An important observation is that an ordered product of gauge field group elements along a closed curve of links C, stays in the same conjugacy class under all gauge transformations:

$$U_C = U_{i_1 i_2} U_{i_2 i_3} \cdots U_{i_n i_1} \tag{5.21}$$

$$U_C \mapsto g_{i_1} U_{i_1 i_2} g_{i_2}^{-1} g_{i_2} U_{i_2 i_3} \cdots U_{i_n i_1} g_{i_1}^{-1} = g_{i_1} U_C g_{i_1}^{-1} \tag{5.22}$$

Therefore any class function f is gauge invariant, and therefore a candidate for the gauge field action:

$$f(h) = f(ghg^{-1}) \tag{5.23}$$

Furthermore, class functions are invariant under a cyclic permutation of their arguments:

$$f(ghk) = f(g^{-1}ghkg) = f(hkg) = f(kgh) \tag{5.24}$$

Which, in the light of the ordered product (5.21), means the basepoint of the curve C is not of importance.

The class function that reduces to the continuum theory for SU_N lattice gauge theories is the fundamental character $\chi_f(U_p)$ of the simplest closed curve p, the plaquette:

$$U_p = U_{ij} U_{jk} U_{kl} U_{li} \tag{5.25}$$

Taking only the real part of the character and summing over all plaquettes, the gauge field action for SU_N theories becomes:

$$S = -\beta \sum_{p \in \mathscr{P}} \mathrm{Re}\left(\chi_f(U_p)\right) \tag{5.26}$$

where $\mathscr{P}$ is the set of all plaquettes on the lattice. The reality constraint is necessary because the action is a real quantity. It also makes the orientation of the plaquette irrelevant, since $\mathrm{Re}\left(\chi(g)\right) = \mathrm{Re}\left(\chi(g^{-1})\right)$.

In the case of SU_N, typically only the character in the fundamental representation is used, but it is also possible to use actions that contain for example both the fundamental and adjoint representations [Smit (2002)]. For the discrete gauge theories, we will make use of the most general case, and sum over the characters of all representations, each with its own coupling constant:

$$S = -\sum_{\alpha\in\mathscr{R}} \beta_\alpha \sum_{p\in\mathscr{P}} \mathrm{Re}\left(\chi_\alpha(U_p)\right) \tag{5.27}$$

Where $\mathscr{R}$ is the set of irreducible representations of the group, which is finite in the case of finite groups.

5.1.5 Discrete gauge theory actions

As put forward above, the most general gauge field action is of the form (5.27). This formulation, in which the coupling constants are in what we call the *representation basis*, is not the most convenient for an exploration of the phase diagram. Making use of the natural duality for discrete groups between irreducible representations and classes, we will transform (5.27) to a formulation where we have one coupling constant per class A.

For this purpose, we will make use of a class delta function:

$$\delta_A(g) = 1 \text{ if } g \in A, \text{ 0 otherwise} \tag{5.28}$$

Consider now an action of the form:

$$S = -\sum_{A\in\mathscr{C}} \beta_A \sum_{p\in\mathscr{P}} \delta_A(U_p) \tag{5.29}$$

Where $\mathscr{C}$ is the collection of conjugacy classes of the group. We will show that the class couplings β_A can be written in terms of the representation couplings β_α appearing in equation (5.27), which proves that the action defined in equation (5.29) is equivalent to the original action (5.27).

Transformation to class basis

To perform the transformation to the class basis, we need to make use of the following orthogonality relations valid for all finite groups H:

$$\int_H dg\,\chi_\alpha(g)\chi^*_\beta(g) = \delta_{\alpha,\beta} \tag{5.30}$$

$$\sum_{\alpha\in\mathscr{R}} \chi_\alpha(g)\chi^*_\alpha(h) = \frac{|H|}{|A|} \text{ if } g,h \in A \tag{5.31}$$

$$= 0 \text{ otherwise} \tag{5.32}$$

Where $|H|$ is the order of the group H and $|A|$ is the order of the class A, and group integration is defined as follows:

$$\int_H dg\, f(g) = \frac{1}{|H|}\sum_{g\in H} f(g) \tag{5.33}$$

First we will show the delta functions δ_A appearing in (5.29) written as linear combinations of group characters, and then we will derive an expression for the β_A in terms of the β_α.

Equations (5.30) and (5.31) show that the irreducible representations of a group H form an orthonormal set for functions on classes of H. We thus expect the class delta function to be expressible in terms of characters:

$$\delta_A(g) = \sum_{\alpha \in \mathscr{R}} c_\alpha \chi_\alpha(g) \tag{5.34}$$

For some set of constants $\{c_\alpha\}$. Ee multiply both sides of this expression by a character of the same group element in another irrep β and perform the integrations by use of the orthogonality relations (5.30) and (5.31):

$$\begin{aligned} \int_H dg \chi^*_\beta(g)\delta_A(g) &= \sum_{\alpha \in \mathscr{R}} c_\alpha \int_H dg \chi^*_\beta(g)\chi_\alpha(g) \\ \frac{|A|}{|H|}\chi^*_\beta(A) &= \sum_{\alpha \in \mathscr{R}} c_\alpha \delta_{\alpha\beta} = c_\alpha \end{aligned}$$

Where the slightly abusive notation $\chi_\alpha(A)$ means the character of any group element of A in the representation α. This shows that

$$\delta_A(g) = \sum_{\alpha \in \mathscr{R}} \frac{|A|}{|H|}\chi^*_\alpha(A)\chi_\alpha(g) \tag{5.35}$$

This shows that the the difference between (5.27) and (5.29) is just a change of basis:

$$\sum_{A \in \mathscr{C}} \beta_A(\beta_\alpha)\delta_A(g) = \sum_{\alpha \in \mathscr{R}} \beta_\alpha \chi_\alpha(g) \tag{5.36}$$

Where $\beta_A(\beta_\alpha)$ is given by:

$$\beta_A = \sum_\alpha \beta_\alpha \chi_\alpha(A) \tag{5.37}$$

5.2 Operators as order parameters

We have seen in the previous sections that it is possible to formulate a discrete gauge theory on a lattice, in such a way that we have a number of free parameters in the theory: one coupling constant for each class, or alternatively, for each irrep. We expect that different phases will be realized in different regions of the coupling constant space.

To fully probe the phase structure, we need gauge invariant operators. In general these can also be non-local, and it are these non-local operators corresponding to the different sectors of the theory, that characterize the phase structure best.

5.2.1 Elitzur's theorem

First we will show the crucial difference between statistical mechanical systems and gauge systems when it comes to characterizing phases. In the Ising model for example, one can just use the expectation value of the spin variable appearing in the Hamiltonian to characterize between the two phases. If this variable does not gain an expectation value, the disordered phase is realized, and when the expectation value of a single spin is either plus or minus one, an ordered phase sets in and the symmetry is broken.

For gauge theories, one cannot use a single variable appearing in the Hamiltonian or action to characterize the phase: by a series of gauge transformations, a single link variable in a lattice gauge theory can take arbitrary values, while staying in the same vector in Hilbert space.

Here we give the proof that the expectation value of a local non-gauge-invariant operator will always vanish [Elitzur (1975)]. Let ϕ be the complete collection of gauge field variables, $f(\phi$ some quantity we try to use as an order parameter, J an external source field and N the lattice size. The expectation value of ϕ is then:

$$< f(\phi) > = \lim_{J\to 0}\lim_{N\to\infty} < f(\phi) >_{N,J} \tag{5.38}$$

$$< f(\phi) >_{N,J} = \frac{1}{Z_{N,J}}\int D\phi e^{-S(\phi)+J\cdot\phi} f(\phi) \tag{5.39}$$

The order of limits in this case is important. To see this, remember the Ising model: starting in the disordered phase, lowering the temperature will lead to one of the two ordered phases. Either one of these phases, all spins up or all down, is a good candidate, but only one of them will get realized. To go from one of these phases to the other would require the creation of a domain wall, of which the energy scales with the system size N. The correct order in this case, and in (5.38), is then to first take the thermodynamic limit $N\to\infty$ and then turn of the sources.

The claim was that a local quantity not invariant under gauge transformations $\phi \mapsto^g \phi$ is not a good candidate for an order parameter. By non invariance, we mean the following:

$$\int f({}^g\phi) Dg = 0 \tag{5.40}$$

Where the integral is over all gauge transformations on a given field configuration ϕ.

By locality of f, we mean that the function f depends only on a finite set of field variables $\{\phi'\}$. The total collection of field variables is thus partitioned as $\{\phi\} = \{\phi'\}\cup\{\phi''\}$. Consider now a subset of all possible local gauge transformations, namely the ones acting trivially on the $\{\phi''\}$ set of field variables: ${}^g\phi'' = \phi''$. Averaging over these transformations in equation (5.39) and using the invariance of the measure and action under gauge transformations, we obtain:

$$< f(\phi) >_{N,J} = \frac{1}{Z_{N,J}}\int\int D\phi Dg e^{-S(\phi)+J'\cdot{}^g\phi'+J''\cdot\phi''} f({}^g\phi) \tag{5.41}$$

Where the first integral is a path integral over the field variables and the second is an integral over the previously mentioned set of gauge transformations.

Since we take the limit $J\to 0$ in (5.38) anyway, we can consider J to be bounded from above by some parameter ϵ. If we introduce a function $\eta(\epsilon)$ vanishing uniformly with ϵ, the following inequality is derived, which is crucial to the coming argument:

$$|e^{J'\cdot\phi'} - 1| \le \eta(\epsilon) \tag{5.42}$$

Now writing $e^{J'\cdot\phi'} = 1 + (e^{J'\cdot\phi'} - 1)$, the inequality (5.42) can be used to find an upper bound for

equation (5.41):

$$\begin{aligned}
< f(\phi) >_{N,J} &= \frac{1}{Z_{N,J}} \left(\int\int D\phi Dg e^{-S(\phi)} f({}^g\phi) + \int\int D\phi Dg e^{J'.{}^g\phi'} f({}^g\phi) + \int\int D\phi Dg e^{J''.\phi''} f({}^g\phi) \right) \\
&= \frac{1}{Z_{N,J}} \left(\int D\phi e^{-S(\phi)} \left\{ \int f({}^g\phi) Dg \right\} + \int\int D\phi Dg e^{J'.{}^g\phi'} f({}^g\phi) + \int D\phi e^{J''.\phi''} \left\{ \int f({}^g\phi) Dg \right\} \right) \\
&= \frac{1}{Z_{N,J}} \left(\int\int D\phi Dg e^{J'.{}^g\phi'} f({}^g\phi) \right) \\
&= \frac{1}{Z_{N,J}} \left(\int\int D\phi Dg f({}^g\phi) + \int\int (e^{J'.{}^g\phi'} - 1) f({}^g\phi) \right) \\
&= \frac{1}{Z_{N,J}} \left(\int\int (e^{J'.{}^g\phi'} - 1) f({}^g\phi) \right) \\
&\leq \eta(\epsilon) \sup(f)
\end{aligned}$$

Which boils down to, when taking the limits in equation (5.38):

$$< f(\phi) >= 0 \tag{5.43}$$

Proving that gauge invariant quantities are required to characterize phases in a physical theory with local gauge invariance.

5.2.2 Wilson loop W_α

The best-known order parameter in gauge theories is the *Wilson loop*. The physical interpretation of this operator is the insertion of a particle-antiparticle pair at some timeslice, letting them propagate and annihilating them at some later time.

In the continuum, the Wilson loop operator $W_\alpha(\Omega)$ for a source charged as irrep α around a closed loop Ω is given by the following expression:

$$W_\alpha(\Omega) = \chi_\alpha \left(\mathrm{P} \exp(ig \int_\Omega dx^\mu A_\mu(x)) \right) \tag{5.44}$$

This expression amounts to parallel transport around a closed curve.

On the lattice, we have seen that parallel transport is taken care of by the link variables U_{ij}. Therefore the Wilson loop in a lattice gauge theory takes a particularly simple form:

$$W_\alpha(\Omega) = \chi_\alpha(U_\Omega) = \chi_\alpha(U_{12} U_{23} \cdots U_{N1}) \tag{5.45}$$

Where the order of multiplication of the link variables is of importance in the case of nonabelian groups H, like path ordering in the continuum case.

5.2.3 't Hooft loop H^A

In addition to the charges, there are also the magnetic fluxes in gauge theories in two spatial dimensions. Therefore we need to construct an operator thar creates a flux-antiflux pair at a certain timeslice that can propagate in time and annihilate at some later timeslice.

There exist many papers in the literature concerned with the central $\mathbb{Z}_N$ fluxes of an SU_N theory. The operator ϕ defined in (3.19) is the operator creating such excitations in a Hamiltonian formalism. The Euclidean lattice gauge theory equivalent of this operator is studied [in the light of quark confinement [de Forcand et al. (2001)].

The generalization of these loops to the case of nonabelian fluxes, where the gauge invariant notion of a flux is not given by a group element, but by a conjugacy class, was put forward in [Alford and March-Russell (1992)] and [Lo (1995)].

Construction

To construct the correct operator, three things have to be kept in mind. First of all, we expect there to be one operator for each conjugacy class in the group. Secondly, the operator will need to act on the elementary plaquette, since a nonzero plaquette in a discrete lattice gauge theory means there is a flux present. Finally, Elitzur's theorem requires the operator to be gauge invariant.

We want to make sure that in every configuration we sum over in the path integral, an extra flux pair is inserted along some closed loop. Because the fluxes live on the plaquettes of the lattice, we introduce the notion of the *dual lattice*: the lattice that is obtained by shifting all sites by one half of the lattice distance in all three directions.

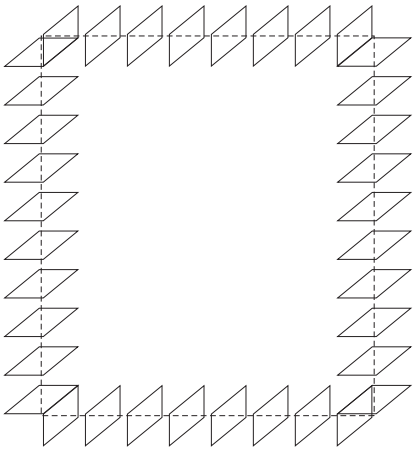

Figure 5.1: A loop Σ^* on the dual lattice (dashed) and its associated plaquettes (solid).

Let Σ^* be a closed loop on this dual lattice. This loop pierces a number of plaquettes on the original lattice, like beads on a string; we denote this set of plaquettes by Σ. The loop Σ^* can be viewed as the worldline of the flux-antiflux pair, if we take it to be timelike. An example of a loop Σ^* with its associated plaquettes Σ is given in figure 5.1.

Let us define a twisted partition sum $\tilde{Z}$ that has an extra flux in class A forced through each plaquette in Σ:

$$\tilde{Z} = \int DU \prod_{p\in\mathscr{P}, p\notin\Sigma} e^{-S(U_p)} \prod_{p'\in\Sigma} \frac{1}{|A|} \sum_{g\in A} e^{-S(gU_p)} \tag{5.46}$$

Having defined this twisted partition sum, the expectation value of an 't Hooft loop $H^A(\Sigma^*)$ is:

$$< H^A(\Sigma^*) >= \frac{\tilde{Z}}{Z} \tag{5.47}$$

It might seem strange, and is indeed difficult to work with, to define an operator as a modification of the partition sum. It is therefore more convenient to write down the operator $H^A(\Sigma^*)$ as a normal

operator, that can be plugged into the path integral:

$$H^A(\Sigma^*) = \prod_{p\in\Sigma} \frac{1}{|A|} \sum_{g\in A} e^{S(U_p)-S(gU_p)} \tag{5.48}$$

The equivalence to (5.47) can be seen by plugging the above expression into the path integral: the $e^{S(U_p)}$ removes the original Boltzmann factor of the plaquette U_p and replaces it by $e^{-S(gU_p)}$.

A final remark has to be made. The summation over the conjugacy class A in expression (5.48) ensures gauge invariance. Under gauge transformations the plaquette product transforms at most as $U_p \mapsto hU_ph^{-1}$, and the action is a cyclic function, so the summation over g can be written as a summation over $h^{-1}gh$. When summing over a class this transformation is immaterial, so gauge invariance is ensured.

5.2.4 Dyonic loop D^A_α

The more exotic excitations in discrete gauge theories are the dyons. We do not know of any literature that described a procedure to construct an Euclidean lattice gauge theory operator corresponding to these sectors. Here we show our attempt to construct an operator for a give dyonic sector with flux A and centralizer charge α. Physical intuition tells us that this operator has to be some soft of combination of a Wilson loop and an 't Hooft loop, since it contains both electric and magnetic degrees of freedom.

However, in this light a technical difficulty arises. The electric part of the dyon does not form a representation of the full group H, the dyonic sectors carry only centralizer charge. However, since the group elements living on the links of the lattice live in the full group H, it is not directly clear how to take the trace of the Wilson loop. Our proposal for the dyonic operator D^A_α tackles this problem, as we will describe in the following.

Outline

The idea is as follows. First we introduce an 't Hooft loop H^A to insert a closed loop of flux on the real lattice. Then we will take a loop on the real lattice, neighbouring the loop on the dual lattice, to draw a Wilson loop.

This Wilson loop will have to be traced in a centralizer representation. For this purpose, we will construct a map from the full group H to the centralizer subgroup ${}^AN$. After applying the map, it is possible to take the character of the Wilson loop group element in the centralizer representation α.

Construction

Let us first pick a loop Σ^* on the dual lattice. On this loop we put an 't Hooft loop for the class A, as in equation (5.48). For the Wilson loop, we pick a loop Ω on the real lattice. This loop can be obtained by shifting each dual lattice site of Σ^* inwards into the loop. This construction is clarified in figure 5.2.

Now we need to take the character of the electric part of the dyon in a centralizer representation α. For this purpose, we construct a map from the full group H to the centralizer subgroup ${}^AN$. This map is called Θ, and is made explicit in equations (4.30) to (4.33):

$$\Theta : (A\times H) \rightarrow {}^AN \tag{5.49}$$

$$(h,g) \mapsto \tilde{g} \tag{5.50}$$

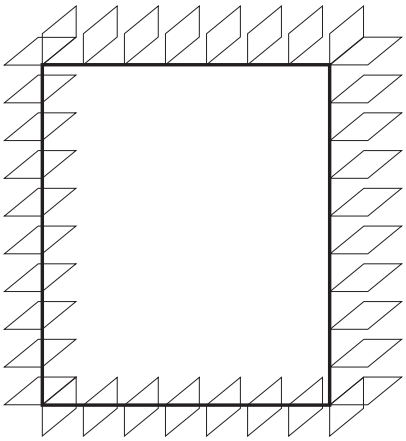

Figure 5.2: A dyonic loop, consisting of a set of plaquettes Σ (thin) and a closed loop of links Ω (fat).

We will give a concrete example of this construction for the group $\overline{D_2}$ in the final chapter. With the use of the map Θ, the electric part of the dyon is captured in the ordered product of links U_Ω, and we propose the following operator D^A_α:

$$D^A_\alpha(\Sigma^*,\Omega) = \left(\prod_{p\in\Sigma}\frac{1}{|A|}\sum_{g\in A} e^{S(U_p)-S(gU_p)}\right)\left(\frac{1}{|A|}\sum_{h\in A}\chi_\alpha(\Theta(h,U_\Omega))\right) \tag{5.51}$$

Two final remarks still have to be made to conclude the discussion regarding D^A_α.

Gauge invariance

The first remark concerns gauge invariance of equation (5.51). The gauge invariance of the flux part was already discussed in the section defining the 't Hooft loop. The electric part is also made gauge invariant by summing over the conjugacy class. Since the map Θ has the following property:

$$\Theta(h, gU_\Omega g^{-1}) = \Theta(g^{-1}hg, U_\Omega) \tag{5.52}$$

and the Wilson loop transforms at most as

$$U_\Omega \mapsto gU_\Omega g^{-1} \tag{5.53}$$

the sum on the right hand side in equation (5.51) is clearly gauge invariant.

Ribbon element

The other remark has to do with the shape of Ω. In the definition given above, the loops Ω and Σ^* have zero linking number. When we allow nonzero linking numbers, we expect that the topological spin factor of the dyonic sector will be obtained. Suppose we have a loop $\tilde{\Omega}$ that has linking number 1 with the loop Σ^*, and a loop Ω with zero linking number with Σ^*. This construction is clarified in figure 5.3. The ribbon element $c(A,\alpha)$ for the dyonic sector Π^A_α will now be given by the following expectation value:

$$c(A,\alpha) = \frac{< D^A_\alpha(\Sigma^*,\tilde{\Omega}) >}{< D^A_\alpha(\Sigma^*,\Omega) >} \tag{5.54}$$

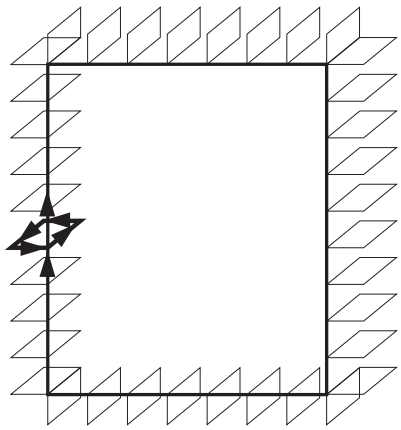

Figure 5.3: A dyonic loop with linking number 1

5.3 Location of gauge invariant magnetic condensates in the parameter space

By studying the discrete gauge theory based on the group $\overline{D_2}$, we have found a general principle to realize a magnetic condensate by tweaking the coupling constants in the gauge action. We identify the gauge invariant magnetic condensates by studying the behaviour of the 't Hooft loop operator in the different regions of parameter space.

In this parameter space, we found regions where the 't Hooft loop $H^A(\Sigma^*)$ becomes independent of the loop size of Σ^*. These are the regions we identify with a broken theory due to a condensate of the Π_1^A sector. The following general principle has been found to locate these regions.

We first work out the set of elements K_A generated by the class A. This is a normal subgroup of the full group H. Then we identify the set of classes of H corresponding to the elements of K_A. We call this set of classes $\mathscr{K}_A$. For each class B not appearing in $\mathscr{K}_A$, the coupling β_B is set to zero, leaving the following action:

$$S(U_p) = -\sum_{C \in \mathscr{K}_A} \beta_C \delta_C(U_p) \tag{5.55}$$

When these couplings β_C are all approximately equal, and larger than some critical value, we found that the Π_1^A condensate is realized.

We have no analytical proof of the above statements, but Monte Carlo simulations support the above view.

5.4 Performing calculations

Of course any formulation of a physical theory is only as useful as the calculations it allows. Although continuum quantum field theory is plagued by many infinities, the lattice formulation is much better defined. Also, the lattice formulation makes a clear connection between classical statistical mechanics and quantum field theory after the Wick rotation: a path integral with weighing factor $e^{-\beta S}$ is mathematically equivalent to a classical statistical mechanical system with Boltzmann factor $e^{-\beta H}$.

This latter relation allows us to apply two methods developed in the realm of statistical mechanics to lattice gauge theory: the strong coupling expansion [Balian et al. (1975b)] and the Monte Carlo simulation. The latter method allows field theory problems to be tackled efficiently on a computer [Thijssen (2007)]. In addition to these two methods, also weak coupling expansions can be made in a systematic fashion in the case of discrete gauge groups.

5.4.1 Strong coupling expansions

It is amusing to note that, contrary to the continuum setting, perturbative expansions in the strongly coupled regime are easily performed on the lattice. To perform these calculations, we will expand the Boltzmann factor in the path integral in terms of characters, and then use orthogonality relations between the group representations and classes to obtain terms of higher and higher accuracy. The terms correspond to diagrams on the lattice, making a systematic expansion possible.

Character expansions

In order to expand the weighing factor e^{-S} in the path integral, we require character expansions: the characters of the group form a complete basis for the functions on the conjugacy classes. This technique was also used in the derivation of equation (5.35), the expansion of the class delta function in terms of characters.

Let us briefly recall the orthogonality relations for finite groups (5.30) and (5.31):

$$\int_H dg \chi_\alpha(g)\chi^*_\beta(g) = \delta_{\alpha,\beta} \tag{5.56}$$

$$\sum_{\alpha\in\mathscr{R}} \chi_\alpha(g)\chi^*_\alpha(h) = \frac{|H|}{|A|} \text{ if } g,h \in A \tag{5.57}$$

$$= 0 \text{ otherwise} \tag{5.58}$$

The above relations can be used to expand the Boltzmann factor $e^{-S(U_p)}$, which is a function on conjugacy classes of the group, since the action itself is a function on conjugacy classes. Let us write the Boltzmann factor as a linear combination of group characters:

$$e^{-S(U_p)} = \sum_{\alpha\in\mathscr{R}} d_\alpha c_\alpha \chi_\alpha(U_p) \tag{5.59}$$

Where we have written the coefficients of the expansion as a product of the dimensionality d_α of the irrep α, and a coefficient c_α, to be determined. These latter coefficients can be found by multiplying both sides of (5.59) with $\chi^*_\beta(U_p)$ and integrating over the full group:

$$\int_H dU_p \chi^*_\beta(U_p) e^{-S(U_p)} = \sum_{\alpha\in\mathscr{R}} d_\alpha c_\alpha \int_H dU_p \chi_\alpha(U_p)\chi^*_\beta(U_p) \tag{5.60}$$

$$= \sum_{\alpha\in\mathscr{R}} d_\alpha c_\alpha \delta_{\alpha\beta} \tag{5.61}$$

$$d_\alpha c_\alpha = \int_H dU_p \chi^*_\alpha(U_p) e^{-S(U_p)} \tag{5.62}$$

This allows the partition sum to be expanded as follows (with analogous expression for quantum

expectation values):

$$Z = \int DU e^{-S(U_p)} \tag{5.63}$$

$$= \int_H \prod_{ij} dU_{ij} \prod_{p\in\mathscr{P}} e^{-S(U_p)} \tag{5.64}$$

$$= \int_H \prod_{ij} dU_{ij} \prod_{p\in\mathscr{P}} \left(\sum_{\alpha\in\mathscr{R}} c_\alpha d_\alpha \chi_\alpha(U_p) \right) \tag{5.65}$$

$$= c_1^{|\mathscr{P}|} \int_H \prod_{ij} dU_{ij} \prod_{p\in\mathscr{P}} \left(1 + \sum_{\alpha\in\mathscr{R},\alpha\neq 1} \frac{c_\alpha d_\alpha}{c_1} \chi_\alpha(U_p) \right) \tag{5.66}$$

Where the trivial representation has been split off for later calculational convenience and $|\mathscr{P}|$ is the number of plaquettes. This relation is exact, no approximations have been made. Furthermore, in our setting, where the groups are finite, the sum over representations is finite (note that in the case of Lie groups, this is more tedious, since these have an infinite number of irreducible representations).

Wilson loop: area law

As an example, let us calculate the expectation value of the Wilson loop in the strongly coupled regime:

$$< W_\alpha(\Omega) > = \frac{1}{Z} \int DU e^{-S(U_p)} \chi_\alpha(U_\Omega) \tag{5.67}$$

$$= \int_H \prod_{ij} dU_{ij} \prod_{p\in\mathscr{P}} \left(\sum_{\alpha\in\mathscr{R}} c_\alpha d_\alpha \chi_\alpha(U_p) \right) \chi_\alpha(U_\Omega) \tag{5.68}$$

So far, this expression is exact. Now, since we integrate over the group, the only terms contributing are the ones that form singlets (transform trivially under the group). Singlets can be formed for a given link integration by picking two plaquettes sharing a link U_{ij} in (5.68), and use the following identity:

$$\int_H dU_{ij} \chi_\alpha(V_1 U_{ij}) \chi_\beta(U_{ij}^{-1} V_2) = \frac{\delta_{\alpha\beta}}{d_\alpha} \chi_\alpha(V_1 V_2) \tag{5.69}$$

This relation, visualized in figure 5.4, can be used iteratively to integrate out more and more links.

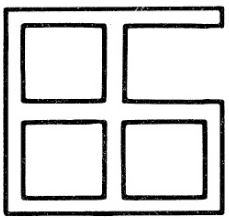

Figure 5.4: Integrating out one link after tiling a 2×2 Wilson loop with four plaquettes.

The leading order term in expression (5.68) then comes from tiling the inside of the Wilson loop

with plaquettes from the Boltzmann factor:

$$< W_\alpha(\Omega) >= d_\alpha \left(\frac{c_\alpha}{c_1}\right)^A \tag{5.70}$$

With A the area of the Wilson loop. Higher order corrections can be found by "decorating" the

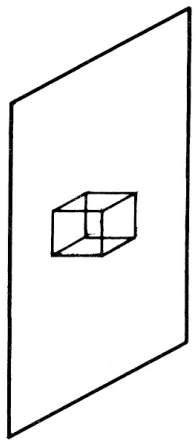

Figure 5.5: Decorating the plaquettes inside the Wilson loop with a little house, leading to corrections to the first order expansion.

tiled loop. The first correction corresponds to a little house placed anywhere inside the loop, as visualized in figure 5.5. Since we can place this decoration in $2A$ different ways, the expression for the Wilson loop expectation value becomes:

$$< W_\alpha(\Omega) >= d_\alpha \left(\frac{c_\alpha}{c_1}\right)^A + d_\alpha 2A \left(\frac{c_\alpha}{c_1}\right)^{A+4} \tag{5.71}$$

By using different diagrams, for some representations also perimeter law behaviour can be deduced. Since we will not be needing this, it will not be discussed here, but for discussion see for example [Smit (2002)].

5.4.2 Weak coupling expansion

The weak coupling expansions in lattice gauge theory are perturbative expansions around the classical extremum of the action. The first step is thus to find the classical configuration, which contributes dominantly to the path integral. This can not be done in all cases, but we give here an example in which the calculation is relatively straightforward: the calculation of the expectation value of the Wilson loop in a $\mathbb{Z}_2$ gauge theory.

The plaquette action for a $\mathbb{Z}_2$ gauge theory is given by:

$$S = -\beta\chi(U_p) \tag{5.72}$$

Where the character is in the nontrivial irrep of the group, $\chi(U_p) = \pm 1$. For large β, the dominant contribution to the path integral is given by the configurations in which all plaquettes are $+1$. This means, that modulo gauge transformations, all U_{ij} are $+1$.

Let us work out the expectation value of a Wilson loop in this regime. The value of a Wilson loop around a curve Ω of length L is +1 in the dominant configuration. The Boltzmann factor for this configuration is $e^{\beta N}$, where N is the total number of plaquettes (equalling the total number of links).

The first correction comes from configurations where one link is flipped. This can be done at N different locations. The Boltzmann factor for these configurations is $e^{\beta(N-8)}$, since in our three-dimensional lattice a single link is associated to four plaquettes, and for these plaquettes the values shifts two units (+1 to -1). For L of these flips, the Wilson loop value changes from +1 to -1, and for $N-L$ of the flips, the Wilson loop stays the same. To first order then, the expectation value for the Wilson loop operator becomes:

$$< W(\Omega) > = \frac{1e^{\beta N} + 1(N-L)e^{\beta(N-8)} + (-1)Le^{\beta(N-8)}}{e^{\beta N} + Ne^{\beta(N-8)}} \tag{5.73}$$

$$= \frac{1 + Ne^{-8\beta} - 2Le^{-8\beta}}{1 + Ne^{-8\beta}} \tag{5.74}$$

$$\approx 1 - 2Le^{-8\beta} \tag{5.75}$$

Where we have used the approximation $\frac{1}{1-x} \approx 1 + x$ and kept only leading order terms in β. As we see, in this regime, the Wilson loop falls off with its perimeter.

5.4.3 Monte Carlo Methods

Necessity

Imagine we desire to calculate the expectation value of some operator on a computer in a numerical simulation. How do we approach this? The naive way would be something along the following lines: we define some finite lattice and impose the appropriate boundary conditions, find some way to generate all the configurations of the gauge field and evaluate the operator in each of these configurations. Then for each configuration we multiply the value of the operator in that configuration by its Boltzmann factor, add all these contributions and divide by Z.

This might seem appealing, but this approach is entirely unfeasible. A typical lattice size is 8^3, which means there are $8^3 = 512$ dynamical variables that have to be integrated over. For simplicity, take the simplest group, $\mathbb{Z}_2$, having two elements. This situation has already $2^{512} \approx 10^{154}$ configurations in the path integral, which is such an astronomically high number that all hope of using this scheme for a numerical analysis must be abandoned.

A solution is to construct an algorithm that generates the configurations that dominate the path integral, each with probability e^{-S}, and sample those with equal weight. This method goes by the name of Monte Carlo. For an extensive treatment, see for example the series of (review) articles in [Rebbi (1983)].

Generalities

A general Monte Carlo algorithm works as follows. We start with some initial configuration of variables (in the lattice gauge theory setting, the link variables U_{ij}). We denote this configuration by $C^{(1)}$. The desired operator O is sampled in this configuration. Then we generate a new configuration $C^{(2)}$ from the old one, and sample O again, and so on. To obtain true quantum expectation values, the configuration $C^{(2)}$ should not be deterministically linked to $C^{(1)}$: only a transition probability $p(C^{(1)} \to C^{(2)}$ should be defined for each of these steps.

We want this probability p to be defined in such a way that after some finite number of steps n_0, the distribution of generated configurations closely approximates the Boltzmann distribution e^{-S}. If this is the case, we calculate quantum expectation values as follows:

$$< O >= \frac{1}{n} \sum_{k=n_0+1}^{n_0+n} O(C^{(k)}) \tag{5.76}$$

Where $O(C^{(k)})$ is the value of the operator O, sampled in configuration $C^{(k)}$. To ensure that the generated configurations approximate the Boltzmann distribution, we must implement the *detailed balance* condition:

$$\frac{p(C \to C')}{p(C' \to C)} = \frac{e^{-S(C')}}{e^{-S(C)}} \tag{5.77}$$

Heat bath algorithm

The algorithm used in our discrete gauge theory Monte Carlo simulation, is called the *heat bath* algorithm. It functions as follows. We start with some initial configuration of link variables $C^{(1)}$. We then update all links in lexicographic order, a process called a *sweep*, and arrive at a new configuration $C^{(2)}$. The updating process for each link is the following.

Consider the link U_{ij}. We identify which plaquettes contain this link: in three dimensions, there are four such plaquettes. Now we calculate, for each element $g \in H$, what the sum of the plaquette actions for each of these four plaquettes would be come if U_{ij} were to be replaced by g. This gives a set of numbers:

$$\{S_{g_1}, S_{g_2}, \cdots, S_{g_{|H|}}\} \tag{5.78}$$

Where S_{g_i} is the sum of the four plaquette actions with U_{ij} replaced with g_i. We now calculate a localized partition sum $Z_{U_{ij}}$:

$$Z_{U_{ij}} = \sum_{g \in H} e^{-S_g} \tag{5.79}$$

Which can be used to calculate a set of probabilities $\{p(g)\}_{g \in H}$ for each group element g:

$$p(g) = \frac{e^{-S_g}}{Z_{U_{ij}}} \tag{5.80}$$

We then update U_{ij} to a new value using the random number generator of the computer, according to the set of probabilities (5.80). It is trivial to check that this procedure obeys the detailed balance condition (5.77).

Chapter 6

$\overline{D_2}$ gauge theory

In this chapter we will apply all that has been learned thusfar to a concrete example. We choose a model based on the group $\overline{D_2}$, a nonabelian group with eight elements, which can be seen as a subgroup of SU_2 or, alternatively, as the group of quaternions. In the former setting it is often known as the *double dihedral group*. In the latter setting one also tends to find the notation Q.

We will first briefly discuss the structure of the group, and then move on to the representation theory of the quantum double constructed from this group to study the possible sectors. Then we will work out the symmetry breaking by magnetic condensates using the representation view. Finally, and this is where new results come in, we try to realize those condensates by going through the phase space of our lattice model.

For the representation theory, we use the notation in [Bais et al. (1992)] and follow their discussion.

6.1 $\overline{D_2}$ and D($\overline{D_2}$)

We will first briefly describe the group structure of $\overline{D_2}$ by looking at what we know something of: SU_2. It is useful to develop some feeling for this group, as we will be performing some intricate group theoretical manipulations later on.

6.1.1 The group and its representations

Subgroup of SU_2

A common method of developing intuition on Lie groups is by drawing a schematic picture of its parameter space. For SU_2, the parameter space is a filled sphere S_2 of radius 2π in three-space, with all points on the surface identified with eachother.

If we draw a cartesian set of axes inside of the sphere, and let the origin coincide with the center of it, we can easily see what is going on. We identify the identity element of the group with the origin. All three axes run from 0 to 2π, and each point on such an axis is identified with an SU_2 rotation by an amount corresponding to the distance from the origin, along the appropriate axis in group space.

So for example, the point lying on the x-axis at a distance π from the origin corresponds to the SU_2 group element that is represented by $i\sigma_x$ in the spinor representation. We can see this goes well by performing two successive rotations of this type, leaving us on the origin. In spinor

representation this element would be represented by $i^2\sigma_x^2 = -1$, which makes sense, since a spinor flips sign when rotated by 2π along any axis.

This picture gives us a neat way of approaching $\overline{D_2}$: keep only identity, the rotations by π and $-\pi$ along each of the three axes, and the -1 element. This gives us eight elements, and since simple reasoning tells us that the rotations along π and $-\pi$ must belong to the same conjugacy class, five classes.

In the rest of this work, we will use the following notation for the group elements. Let e denote the identity element, $\overline{e}$ the -1 element and let the rotations around one of the axes i by π or $-\pi$ be given by X_i and $\overline{X}_i$, respectively ($i = 1,2,3$).

Now, with the appropriate abuse of notation we will use the same symbols for the classes, but in square brackets. The central elements are alone in their classes, which will be refered to by $[e]$ and $[\overline{e}]$. The rotations render three classes of order two: $[X_1]$, $[X_2]$ and $[X_3]$.

Representations

Since there are five classes, there must also be five irreducible representations. After some algebra one discovers they are: one two-dimensional, three nontrivial one-dimensional and the trivial irrep. We label them as follows: the trivial irrep is called 1, the nontrivial three one-dimensional ones are J_i ($i = 1,2,3$) and the twodimensional or *doublet* irrep is named χ. The latter doublet irrep is basically an induced representation that originates from the spinor representation of SU_2, and represents the X_i and $\overline{X}_i$ elements by $i\sigma_i$ and $-i\sigma_i$, whereas the identity element and the -1 element are represented by respectively plus and minus the identity matrix.

At the end of the day we arrive at the following character table:

Table 6.1: Character table for $\overline{D_2}$

$\overline{D_2}$	$[e]$	$[\overline{e}]$	$[X_1]$	$[X_2]$	$[X_3]$
1	1	1	1	1	1
J_1	1	1	1	-1	-1
J_2	1	1	-1	1	-1
J_3	1	1	-1	-1	1
χ	2	-2	0	0	0

Centralizers

To construct the quantum double irreducible representations, we also need the centralizer of each of the conjugacy classes. For the two central elements e and $\overline{e}$, this is trivial: the entire group commutes by definition, so their centralizer group is $\overline{D_2}$. For the three $[X_i]$ classes, the best method to find out what the centralizer is, is probably just by picking a representative element and trying which elements in the group commute with it.

It turns out that the centralizers for all these three classes are isomorphic, which was to be expected since the high level of symmetry relating them. For each class $[X_i]$, the group elements commuting with a representative of this class are e, $\overline{e}$, X_i and $\overline{X}_i$. This set of elements itself forms a group again, which can be found out by multiplying them together. This group is the cyclic group of order four, $\mathbb{Z}_4$ which has four irreps, since it is an abelian group with four elements.

We denote the $\mathbb{Z}_4$ irreps by Γ^j ($j = 0,1,2,3$), with Γ^0 the identity irrep. To conclude, we give the centralizers of each of the classes of $\overline{D_2}$ and the irreps of $\mathbb{Z}_4$ below:

Table 6.2: Conjugacy classes of $\overline{D_2}$ and their centralizers

Class	Centralizer
$[e] = e$	$\overline{D_2}$
$[\overline{e}] = \overline{e}$	$\overline{D_2}$
$[X_1] = \{X_1, \overline{X}_1\}$	$\mathbb{Z}_4 \simeq \{e, X_1, \overline{e}, \overline{X}_1\}$
$[X_2] = \{X_2, \overline{X}_2\}$	$\mathbb{Z}_4 \simeq \{e, X_2, \overline{e}, \overline{X}_2\}$
$[X_3] = \{X_3, \overline{X}_3\}$	$\mathbb{Z}_4 \simeq \{e, X_3, \overline{e}, \overline{X}_3\}$

Table 6.3: Character table for $\mathbb{Z}_4$

$\mathbb{Z}_4$	e	X_i	$\overline{e}$	$\overline{X}_i$
Γ^0	1	1	1	1
Γ^1	1	i	-1	$-i$
Γ^2	1	-1	1	-1
Γ^3	1	$-i$	-1	i

Where we will sometimes denote the trivial irrep of $\mathbb{Z}_4$ by 1 instead of Γ^0.

6.1.2 Representations of $D(\overline{D_2})$

The full representation theory of $D(\overline{D_2})$ has been worked out in the literature [de Wild Propitius and Bais (1995)]. We use the notation Π_α^A, where A is a class and α the representation of its centralizer.

Vacuum sector

The vacuum sector consists of the trivial group element e, paired with the trivial irrep 1 of the full group $\overline{D_2}$:

$$\{\Pi_1^e\} \tag{6.1}$$

Pure charges

The pure charges in the theory are found by pairing the trivial flux e with any of the irreps of the full group:

$$\{\Pi_{J_1}^e, \Pi_{J_2}^e, \Pi_{J_3}^e, \Pi_\chi^e\} \tag{6.2}$$

Pure fluxes

The pure fluxes are given by pairing any one of the classes with the trivial irrep:

$$\{\Pi_1^{\overline{e}}, \Pi_1^{X_1}, \Pi_1^{X_2}, \Pi_1^{X_3}\} \tag{6.3}$$

Dyons

The dyons of $D(\overline{D_2})$ fall into two classes: those carrying $[\overline{e}]$ flux, which carry irreps of the full group as electric charge, and those carrying $[X_i]$ flux and $\mathbb{Z}_4$ charge:

$$\{\Pi^{\overline{e}}_{J_1}, \Pi^{\overline{e}}_{J_2}, \Pi^{\overline{e}}_{J_3}, \Pi^{\overline{e}}_{\chi}\} \tag{6.4}$$

$$\{\Pi^{X_1}_{\Gamma^1}, \Pi^{X_1}_{\Gamma^2}, \Pi^{X_1}_{\Gamma^3}, \Pi^{X_2}_{\Gamma^1}, \Pi^{X_2}_{\Gamma^2}, \Pi^{X_2}_{\Gamma^3}, \Pi^{X_3}_{\Gamma^1}, \Pi^{X_3}_{\Gamma^2}, \Pi^{X_3}_{\Gamma^3}\} \tag{6.5}$$

All in all thus, there are 21 sectors: the vacuum, four charges, four fluxes and thirteen dyons.

6.1.3 Fusion rules

The fusion rules between the different sectors have also been worked out previously [de Wild Propitius and Bais (1995)]. We restate their results, which we require to analyze the symmetry breaking. The fusion rules between electric sectors is given by the representation ring of the group $\overline{D_2}$

$$\Pi^{e}_{J_i} \times \Pi^{e}_{J_i} = \Pi^{e}_{1}, \qquad \Pi^{e}_{J_i} \times \Pi^{e}_{J_j} = \Pi^{e}_{J_k} \tag{6.6}$$

$$\Pi^{e}_{J_i} \times \Pi^{e}_{\chi} = \Pi^{e}_{\chi}, \qquad \Pi^{e}_{\chi} \times \Pi^{e}_{\chi} = \Pi^{e}_{1} + \sum_i \Pi^{e}_{J_i} \tag{6.7}$$

Where i, j, k range from 1 to 3 and $i \neq j$, $i \neq k$, $j \neq k$. The dyons with $[\overline{e}]$ flux are obtained by pairing the flux with any of the electric charges:

$$\Pi^{e}_{J_i} \times \Pi^{\overline{e}}_{1} = \Pi^{\overline{e}}_{J_i} \qquad \Pi^{e}_{\chi} \times \Pi^{\overline{e}}_{1} = \Pi^{\overline{e}}_{\chi} \tag{6.8}$$

The remaining dyons in the spectrum are constructed as follows

$$\Pi^{e}_{J_i} \times \Pi^{X_i}_{\Gamma^0} = \Pi^{X_i}_{\Gamma^0}, \qquad \Pi^{e}_{J_j} \times \Pi^{X_i}_{\Gamma^0} = \Pi^{X_i}_{\Gamma^2}, \qquad \Pi^{e}_{\chi} \times \Pi^{X_i}_{\Gamma^0} = \Pi^{X_i}_{\Gamma^1} + \Pi^{X_i}_{\Gamma^3} \tag{6.9}$$

We have now constructed all 21 sectors of the spectrum. The remaining set of fusion rules is

$$\Pi^{\overline{e}}_{1} \times \Pi^{\overline{e}}_{1} = \Pi^{e}_{1}, \qquad \Pi^{\overline{e}}_{1} \times \Pi^{X_i}_{\Gamma^{0,2}} = \Pi^{X_i}_{\Gamma^{0,2}}, \qquad \Pi^{\overline{e}}_{1} \times \Pi^{X_i}_{\Gamma^{1,3}} = \Pi^{X_i}_{\Gamma^{3,1}} \tag{6.10}$$

$$\Pi^{e}_{J_i} \times \Pi^{X_i}_{\Gamma^{1,3}} = \Pi^{X_i}_{\Gamma^{1,3}}, \qquad \Pi^{e}_{J_j} \times \Pi^{X_i}_{\Gamma^{1,3}} = \Pi^{X_i}_{\Gamma^{3,1}}, \qquad \Pi^{e}_{\chi} \times \Pi^{X_i}_{\Gamma^{1,3}} = \Pi^{X_i}_{\Gamma^0} + \Pi^{X_i}_{\Gamma^0} \tag{6.11}$$

$$\begin{aligned}
\Pi^{X_i}_{\Gamma^{0,2}} \times \Pi^{X_i}_{\Gamma^{0,2}} &= \Pi^{e}_{1} + \Pi^{\overline{e}}_{1} + \Pi^{e}_{J_i} + \Pi^{\overline{e}}_{J_i} && (6.12)\\
\Pi^{X_i}_{\Gamma^{0,2}} \times \Pi^{X_j}_{\Gamma^{0,2}} &= \Pi^{X_k}_{\Gamma^0} + \Pi^{X_k}_{\Gamma^2} && (6.13)\\
\Pi^{X_i}_{\Gamma^{0,2}} \times \Pi^{X_i}_{\Gamma^{1,3}} &= \Pi^{e}_{\chi} + \Pi^{\overline{e}}_{\chi} && (6.14)\\
\Pi^{X_i}_{\Gamma^{0,2}} \times \Pi^{X_j}_{\Gamma^{1,3}} &= \Pi^{X_k}_{\Gamma^1} + \Pi^{X_k}_{\Gamma^3} && (6.15)\\
\Pi^{X_i}_{\Gamma^{1,3}} \times \Pi^{X_i}_{\Gamma^{1,3}} &= \Pi^{e}_{1} + \Pi^{e}_{J_i} + \Pi^{\overline{e}}_{J_j} + \Pi^{\overline{e}}_{J_k} && (6.16)\\
\Pi^{X_i}_{\Gamma^{1,3}} \times \Pi^{X_j}_{\Gamma^{1,3}} &= \Pi^{X_k}_{\Gamma^0} + \Pi^{X_k}_{\Gamma^2} && (6.17)
\end{aligned}$$

6.2 Breaking: quantum double analysis using representations

In this section we work out the effect of gauge invariant magnetic condensates in the $\overline{D_2}$ gauge theory. We have chosen the magnetic sector since these condensates are realizable on the lattice using a pure gauge action. Here we will approach the problem using the quantum double formulation, and later we will compare this to lattice results.

First we will explicitly work out the breaking using the representation-theoretic approach [Bais and Slingerland (2007)]. The results will turn out to be equivalent to the algebraic approach [Bais et al. (2003)], of which we will just give the conclusions.

6.2.1 Condensation of $\Pi_1^{\overline{e}}$

First we will discuss the situation where the $\Pi_1^{\overline{e}}$ sector is condensed. This representation is one dimensional, so identification with the vacuum sector of the broken theory can be performed without requiring branching of representations:

$$\Pi_1^{\overline{e}} \to \Pi_1^e \tag{6.18}$$

Since the $[\overline{e}]$ were formed by fusing pure charges with pure $[\overline{e}]$ fluxes, see equation (6.8), these dyons become pure charges in the broken theory:

$$\Pi_\alpha^{\overline{e}} \to \Pi_\alpha^e \tag{6.19}$$

For all irreps α. Equation (6.10) shows that the in the broken theory, the two odd $\mathbb{Z}_4$ charges carried by some of the dyons, become indistinguishable. Together with equation (6.14), the identification becomes

$$\Pi_{\Gamma^1}^{X_i}, \Pi_{\Gamma^3}^{X_i} \to \Pi_\chi^{X_i} \tag{6.20}$$

From the above step we can see that the $[X_i]$ fluxes in the broken phase need to be abelian, since we require the dimensionalities of the representations to be equal on both sides of the arrow. The dyonic excitations can thus carry irreps of the full group.

Equation (6.12) shows that fusing two identical $[X_i]$ dyons with even $\mathbb{Z}_4$ charge can decay into the vacuum of the broken theory in two different ways, since we have made the identification (6.18). This is an undesirable situation, so we require these dyons to branch into multiple sectors in the new vacuum. To be consistent with equation (6.9), the correct identification is the following:

$$\Pi_{\Gamma^0}^{X_i} \quad \to \quad \Pi_1^{X_i} + \Pi_{J_i}^{X_i} \tag{6.21}$$

$$\Pi_{\Gamma^2}^{X_i} \quad \to \quad \Pi_{J_j}^{X_i} + \Pi_{J_k}^{X_i} \tag{6.22}$$

With the above identifications, the fusion rules are consistent. The spectrum of the broken phase (including confined excitations) is

$$\{\Pi_1^e, \Pi_{J_i}^e, \Pi_\chi^e, \Pi_1^{X_i}, \Pi_{J_j}^{X_i}, \Pi_\chi^{X_i}\} \tag{6.23}$$

Without the constraint $i \neq j$. The electric sectors Π_α^e fuse as before

$$\Pi_{J_i}^e \times \Pi_{J_i}^e = \Pi_1^e, \qquad \Pi_{J_i}^e \times \Pi_{J_j}^e = \Pi_{J_k}^e \tag{6.24}$$

$$\Pi_{J_i}^e \times \Pi_\chi^e = \Pi_\chi^e, \qquad \Pi_\chi^e \times \Pi_\chi^e = \Pi_1^e + \sum_i \Pi_{J_i}^e \tag{6.25}$$

The magnetic sectors $\Pi_1^{X_i}$ have become one dimensional and obey the relations

$$\Pi_1^{X_i} \times \Pi_1^{X_i} = \Pi_1^e, \qquad \Pi_1^{X_i} \times \Pi_1^{X_j} = \Pi_1^{X_k} \tag{6.26}$$

And the dyons are created according to the following rule

$$\Pi_1^{X_i} \times \Pi_\alpha^e = \Pi_\alpha^{X_i} \tag{6.27}$$

For $\alpha = 1, J_1, J_2, J_3, \chi$.

These expressions and their combinations give the full set of fusion rules. We still have to determine the effective unconfined theory. For an excitation in the broken phase to be unconfined, all of its "parent" sectors appearing on the left hand side of the identifications have to braid trivially with the condensed sector $\Pi_1^{\overline{e}}$.

The Π_χ^e sector of the unbroken phase braids nontrivially with $\Pi_1^{\overline{e}}$, which can be read off in table 6.1. We therefore find the sectors of the broken theory carrying χ electric charge to be confined. The unconfined set of sectors is then

$$\{\Pi_1^e, \Pi_{J_i}^e, \Pi_1^{X_i}, \Pi_{J_j}^{X_i}\} \tag{6.28}$$

Where here $i \neq j$ is not implied. This leaves 16 sectors: three pure charges, three pure fluxes and nine dyons. We can see that the fusion algebra of these sectors closes on itself.

The last step is the identification of the group $\tilde{H}$, of which (6.28) is the set of irreducible representations of $D(\tilde{H})$. This group can be found relatively straightforward in this case.

We search for an abelian group, since all irreps in (6.28) are one dimensional. The number of elements needs to be four, since we have four classes and irreps. Furthermore, all elements are selfconjugate and multiplying two nontrivial elements give the third nontrivial element. The group that has all of these properties is $\mathbb{Z}_2 \times \mathbb{Z}_2$. We therefore conclude that the effective unconfined theory is described by the symmetry algebra $D(\mathbb{Z}_2 \times \mathbb{Z}_2)$.

6.2.2 Condensation of $\Pi_{\Gamma^0}^{X_i}$

There are three additional broken phases, corresponding to condensation of the $\Pi_{\Gamma^0}^{X_i}$ sectors. Since their role in the group is so similar, these three cases are equivalent to each other, and we will study only the condensation of $\Pi_{\Gamma^0}^{X_1}$.

Since this quantum double irrep is two dimensional it cannot directly be identified with the vacuum: it will branch into the vacuum plus some as yet unknown onedimensional irrep

$$\Pi_{\Gamma^0}^{X_1} \to \Pi_1^e + \Pi_\alpha^A \tag{6.29}$$

Equation (6.9) immediately prescribes this unknown irrep

$$\Pi_{\Gamma^0}^{X_1} \to \Pi_1^e + \Pi_{J_1}^e \tag{6.30}$$

The second identity in equation (6.10) leads to the identification

$$\Pi_\alpha^{\overline{e}} \to \Pi_\alpha^e \tag{6.31}$$

This relation, which is equivalent to the condensation of $\Pi_1^{\overline{e}}$ discussed previously, in addition with equation (6.13) leads to the following set of identifications

$$\Pi_{\Gamma^2}^{X_1} \rightarrow \Pi_{J_2}^e + \Pi_{J_3}^e \tag{6.32}$$
$$\Pi_{\Gamma^0}^{X_2} \rightarrow \Pi_1^X + \Pi_{J_1}^X \tag{6.33}$$
$$\Pi_{\Gamma^2}^{X_2} \rightarrow \Pi_{J_2}^X + \Pi_{J_3}^X \tag{6.34}$$
$$\Pi_{\Gamma^0}^{X_3} \rightarrow \Pi_1^X + \Pi_{J_1}^X \tag{6.35}$$
$$\Pi_{\Gamma^2}^{X_3} \rightarrow \Pi_{J_2}^X + \Pi_{J_3}^X \tag{6.36}$$

Where we have introduced the central flux $[X]$ for the broken phase. This prescribes the identifications of the dyons carrying even $\mathbb{Z}_4$ charge. The oddly charged dyons have their behaviour fixed by equation (6.14), leading to the identifications

$$\Pi_{\Gamma^1}^{X_1}, \Pi_{\Gamma^3}^{X_1} \rightarrow \Pi_\chi^e \tag{6.37}$$
$$\Pi_{\Gamma^1}^{X_2}, \Pi_{\Gamma^3}^{X_2}, \Pi_{\Gamma^1}^{X_3}, \Pi_{\Gamma^3}^{X_3} \rightarrow \Pi_\chi^X \tag{6.38}$$

The spectrum of excitations, unconfined and confined, in the broken phase is thus given by

$$\{\Pi_1^e, \Pi_{J_i}^e, \Pi_\chi^e, \Pi_1^X, \Pi_{J_i}^X, \Pi_\chi^X\} \tag{6.39}$$

Where the electric sectors obey the same fusion algebra as in the unbroken phase

$$\Pi_{J_i}^e \times \Pi_{J_i}^e = \Pi_1^e, \qquad \Pi_{J_i}^e \times \Pi_{J_j}^e = \Pi_{J_k}^e \tag{6.40}$$

$$\Pi_{J_i}^e \times \Pi_\chi^e = \Pi_\chi^e, \qquad \Pi_\chi^e \times \Pi_\chi^e = \Pi_1^e + \sum_i \Pi_{J_i}^e \tag{6.41}$$

And the fusion rules for magnetic and dyonic sectors are fixed by the following relations

$$\Pi_1^X \times \Pi_1^X = \Pi_1^e, \qquad \Pi_\alpha^e \times \Pi_1^X = \Pi_\alpha^X \tag{6.42}$$

The trivial braiding condition reduces the set (6.39) to the spectrum of unconfined sectors. All nontrivial pure charges, except $\Pi_{J_1}^e$, braid nontrivially with the condensed sector $\Pi_{\Gamma^0}^{X_1}$, as we can read off from the character table 6.1. This leaves the following unconfined spectrum

$$\{\Pi_1^e, \Pi_{J_1}^e, \Pi_1^X, \Pi_{J_1}^X\} \tag{6.43}$$

Again we see that the fusion algebra of these sectors closes. There are four sectors left, the vacuum, a charge, a flux and a dyon. All of these are selfconjugate. This fixes the group describing the effective unconfined theory to $\mathbb{Z}_2$.

6.3 Breaking: quantum double analysis using the algebra

From the algebraic approach to quantum double symmetry breaking, a general result exists for the case of gauge invariant magnetic condensates [Bais et al. (2003)]. In the case of a condensed Π_1^A sector in a H gauge theory, the unconfined symmetry algebra is found as follows. First one has to work out the set of elements of H that is generated by the elements of A. This set K is a normal subgroup. The unconfined symmetry algebra is then given by $D(H/K)$.

6.3.1 Condensation of $\Pi_1^{\overline{e}}$

The group K generated by the class $[\overline{e}]$ is isomorphic to $\mathbb{Z}_2$. Therefore the unconfined symmetry algebra is given by $D(\overline{D_2}/\mathbb{Z}_2)$. The most straightforward way to calculate this factor group is by writing each element of $\overline{D_2}$ up to a factor of $\overline{e}$. This leads to the following identifications between elements of $\overline{D_2}$ and $\overline{D_2}/\mathbb{Z}_2$

$$e, \overline{e} \rightarrow e \tag{6.44}$$
$$X_1, \overline{X}_1 \rightarrow X_1 \tag{6.45}$$
$$X_2, \overline{X}_2 \rightarrow X_2 \tag{6.46}$$
$$X_3, \overline{X}_3 \rightarrow X_3 \tag{6.47}$$

The relations obeyed by the elements of the factor group is identical to the group structure of the group $\mathbb{Z}_2 \times \mathbb{Z}_2$. We therefore conclude that the unconfined symmetry algebra is given by $D(\mathbb{Z}_2 \times \mathbb{Z}_2)$, which is equivalent to the result we obtained by using the representation approach to symmetry breaking.

6.3.2 Condensation of $\Pi_{\Gamma^0}^{X_i}$

Let us again consider the case where $\Pi_{\Gamma^0}^{X_1}$ is condensed. The class $[X_1]$ generates a $\mathbb{Z}_4$ group K

$$K = \{e, \overline{e}, X_1, \overline{X}_1\} \tag{6.48}$$

By writing every element of $\overline{D_2}$ up to factors in K, we have only two elements left, a nontrivial element X and the group unit e

$$e, \overline{e}, X_1, \overline{X}_1 \rightarrow e \tag{6.49}$$
$$X_2, \overline{X}_2, X_3, \overline{X}_3 \rightarrow X \tag{6.50}$$

These elements obey the group structure of $\mathbb{Z}_2$. The unconfined symmetry algebra is therefore $D(\mathbb{Z}_2)$, equivalent to what we found using the representations to break the symmetry.

6.3.3 Summary

Here we recapitulate the results we have found before using both the representation and algebraic view.

Table 6.4: Gauge invariant magnetic condensates in the $\overline{D_2}$ theory

Condensed sector	K	Unconfined algebra
$\Pi_1^{\overline{e}}$	$\mathbb{Z}_2$	$D(\mathbb{Z}_2 \times \mathbb{Z}_2)$
$\Pi_1^{X_1}$	$\mathbb{Z}_4$	$D(\mathbb{Z}_2)$
$\Pi_1^{X_2}$	$\mathbb{Z}_4$	$D(\mathbb{Z}_2)$
$\Pi_1^{X_3}$	$\mathbb{Z}_4$	$D(\mathbb{Z}_2)$

6.4 Lattice formulation

We now proceed to the lattice formulation of $\overline{D_2}$ gauge theory. We will first write down the most general action for this theory, and write down the linear combinations of characters that realize the delta functions on classes. Then we make explicit the map Θ which maps elements of $\overline{D_2}$ to the $\mathbb{Z}_4$ centralizer group of the $[X_i]$ classes.

6.4.1 Actions

The most general action in the representation basis is the following:

$$\begin{aligned} S_{\text{gauge}} &= -\beta_{J_1}\chi_{J_1}(U_p) \\ &+ -\beta_{J_2}\chi_{J_2}(U_p) \\ &+ -\beta_{J_3}\chi_{J_3}(U_p) \\ &+ -\beta_{\chi}\chi_{\chi}(U_p) \end{aligned} \tag{6.51}$$

As has been stressed earlier, the phase diagram becomes more transparent by transforming this action to one containing delta functions on classes, with one coupling for each class. This can be done by applying formula (5.35), and leads to the linear combinations of characters given in table 6.5.

Table 6.5: Class actions for $\overline{D_2}$ in terms of the characters

Class A	Action S
$[e]$	$-\frac{1}{8}\left(1+\chi_{J_1}(U_p)+\chi_{J_2}(U_p)+\chi_{J_3}(U_p)+2\chi_{\chi}(U_p)\right)$
$[\overline{e}]$	$-\frac{1}{8}\left(1+\chi_{J_1}(U_p)+\chi_{J_2}(U_p)+\chi_{J_3}(U_p)-2\chi_{\chi}(U_p)\right)$
$[X_1]$	$-\frac{1}{4}\left(1+\chi_{J_1}(U_p)-\chi_{J_2}(U_p)-\chi_{J_3}(U_p)\right)$
$[X_2]$	$-\frac{1}{4}\left(1-\chi_{J_1}(U_p)+\chi_{J_2}(U_p)-\chi_{J_3}(U_p)\right)$
$[X_3]$	$-\frac{1}{4}\left(1-\chi_{J_1}(U_p)-\chi_{J_2}(U_p)+\chi_{J_3}(U_p)\right)$

This leads to the following most general action in the class basis

$$\begin{aligned} S &= -\beta_{[e]}\delta_{[e]}(U_p) \\ &+ -\beta_{[\overline{e}]}\delta_{[\overline{e}]}(U_p) \\ &+ -\beta_{[X_1]}\delta_{[X_1]}(U_p) \\ &+ -\beta_{[X_2]}\delta_{[X_1]}(U_p) \\ &+ -\beta_{[X_3]}\delta_{[X_1]}(U_p) \end{aligned} \tag{6.52}$$

Which will be the action we will use in the following sections.

6.4.2 The map Θ required for the dyonic operators

To make the dyonic operators (5.51) for the theory explicit, we need to construct the map Θ defined in equation (4.32). We will give the full map in the case of a flux in the class $[X_1]$. In this class, there are two possibilities for ${}^{[X_1]}h_i$: either X_1 or $\overline{X}_1$. We label the class by picking X_1 as the ${}^{[X_1]}h_1$ element, and X_2 as the ${}^{[X_1]}x_2$ element. Now we can construct the table 6.6 for the map Θ.

Table 6.6: The map Θ for the entire group $\overline{D_2}$, with flux in $[X_1]$

${}^{[X_1]}h_i$	${}^{[X_1]}x_i$	g	${}^{[X_1]}h_k$	${}^{[X_1]}x_k$	$\tilde{g}$
X_1	e	e	X_1	e	e
X_1	e	$\overline{e}$	X_1	e	$\overline{e}$
X_1	e	X_1	X_1	e	X_1
X_1	e	$\overline{X}_1$	X_1	e	$\overline{X}_1$
X_1	e	X_2	$\overline{X}_1$	X_2	e
X_1	e	$\overline{X}_2$	$\overline{X}_1$	X_2	$\overline{e}$
X_1	e	X_3	$\overline{X}_1$	X_2	X_1
X_1	e	$\overline{X}_3$	$\overline{X}_1$	X_2	$\overline{X}_1$
$\overline{X}_1$	X_2	e	$\overline{X}_1$	X_2	e
$\overline{X}_1$	X_2	$\overline{e}$	$\overline{X}_1$	X_2	$\overline{e}$
$\overline{X}_1$	X_2	X_1	$\overline{X}_1$	X_2	$\overline{X}_1$
$\overline{X}_1$	X_2	$\overline{X}_1$	$\overline{X}_1$	X_2	X_1
$\overline{X}_1$	X_2	X_2	X_1	e	$\overline{e}$
$\overline{X}_1$	X_2	$\overline{X}_2$	X_1	e	e
$\overline{X}_1$	X_2	X_3	X_1	e	$\overline{X}_1$
$\overline{X}_1$	X_2	$\overline{X}_3$	X_1	e	X_1

6.5 Breaking: lattice analysis

In this section we present the results of putting the $\overline{D_2}$ gauge theory on the lattice. We have studied the behaviour of the operators defined previously in different regions of the phase diagram. We were able to identify the phases corresponding to condensation of the $\Pi_1^{\overline{e}}$ and $\Pi_{\Gamma^0}^{X_i}$ irreps of the quantum double $D(\overline{D_2})$.

We have studied the behaviour of the Wilson, 't Hooft and dyonic loops in these broken phases. We have found it possible to determine whether different sectors were confined or unconfined. We have however not yet found a method to study the branching of a sector of the unbroken theory into multiple sectors of the broken theory.

We still do not fully understand this process in the language of the lattice. Most likely one will have to calculate expectation values of multiple linked operators. For example, in the $[\overline{e}]$ condensate, the pure $[X_1]$ flux decays into a pure flux plus a dyon:

$$\Pi_{\Gamma^0}^{X_1} \to \Pi_1^{X_1} + \Pi_{J_1}^{X_1} \tag{6.53}$$

To be able to detect this J_1 charge, we would have to first introduce the operator $H^{X_1}(\Sigma^*)$ in the $[\overline{e}]$ vacuum, and then a second 't Hooft operator $H^A(\Xi^*)$ for a loop Ξ^* linked with the loop Σ^*. If we then calculate the expectation value

$$\frac{< H^{X_1}(\Sigma^*) H^A(\Xi^*) >}{< H^{X_1}(\Sigma^*) >< H^A(\Xi^*) >} \tag{6.54}$$

Then we expect this to have the value $\chi_{J_1}(A)$, since a J_1 charge encircles a A flux once, thus allowing the charge to be determined by probing with all fluxes A.

We were however not able to perform these measurements, due to lack of computing power. Below we do present the behaviour of the operators corresponding to the excitations of the unbroken phase in the different phases of the theory.

6.5.1 Phase diagram

We present two different cross sections of the large phase space of the $\overline{D_2}$ theory. First we will discuss the phase diagram in figure 6.1, which contains the realizations of the trivial phase and the $[\overline{e}]$ condensed phase. After this we will discuss the diagram in figure 6.2, which realizes the $[X_1]$ condensate.

The diagrams have been produced by sweeping across sections in phase space in our Monte Carlo simulation. At each point the behaviour of the 't Hooft operator has been probed to check whether some flux might have condensed. Monte Carlo measurements were done on a 6^3 lattice.

Trivial phase and $[\overline{e}]$ condensate

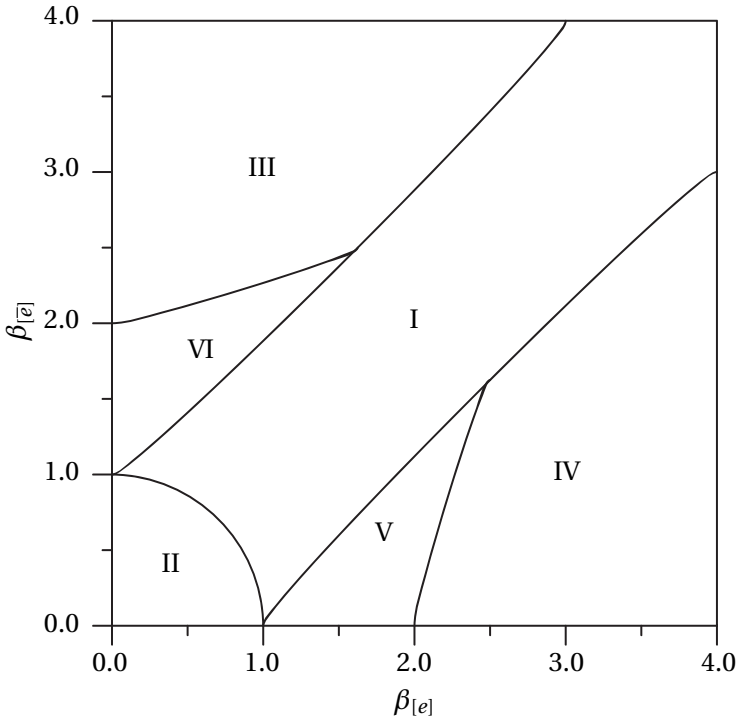

Figure 6.1: Cross section of the phase diagram of $\overline{D_2}$ gauge theory. The plane is chosen such that the horizontal axis represents $\beta_{[e]} = 0...4$ and the vertical axis represents $\beta_{[\overline{e}]} = 0...4$. All other couplings are zero. The regions I to VI are discussed in the text.

In figure 6.1 we have denoted six different regions. We will discuss them one by one.

I. The $[\overline{e}]$ condensed phase. Here the 't Hooft operator for the $[\overline{e}]$ fluxes obtains expectation value 1, regardless of size. Further aspects of this phase are discussed further on in the text, but they seem to coincide with the quantum double analysis presented earlier.

II. The strongly coupled phase. Here all the 't Hooft operators obtain expectation value 1 independent of their size, so all fluxes seem to condense.

III. In this region a configuration is realized in which all plaquettes are $[\overline{e}]$ valued. The Wilson loop operator for the χ charge in this region flips sign as a function of area, which is to be expected since it encloses either an odd or an even number of $[\overline{e}]$ fluxes, depending on whether the area is an odd or even number. Behaviour like this is not found in the literature to our knowledge, but seems reminiscent of the antiferromagnet known from condensed matter theory. We could define gauge-invariant probing operators for this phase, for example a Wilson loop with a $(-1)^A$ in front of it. This operator would behave nicely, and is still gauge invariant.

IV. The trivial phase. All 't Hooft operators have perimeter law behaviour, and there is no electric confinement.

V. Transition region between the different neighbouring phases. The 't Hooft operators have very unstable behaviour, and seem to blow up as their sizes get larger. We regard this region as an artifact of the finite lattice size.

VI. Same as V.

$[X_1]$ condensate

Now we will discuss the different regions in figure 6.2.

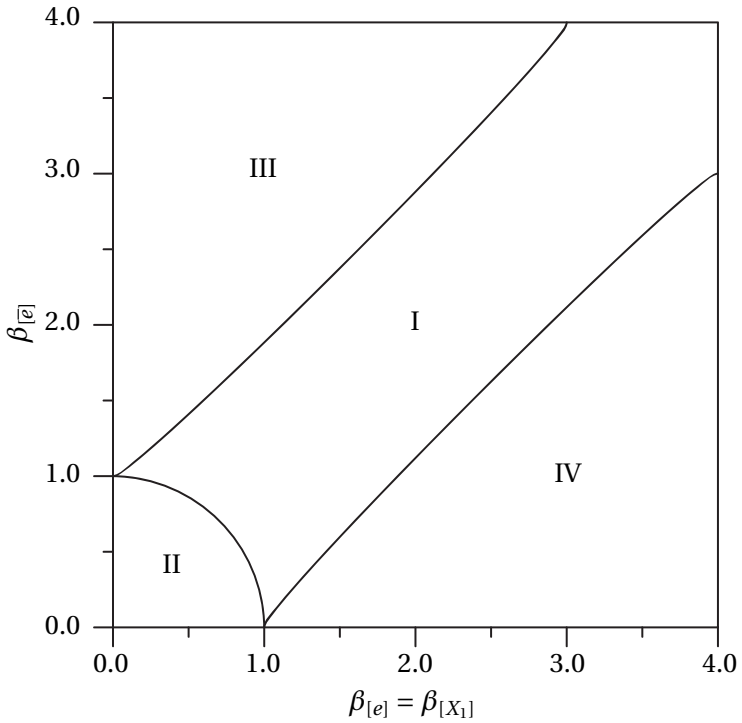

Figure 6.2: Cross section of the phase diagram of $\overline{D_2}$ gauge theory. The plane is chosen in such a way that the horizontal axis represents $\beta_{[e]} = \beta_{[X_1]} = 0...4$ and the vertical axis represents $\beta_{[\overline{e}]} = 0...4$. The other couplings are set to zero. The regions I to IV are discussed in the text

I. The $[X_1]$ condensed phase. The 't Hooft operator for the $[X_1]$ class gets expectation value 1 regardless of size. This phase is described further on in this chapter.

II. Strongly coupled phase for the $\overline{D_2}$ theory. All 't Hooft operators, regardless of loop size, have expectation value 1.

III. All plaquettes are valued $\overline{e}$, and the same remarks given earlier apply.

IV. The 't Hooft operator for the $[X_1]$ flux would indicate an $[X_1]$ condensate, but the Wilson loops also flip sign here.

6.5.2 No condensate

The situation with no condensed magnetic degrees of freedom is both the easiest to realize and to understand conceptually. We expect that the most dominant contributions to the path integral to come from the configurations where all of the plaquettes are the group unit, except for small flux-antiflux pairs that pop in and out of existence.

The action that realizes the trivial vacuum is the one where all of the couplings in (6.52) are zero, except $\beta_{[e]}$:

$$S = -\beta_{[e]}\delta_{[e]}(U_p) \tag{6.55}$$

If $\beta_{[e]}$ becomes larger than approximately 1.0, the trivial vacuum is realized. What do we expect from what we know from the quantum double analysis? Since the full symmetry algebra is realized, all electric and all magnetic degrees of freedom should be free. In the lattice gauge theory setting, this means that all of our Wilson loops and all of our 't Hooft loops should decay according to a perimeter law.

Wilson loops

Since the dominant configuration in the path integral is the one where all the links are the group unit (modulo gauge transformations), we can perform a weak coupling expansion around this configuration. Just for clarity, let us repeat that the expression for a Wilson loop in irrep α around a loop Ω of length L is:

$$< W_\alpha(\Omega) >= \frac{1}{Z}\int \prod_{ij} dU_{ij} \prod_p e^{-S(U_p)} \chi_\alpha(U_\Omega) = \frac{\int \prod_{ij} dU_{ij} \prod_p e^{-S(U_p)} \chi_\alpha(U_\Omega)}{\int \prod_{(ij)} dU_{ij} \prod_p e^{-S(U_p)}} \tag{6.56}$$

Where U_Ω is the ordered product of link variables around the loop Ω.

Let us first work out the denominator, since this is equal for all irreps. The dominant contribution comes from the configuration where all plaquettes are unity. Up to gauge transformations, this configuration is realized by letting all the links be unity, so this contribution is $e^{\beta_{[e]}N}$ since we have N plaquettes.

Now consider the first order quantum correction to this. If we make one link different from unity, this changes the flux on four plaquettes. On these plaquettes the Boltzmann factor changes to 1. We can change the link to seven different values since we have a group of order eight, and we can pick the link we want to change in N different ways.

Taking this into account we obtain to first order:

$$Z = e^{\beta_{[e]}N} + 7Ne^{\beta_{[e]}(N-4)} = e^{\beta_{[e]}N}\left(1 + 7Ne^{-4\beta[e]}\right) \tag{6.57}$$

Now let us work out the numerator for the J_i irreps. The result turns out to be the same for all three of them, but let us pick J_1 just to be concrete. In the dominant configuration, all of the links on Ω will be unity, so the character of U_Ω will equal 1. The leading order term in the numerator is therefore $e^{\beta_{[e]}N}$.

Let us include the first quantum corrections. Again we consider changing one link, but we need to treat the links on Ω differently from the links off Ω, since this will change the value of the ordered product U_Ω, and will thus alter the value of the Wilson loop. First let us change a link on Ω. Clearly this will change the flux on four plaquettes, and there are L different places to put it. Again we can change the link to seven different values, but now some carefulness is required. If we change the link value to $\overline{e}$, X_1 or $\overline{X}_1$, the Wilson loop is unchanged, which can be read off from the character table 6.1. On the other hand, for the four other X_i group elements the Wilson loop value becomes -1. All in all these corrections sum up to $-Le^{\beta_{[e]}(N-4)}$. Finally, we must consider changing a link off the Wilson loop. This can be done on seven different ways, at $N-L$ locations. In all these instances the character of U_Ω equals 1.

Summing the contributions of the numerator, we obtain the following expression for the expectation value of the Wilson loop:

$$\begin{aligned} < W_{J_1}(\Omega) > &= \frac{e^{\beta_{[e]}N} - Le^{\beta_{[e]}(N-4)} + 7(N-L)e^{\beta_{[e]}(N-4)}}{e^{\beta_{[e]}N} + 7Ne^{\beta_{[e]}(N-4)}} && (6.58)\\ &= \frac{1+7Ne^{-4\beta_{[e]}} - 8Le^{-4\beta_{[e]}}}{1+7Ne^{-4\beta_{[e]}}} && (6.59)\\ &\approx 1 - 8Le^{-4\beta_{[e]}} && (6.60) \end{aligned}$$

Where the expressions for the irreps J_2 and J_3 are completely identical.

To calculate the expectation value for the χ irrep, we repeat the above procedure. The contribution from the configuration where all links are unity equals $2e^{\beta_{[e]}N}$, since χ is a two-dimensional irrep. Changing one link off Ω, we obtain a term equalling $14(N-L)e^{\beta_{[e]}(N-4)}$, just as in the J_i case. Changing a link on Ω to one of the X_i gives a Wilson loop equalling zero, and changing a link to $\overline{e}$ gives a contribution $-2Le^{\beta_{[e]}(N-4)}$. At the end of the day, we obtain the following expression, which turns out to be twice (6.58):

$$\begin{aligned} < W_\chi(Q) > &= \frac{2e^{\beta_{[e]}N} - 2Le^{\beta_{[e]}(N-4)} + 27(N-L)e^{\beta_{[e]}(N-4)}}{e^{\beta_{[e]}N} + 7Ne^{\beta_{[e]}(N-4)}} && (6.61)\\ &= 2\frac{1+7Ne^{-4\beta_{[e]}} - 8Le^{-4\beta_{[e]}}}{1+7Ne^{-4\beta_{[e]}}} && (6.62)\\ &\approx 2 - 16Le^{-4\beta_{[e]}} && (6.63) \end{aligned}$$

It can immediately be seen that all of these loops fall off with their perimeters. To illustrate this concretely, we give one graph in figure 6.3, showing the expectation value of the the W_χ loop against its perimeter. As said, all graphs can be found at the end of the chapter. We see that the Monte Carlo data is in excellent agreement with analytical expression (6.61).

't Hooft loops

We will now proceed to the 't Hooft loops in the trivial vacuum. Let us quickly recall the expression (5.48) for an 't Hooft loop inserting flux in class A along a the set of plaquettes $\Sigma*$, forming a closed

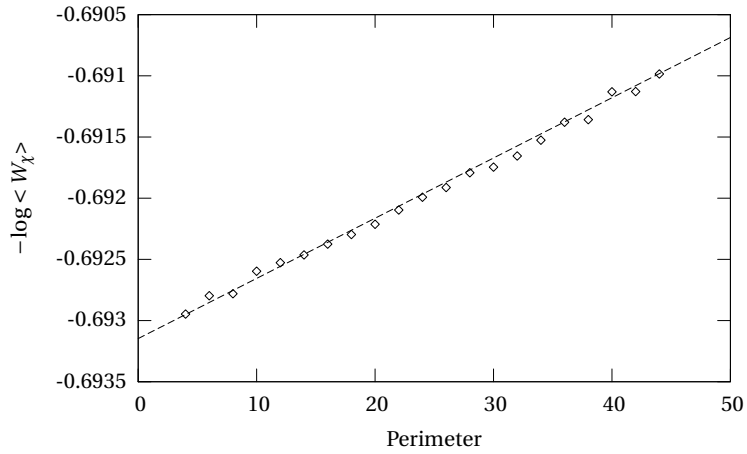

Figure 6.3: Wilson loop behaviour in the trivial vacuum for the χ irrep as a function of perimeter. The Monte Carlo measurements were performed on a $16^2 \times 8$ lattice, $\beta_{[e]} = 3.0$, 10000 sweeps

loop on the dual lattice and piercing a set of plaquettes Σ

$$< H^A(\Sigma*) >= \frac{1}{Z}\int DU \prod_{p\in\mathscr{P}} e^{-S(U_p)} \prod_{p'\in\Sigma*} \frac{1}{|A|}\sum_{g\in A} e^{S(U_{p'})-S(gU_{p'})} \tag{6.64}$$

Although this expression looks quite involved, it is actually quite easily calculated in the trivial vacuum. Even without quantum fluctuations, we already obtain a perimeter law falloff, which turns out to be in excellent agreement with the Monte Carlo measurements. For simplicity we will therefore ignore the quantum fluctuations and use only the first order term.

In the dominant configuration with all links unity, all plaquettes are also unity. If we multiply one of the plaquettes by a nontrivial group element, we change the contribution of that plaquette to the partition sum from $e^{\beta_{[e]}}$ to 1. Therefore, to leading order, the 't Hooft loop expectation value is given by:

$$< H^{[\overline{e}]}(\Sigma*) >=< H^{[X_1]}(\Sigma*) >=< H^{[X_2]}(\Sigma*) >=< H^{[X_3]}(\Sigma*) > = \frac{e^{\beta_{[e]}(N-L)}}{e^{\beta_{[e]}N}} \tag{6.65}$$

$$= e^{-\beta_{[e]}L} \tag{6.66}$$

This seems to be in excellent agreement with the Monte Carlo data we have produced. For illustration, consider figure 6.4.

Dyonic loops

We have not found a way to analytically tackle the problem of calculating the expectation value of the dyonic loops. We were able to perform Monte Carlo simulations for these operators. An illustrative example is given in figures 6.5 and 6.6. The perimeter law behaviour is clearly identifiable, suggesting unconfined excitations.

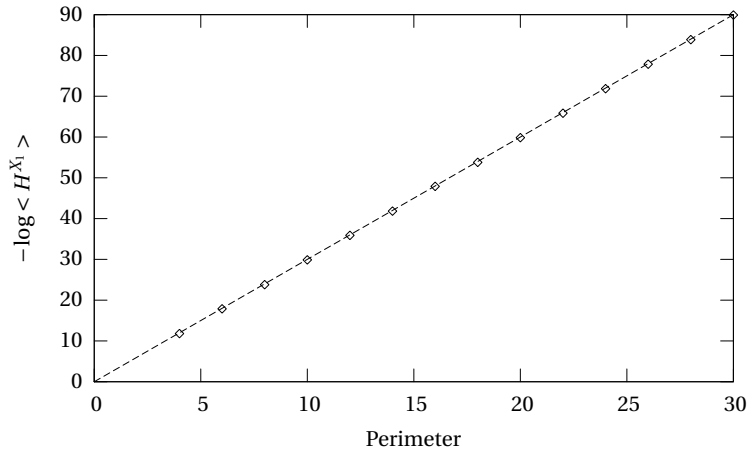

Figure 6.4: 't Hooft loop behaviour in the trivial vacuum for the $[X_1]$ class as a function of perimeter. The Monte Carlo measurements were performed on a $16^2 \times 8$ lattice, $\beta_{[e]} = 3.0$, 1000 sweeps

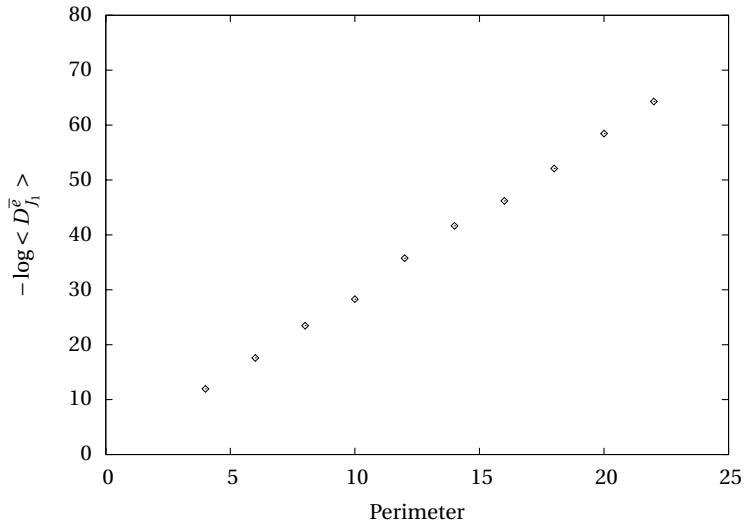

Figure 6.5: Dyonic loop behaviour in the trivial vacuum for the $[\overline{e}]$ flux and J_1 charge as a function of perimeter. The Monte Carlo measurements were performed on a $16^2 \times 8$ lattice, $\beta_{[e]} = 3.0$, 10000 sweeps

Comparison with quantum double analysis

The quantum double analysis predicts that the full symmetry is realized, without any confinement. In our lattice setting, this means that all Wilson and all 't Hooft loops should obey perimeter laws. We have shown both analytically and by Monte Carlo data that this indeed is the case.

6.5.3 $\Pi_1^{\overline{e}}$ condensate

The quantum double analysis tells us that in this phase, the unconfined symmetry algebra is $D(\mathbb{Z}_2 \times \mathbb{Z}_2)$. On the electric side, we expect the three J_i irreps to be free and the χ charge to be confined.

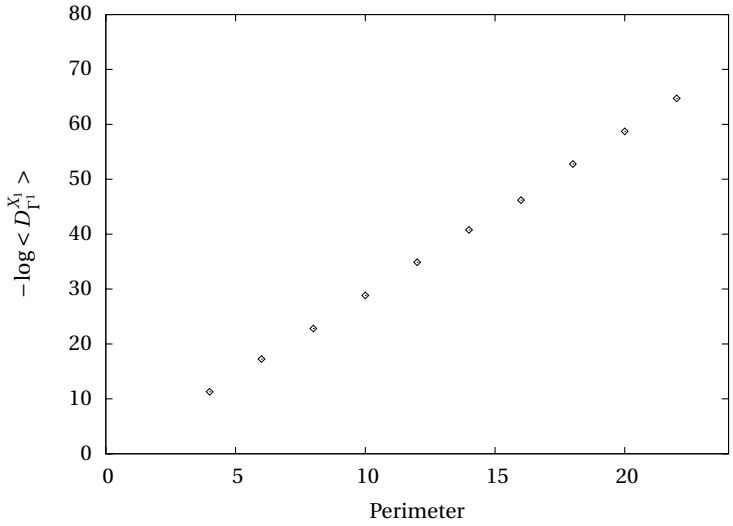

Figure 6.6: Dyonic loop behaviour in the trivial vacuum for the $[X_1]$ flux and Γ^1 charge as a function of perimeter. The Monte Carlo measurements were performed on a $16^2 \times 8$ lattice, $\beta_{[e]} = 3.0$, 10000 sweeps

We expect the three $[X_i]$ fluxes to be the free magnetic excitations. Regarding the dyons, the $[\overline{e}]$ dyons have become pure charges and we also expect their behaviour to be analogous to the pure charge sectors. The dyons carrying $[X_i]$ flux with the even $\mathbb{Z}_4$ representation we expect to be free, whereas the ones carrying odd $\mathbb{Z}_4$ representations will be confined.

The action realizing this condensate is the following, with $\beta_{[e]} \approx \beta_{[\overline{e}]}$:

$$S = -\beta_{[e]}\delta_{[e]}(U_p) - \beta_{[\overline{e}]}\delta_{[\overline{e}]}(U_p) \tag{6.67}$$

Where all other couplings are set to zero.

Wilson loops

Let us start with the irreps that will turn out to be unconfined: the J_i. It is quite clear that we can not naively use the weak coupling perturbation theory used to compute the expressions for the trivial vacuum: a great many configurations contribute to the path integral - this is more or less the essence of a condensed degree of freedom. The configurations that contribute significantly are the ones where, starting from the trivial vacuum, any number of links have been changed to $\overline{e}$, letting closed loops of $[\overline{e}]$ flux run wildly through spacetime.

However, if we pick a special point in the parameter space, life becomes much easier. Let us set $\beta_{[e]}$ exactly equal to $\beta_{[\overline{e}]}$. It is easily seen that this gives our action extra symmetry: there is a local freedom to multiply any one link with the $\overline{e}$ element. This introduces the possibility again to perform perturbation theory, just as in the trivial vacuum.

Introducing this extra symmetry changes the perturbation treatment slightly: since we can can multiply links with $\overline{e}$ at will, we have to identify e and $\overline{e}$, and the X_i and $\overline{X}_i$. The denominator of the Wilson loop expression (6.56) is therefore $e^{\beta_{[e]}N}\left(1+3Ne^{-4\beta_{[e]}}\right)$, since we can only change a given link to three values now. The numerator is also easy once you realize this. All in all we obtain:

$$< W_{J_1}(\Omega) >=< W_{J_2}(\Omega) >=< W_{J_3}(\Omega) > = \frac{1+3Ne^{-4\beta_{[e]}}-6Le^{-4\beta_{[e]}}}{1+3Ne^{-4\beta_{[e]}}} \quad (6.68)$$

$$\approx 1-6Le^{-4\beta_{[e]}} \quad (6.69)$$

This expression, along with Monte Carlo measurements for the J_1 irrep, has been plotted in figure 6.7.

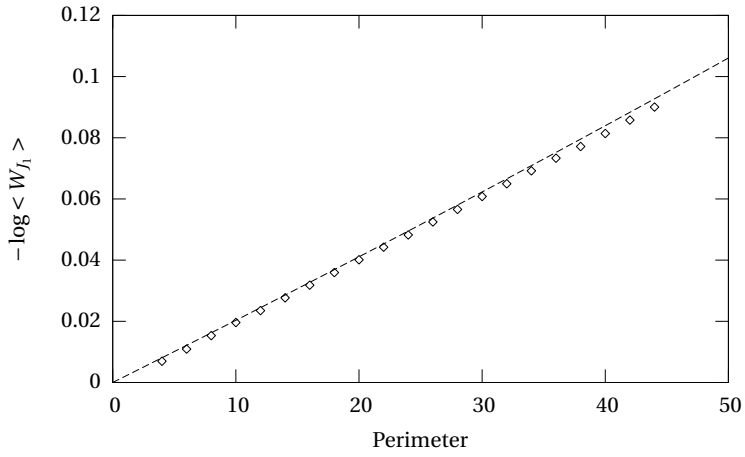

Figure 6.7: Wilson loop behaviour in the $\overline{e}$ condensate of the J_1 irrep as a function of perimeter. The Monte Carlo measurements were performed on a $16^2 \times 8$ lattice, $\beta_{[e]} = \beta_{[\overline{e}]} = 2.0$, 10000 sweeps

As can be seen, the Monte Carlo data and analytic expression back each other up.

Now on to the first example of a confined irrep in our theory. Since the χ charges braid non-trivially with the $[\overline{e}]$ fluxes, we expect the charges to pull a string in the vacuum as we seperate them, leading to linear confinement. This would give an exponential falloff of the expectation value of the Wilson loop of the form e^{-kA}, where k is a constant, and A is the area. This will indeed turn out to be the case.

How do we calculate such a thing analytically? Perturbation theory clearly cannot be used, and the β-parameters are too large to perform a strong coupling expansion. We have not found a general way to calculate this for a general group and general condensate, but for this specific example there is a method.

To arrive here, let us think about what the vacuum looks like again. As has been said before, there are $[\overline{e}]$ loops of all sizes running around. The other excitations present are small flux-antiflux pairs of the $[X_i]$ type. However, the latter are more and more suppressed for larger and larger β. Ignoring them, the configurations that contribute significantly to the path integral are the trivial vacuum and the configurations with any number loops of $[\overline{e}]$ type - of any size.

This is like the strongly coupled vacuum of a $\mathbb{Z}_2$ gauge theory. The plaquette action for such a theory is given by:

$$S = -\gamma\chi(U_p) \quad (6.70)$$

This action, for small but finite γ, is minimized by the trivial vacuum, but in the strongly coupled phase, also the configurations with $[\overline{e}]$ loops of any number and size contribute significantly. We can therefore hope to map the $\overline{D_2}$ problem to an equivalent $\mathbb{Z}_2$ problem.

To perform this mapping, consider the cost of a single $[\overline{e}]$ flux in both theories. In the original theory, assuming that $\beta_{[e]} > \beta_{[\overline{e}]}$, the cost in action of a flux on a single plaquette equals $\beta_{[e]} - \beta_{[\overline{e}]}$. In the $\mathbb{Z}_2$ theory, where the variables are just $+1$ and -1, we change a single plaquette from $+1$ to -1, resulting in an action cost of 2γ.

Our claim is therefore that in this phase, the behaviour of the χ irrep can be described by a strong coupling expansion of the nontrivial irrep in a $\mathbb{Z}_2$ theory described by action (6.70), at coupling:

$$\gamma = \frac{1}{2}\left(\beta_{[e]} - \beta_{[\overline{e}]}\right) \tag{6.71}$$

Now we *do* need to correct for the fact that the χ irrep is two-dimensional, whereas the nontrivial irrep of $\mathbb{Z}_2$ is only one-dimensional. This only gives a factor of 2 in the expectation value for the Wilson loop however.

How does the Wilson loop behave in the strongly coupled $\mathbb{Z}_2$ gauge theory? For this we can use the strong coupling expansion (5.71). First we need to make a character expansion of the Boltzmann factor.

$$\begin{aligned} e^{\gamma\chi(U_p)} &= \cosh\gamma + \sinh\gamma\,\chi(U_p) && (6.72)\\ &= \cosh\gamma\left(1 + \tanh\gamma\,\chi(U_p)\right) && (6.73)\end{aligned}$$

This gives us the following expression for the Wilson loop of a χ irrep in the $[\overline{e}]$ condensed vacuum as a function of the loop Ω:

$$\begin{aligned} < W_\chi(\Omega) >_{\overline{D_2}} = 2 < W(\Omega) >_{\mathbb{Z}_2} &= 2\frac{1}{Z}\int DU\chi(U_\Omega)\prod_{p\in\mathscr{P}}\cosh\gamma\left(1+\tanh\gamma\,\chi(U_p)\right) && (6.74)\\ &\approx 2\left(\tanh\gamma\right)^A + 2A\left(\tanh\gamma\right)^{A+4} && (6.75)\\ &= 2\left(\tanh\frac{1}{2}(\beta_{[e]}-\beta_{[\overline{e}]})\right)^A + 2A\left(\tanh\frac{1}{2}(\beta_{[e]}-\beta_{[\overline{e}]})\right)^{A+4} && (6.76)\end{aligned}$$

Where the area of the loop Ω is given by A, and we have expanded the strong coupling expansion by first filling the loop with plaquettes from the character expansion of the Boltzmann factor, and taking into account the first extra term.

This might all sound a bit far-fetched, but it seems to work out nicely. We plotted both expression (6.74) and the relevant Monte Carlo measurements in figure 6.8, and as can be seen, they are in excellent agreement.

These arguments provide evidence that indeed the condensation of $[\overline{e}]$ fluxes linearly confines the χ charges, as had been alluded to in the beginning of this section.

't Hooft loops

We were not able to find analytical expressions for the 't Hooft loop behaviour of the $[\overline{e}]$ flux. The Monte Carlo measurements however suggest that the operator $H^{\overline{e}}$ obtains a constant value, regardless of its size. The data in figures 6.9 and 6.10 shows the expectation value of the 't Hooft operator associated with the $\overline{e}$ flux as a function of both perimeter and area.

Of course this could be an artifact of our finite lattice. We have however performed these measurements on lattices of various sizes and at different locations in parameter space, and the whole

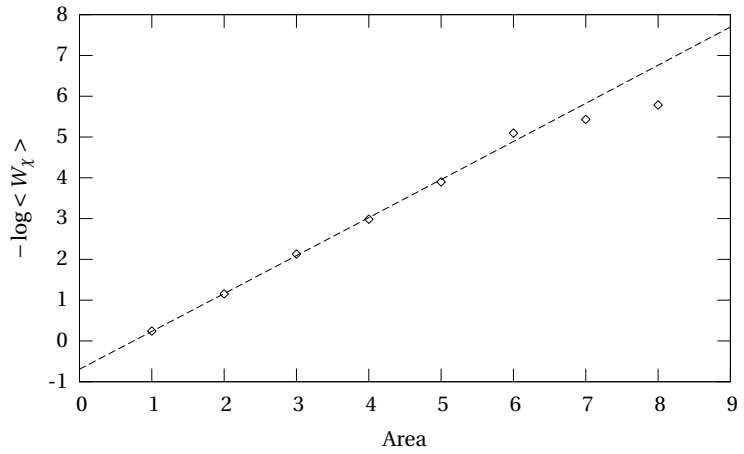

Figure 6.8: Wilson loop behaviour in the $\overline{e}$ condensate of the χ irrep as a function of area. The Monte Carlo measurements were performed on a $16^2 \times 8$ lattice, $\beta_{[e]} = 3.2, \beta_{[\overline{e}]} = 2.4$, 10000 sweeps

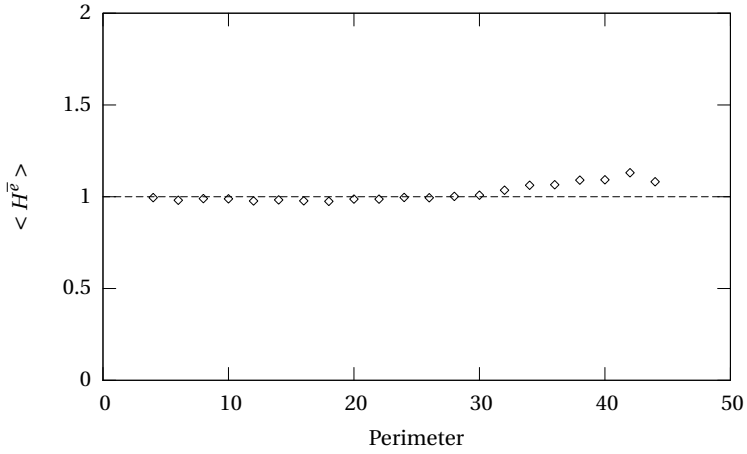

Figure 6.9: 't Hooft loop behaviour in the $[\overline{e}]$ condensate for the $[\overline{e}]$ class as a function of perimeter. Please note that the scale is not logarithmic. The Monte Carlo measurements were performed on a $16^2 \times 8$ lattice, $\beta_{[e]} = 3.0$, $\beta_{[\overline{e}]} = 2.8$, 1000 sweeps

region I in figure 6.1 seems to show this behaviour. It is still very desirable to give some analytic proof of this, but to our knowledge there are no methods to perform this calculation.

As can be seen, the Monte Carlo data supports our notion of flux condensation very well. The data for the larger loops, at the right side of both of the graphs, the Monte Carlo data seems to somewhat walk away from our prediction. This should be understood as arising from a statistical problem: on our finite lattice, there are many more small loops that can be drawn than large loops.

On to the other fluxes. From the quantum double analysis, we know that gauge invariant magnetic condensates leave the magnetic part of the group unbroken. Confinement can only occur if the condensate transforms according some electrical irrep of the group. Therefore, we expect the 't Hooft operators belonging to the $[X_1]$, $[X_2]$ and $[X_3]$ fluxes to obey perimeter laws, since they are still available as unconfined excitations after the condensation of the $[\overline{e}]$ fluxes.

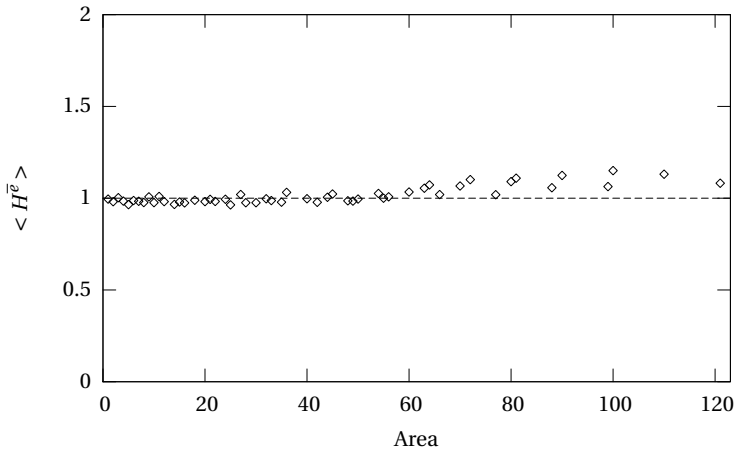

Figure 6.10: 't Hooft loop behaviour in the $[\overline{e}]$ condensate for the $[\overline{e}]$ class as a function of area. Please note that the scale is not logarithmic. The Monte Carlo measurements were performed on a $16^2 \times 8$ lattice, $\beta_{[e]} = 3.0$, $\beta_{[\overline{e}]} = 2.8$, 1000 sweeps

To obtain an analytical expression for these operators, we use the same trick as before in calculating the Wilson loops for the J_i irreps. If we pick $\beta_{[e]} = \beta_{[\overline{e}]}$, the extra local symmetry that allows us to multiply any link with $\overline{e}$ materializes again, and we can perform a perturbation expansion.

The calculation is completely analogous to the one that led to expression (6.65). Thus the result is:

$$< H^{X_1}(\Sigma *) >=< H^{X_2}(\Sigma *) >=< H^{X_3}(\Sigma *) >\approx e^{-\beta_{[e]} L} \tag{6.77}$$

This is nicely backed up by Monte Carlo data, as we show in figure 6.11 for the $[X_1]$ class.

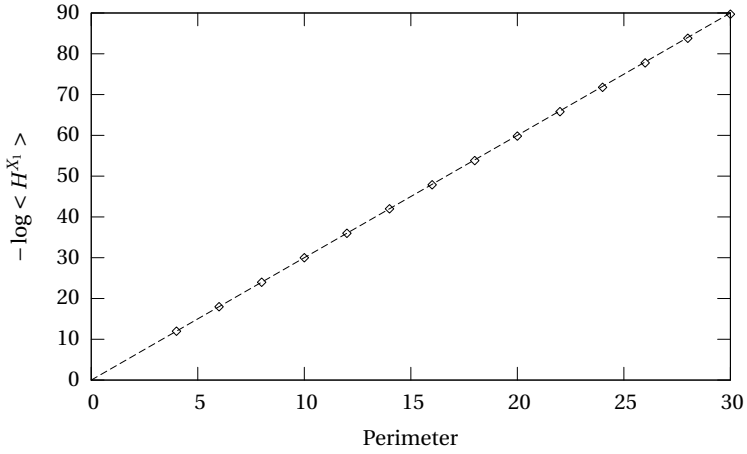

Figure 6.11: 't Hooft loop behaviour in the $[\overline{e}]$ condensate for the $[X_1]$ class as a function of perimeter. The Monte Carlo measurements were performed on a $16^2 \times 8$ lattice, $\beta_{[e]} = \beta_{[\overline{e}]} = 3.0$, 1000 sweeps

Dyonic loops

We expect the dyonic loops associated with $[X_i]$ flux and even $\mathbb{Z}_4$ representations to have perimeter law behaviour and the ones with odd $\mathbb{Z}_4$ representations to have area law behaviour, for the quantum double analysis predicts them to be confined. We were not able to find analytic expressions for the behaviour of these operators, but we do present Monte Carlo data.

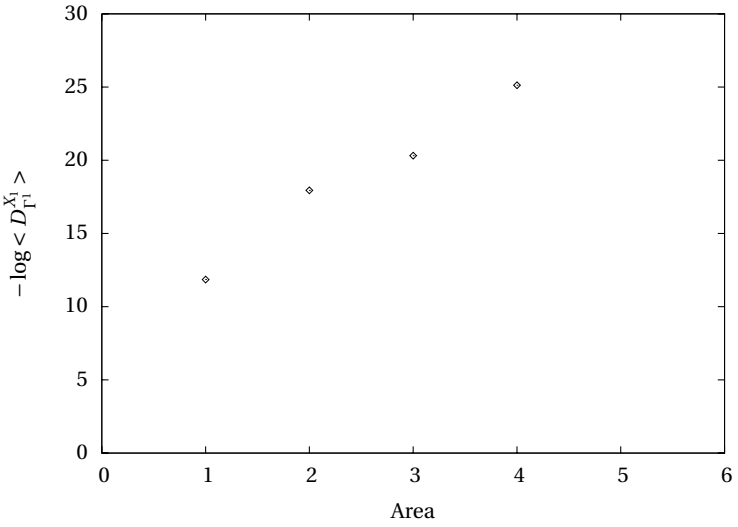

Figure 6.12: Dyonic loop behaviour in the $[\overline{e}]$ condensate for the $[X_1]$ class and Γ^1 charge as a function of area. The Monte Carlo measurements were performed on a $16^2 \times 8$ lattice, $\beta_{[e]} = 3.2, \beta_{[\overline{e}]} = 2.4$, 10000 sweeps

In figure 6.12, we can see the behaviour of the $\Pi^{X_1}_{\Gamma^1}$ excitation. Although the Monte Carlo measurements were difficult to perform, the plot does seem to suggest area law behaviour.

In figure 6.13, the behaviour of the $D^{X_1}_{\Gamma^2}$ operator is plotted. The plot shows perimeter law behaviour, which is what is to be expected for unconfined excitations.

Comparison to quantum double analysis

According to table 6.4 the low energy theory is described by a $\mathbb{Z}_2 \times \mathbb{Z}_2$ gauge theory. There are three nontrivial electric sectors that are all self conjugate. Furthermore, after fusing two different electric charges, one is left with the third. This is the same algebra as obeyed by the representations J_i, which Monte Carlo data tells us are the unconfined electric excitations.

On the magnetic part, the constancy of the 't Hooft operator for the $[\overline{e}]$ tells us this sector is removed from the spectrum. All three $[X_i]$ fluxes also obey perimeter laws. In principle however, it could be that the residual electric charges could not discern these fluxes from one another. However, the J_i charges are capable of telling them apart, so we conclude that all three $\Pi^{X_i}_{\Gamma^0}$ fluxes appear in the effective unconfined theory.

Also the dyons with even $\mathbb{Z}_4$ charge appear unconfined, in contradistinction to the ones carrying odd $\mathbb{Z}_4$ charge, whose operators show area law behaviour.

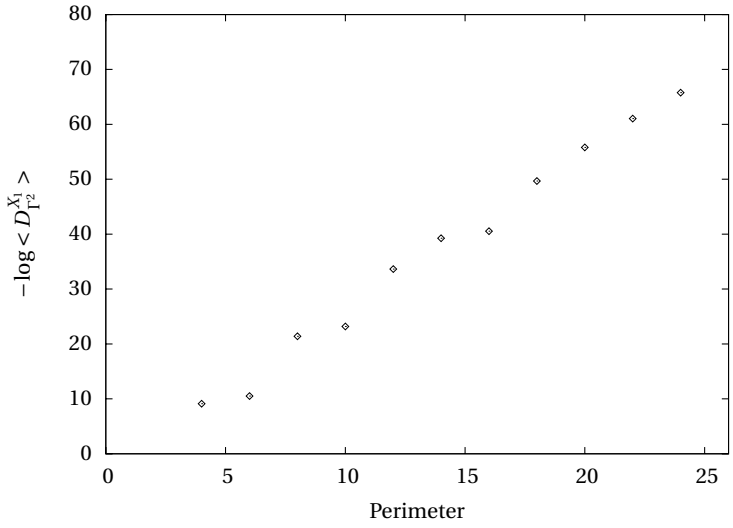

Figure 6.13: Dyonic loop behaviour in the $[\overline{e}]$ condensate for the $[X_1]$ class and Γ^2 charge as a function of perimeter. The Monte Carlo measurements were performed on a $16^2 \times 8$ lattice, $\beta_{[e]} = 3.2, \beta_{[\overline{e}]} = 2.4$, 10000 sweeps

6.5.4 $\Pi^{X_i}_{\Gamma^0}$ condensate

We will focus on the condensation of the $\Pi^{X_1}_{\Gamma^0}$ sector, the other two cases being completely similar. The region in phase space realizing a phase where the $H^{[X_1]}_{\Gamma^0}$ operator obtains a constant expectation value is given by setting in the action

$$S = -\beta_{[e]}\delta_{[e]}(U_p) - \beta_{[\overline{e}]}\delta_{[\overline{e}]}(U_p) - \beta_{[X_1]}\delta_{[X_1]}(U_p) \tag{6.78}$$

the couplings $\beta_{[e]}, \beta_{[\overline{e}]}, \beta_{[X_1]}$ approximately equal and larger than 1.

We were unable to perform analytical calculations in this region, since both the weak coupling and strong coupling methods fail here. Therefore we restrict ourselves to a presentation of the Monte Carlo data.

Wilson loops

The quantum double analysis tells us that the only unconfined charge in this region is the J_1. As presented in figure 6.14, the Wilson loop W_{J_1} indeed has perimeter law behaviour. In figure 6.15, the area law behaviour of W_χ is shown, confirming its confinement.

't Hooft loops

Our criterion for condensation was a constancy of the 't Hooft loop operator. As shown in figure 6.16, the operator H^{X_1} has a constant expectation value in this phase.

It is interesting to note that also the $\Pi^{\overline{e}}_1$ sector becomes condensed in this phase: the 't Hooft loop operator $H^{[\overline{e}]}$ is also constant regardless of its size. Physically, this can be understood in the following way. The fusion rule in equation (6.12) shows that the fusion of two $[X_1]$ fluxes can produce an $[\overline{e}]$ flux. Since there is a macroscopic number of $[X_1]$ fluxes present in the vacuum, they

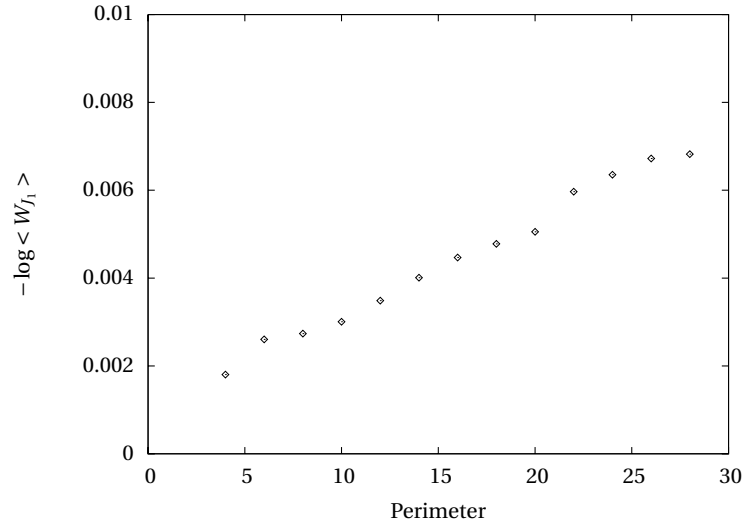

Figure 6.14: Wilson loop behaviour in the $[X_1]$ condensate of the J_1 irrep as a function of perimeter. The Monte Carlo measurements were performed on a $16^2 \times 8$ lattice, $\beta_{[e]} = \beta_{[X_1]} = 2.5, \beta_{[\overline{e}]} = 2.0$, 10000 sweeps

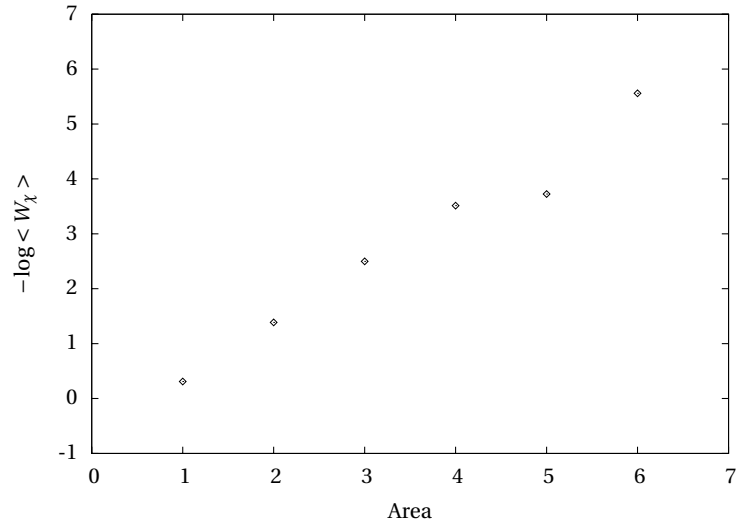

Figure 6.15: Wilson loop behaviour in the $[X_1]$ condensate of the χ irrep as a function of area. The Monte Carlo measurements were performed on a $16^2 \times 8$ lattice, $\beta_{[e]} = \beta_{[X_1]} = 2.5, \beta_{[\overline{e}]} = 2.0$, 10000 sweeps

will constantly meet each other, able to fuse into an $[\overline{e}]$ flux. It is thus to be expected that $H^{\overline{e}}$ also obtains a constant expectation value. The Monte Carlo data for this claim is presented in figure 6.17.

The other 't Hooft loops, H^{X_2} and H^{X_3}, have perimeter law behaviour. We show the result for the $[X_2]$ class in figure 6.18. We will discuss this result below.

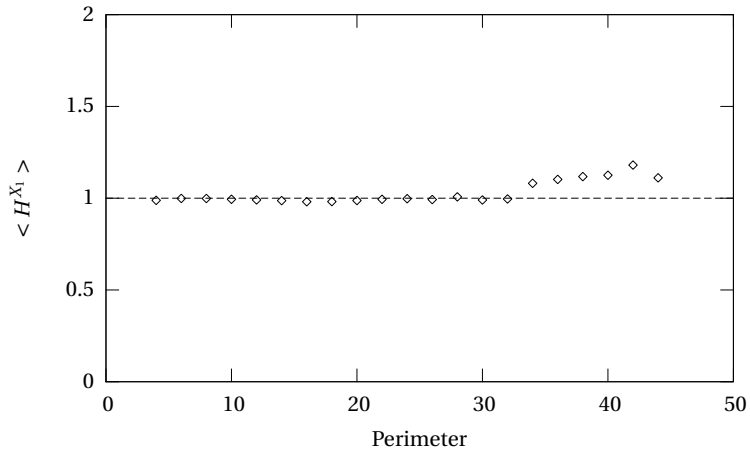

Figure 6.16: 't Hooft loop behaviour in the $[X_1]$ condensate for the $[X_1]$ class as a function of perimeter. Please note that the scale is not logarithmic. The Monte Carlo measurements were performed on a $16^2 \times 8$ lattice, $\beta_{[e]} = \beta_{[X_1]} = 2.5, \beta_{[\overline{e}]} = 2.0$, 1000 sweeps

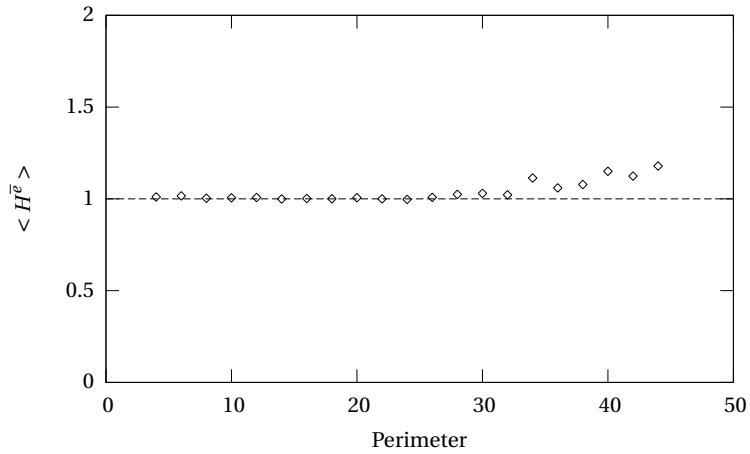

Figure 6.17: 't Hooft loop behaviour in the $[X_1]$ condensate for the $[\overline{e}]$ class as a function of perimeter. Please note that the scale is not logarithmic. The Monte Carlo measurements were performed on a $16^2 \times 8$ lattice, $\beta_{[e]} = \beta_{[X_1]} = 2.5, \beta_{[\overline{e}]} = 2.0$, 1000 sweeps

Dyonic loops

We present here the Monte Carlo measurements for the sectors $\Pi^{X_2}_{\Gamma^2}$, which is unconfined, see figure 6.19 and $\Pi^{X_2}_{\Gamma^1}$ which is confined, see figure 6.20.

Comparison to quantum double analysis

The quantum double breaking scheme predicts that the theory left after condensation of $[X_1]$ is described by $D(\mathbb{Z}_2)$. This means that there is one electric, one magnetic and one dyonic sector; let us compare this to the lattice results.

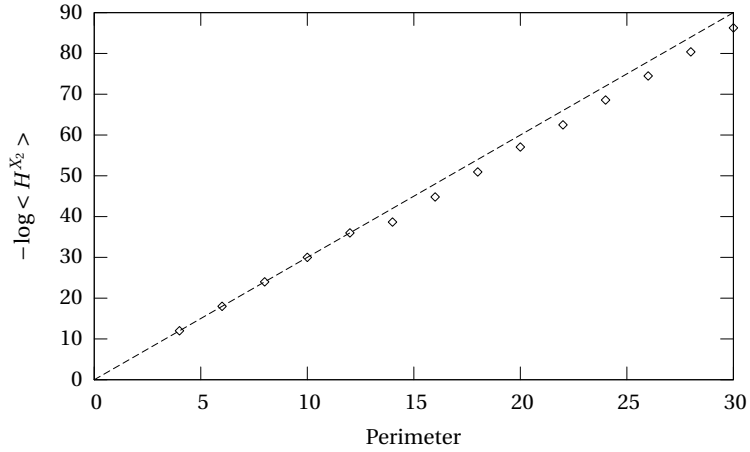

Figure 6.18: 't Hooft loop behaviour in the $[X_1]$ condensate for the $[X_2]$ class as a function of perimeter. The Monte Carlo measurements were performed on a $16^2 \times 8$ lattice, $\beta_{[e]} = \beta_{[X_1]} = 2.5, \beta_{[\overline{e}]} = 2.0$, 1000 sweeps

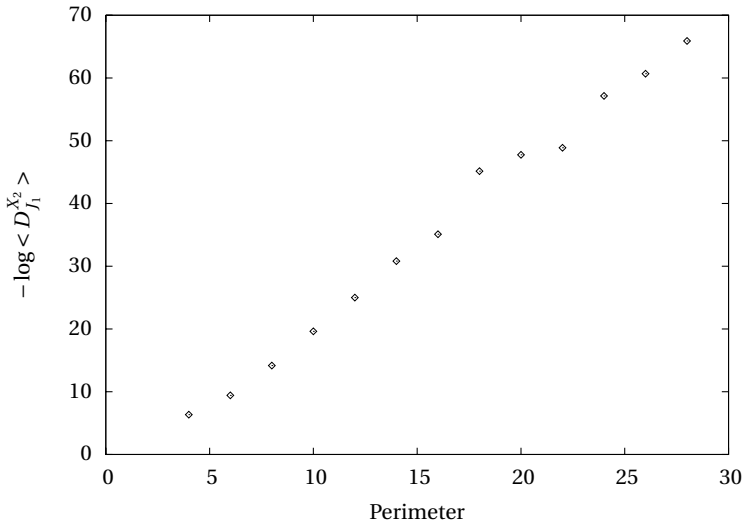

Figure 6.19: Dyonic loop behaviour in the $[X_1]$ condensate for the $[X_2]$ class and Γ^2 charge as a function of perimeter. The Monte Carlo measurements were performed on a $16^2 \times 8$ lattice, $\beta_{[e]} = \beta_{[X_1]} = 2.5, \beta_{[\overline{e}]} = 2.0$, 10000 sweeps

At the electric side, the lattice predicts that there is only one nontrivial irrep that is free: $\Pi^e_{J_1}$. All other electric particles are confined by the background of magnetic flux.

Concerning the fluxes, the lattice calculation tells us the $[\overline{e}]$ flux and the $[X_1]$ flux have condensed, whereas the $[X_2]$ and $[X_3]$ fluxes have perimeter law behaviour, suggesting they are in the spectrum as free excitations. This would seem to contradict what we learn from the quantum double breaking scheme, since this tells us there should be just one nontrivial magnetic sector left. However, let us think more closely. We have only one electric charge, the J_1, left to distinguish between the different fluxes. The character for both of these classes in the J_1 irrep is equal to -1 however, so the only free charge is unable to discern the two. Therefore they have to be identified

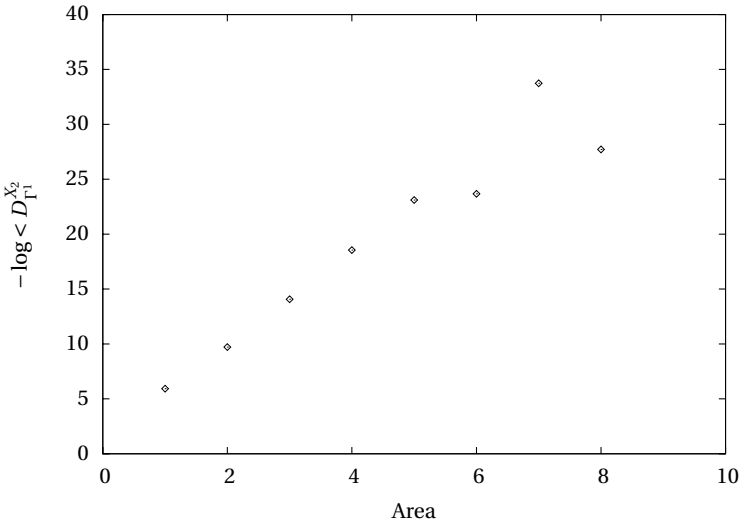

Figure 6.20: Dyonic loop behaviour in the $[X_1]$ condensate for the $[X_2]$ class and Γ^1 charge as a function of area. The Monte Carlo measurements were performed on a $16^2 \times 8$ lattice, $\beta_{[e]} = \beta_{[X_1]} = 2.5, \beta_{[\overline{e}]} = 2.0$, 10000 sweeps

in the effective unconfined theory.

The same argument can be applied to the dyonic sector. The flux carried by the $[X_2]$ and $[X_3]$ dyons cannot be distinguished by the unconfined charges.

6.5.5 Summary

To conclude this section, we recapitulate the results that were obtained. Table 6.7 provides the results for the Wilson and 't Hooft loop operators for the different phases. It describes the behaviour of the Wilson loops and the 't Hooft loops in the different vacua. Perimeter law decay is indicated by P, area law decay by A. Some typical behaviour for the dyons is given in the text, and in appendix B.

Table 6.7: Behaviour of the order parameters W_α and H^A in the different vacua

Condensate	$< W_{J_1} >$	$< W_{J_2} >$	$< W_{J_3} >$	$< W_\chi >$	$< H^{[\overline{e}]} >$	$< H^{[X_1]} >$	$< H^{[X_2]} >$	$< H^{[X_3]} >$
None	P	P	P	P	P	P	P	P
$[\overline{e}]$	P	P	P	A	1	P	P	P
$[X_1]$	P	A	A	A	1	1	P	P
$[X_2]$	A	P	A	A	1	P	1	P
$[X_3]$	A	A	P	A	1	P	P	1

Chapter 7

Conclusions and outlook

We have formulated discrete gauge theories on a spacetime lattice and have formulated operators that capture the full spectrum of quantum double physics. We have given the operators for the Wilson loops W_α corresponding to pure charges, the 't Hooft loops H^A corresponding to pure fluxes and the dyonic loops D^A_α, corresponding to the dyonic sectors. The former two are well-known in the literature while the latter is new, to our knowledge.

The actions we have formulated display a rich phase structure, and we have found methods to identify those regions of the phase space that correspond to magnetic condensates. In these regions, numerical simulations and physical intuition suggest that the 't Hooft operator for a certain flux obtains a constant value, regardless of its size. We would like analytic evidence of this.

The operators, corresponding to the particle-like excitations of the unbroken theory, have been studied in different phases of the $D(\overline{D_2})$ theory. This gives a clear understanding as to which excitations are confined in the presence of a condensate and which are free. This is indicated by area law decay respectively perimeter law decay of the relevant operators. Although we were unable to perform these calculations, we have a clear picture on how to be able to determine which excitations are distinguishable from each other and from the vacuum. This can be done by calculating expectation values of operators which are topologically nontrivially linked with one another.

The question remaining is what to do with representations from the unbroken theory that branch into several irreducible components in the broken phase. We think we have got a picture how to handle this on the lattice in principle, by calculating expectation values of operators with nontrivial topological linking numbers. Alas lack of computer power prohibited us from testing our hypothesis.

The results of the calculations that have been performed, regarding the confinement of excitations, coincide with the results from the quantum group breaking scheme.

Outlook

Some questions remain. The quantum double picture of topological symmetry breaking is well-developed, but the lattice approach still has some shortcomings. Although the formulation of actions and operators seems to be adequate, the calculations are difficult to perform.

Regarding analytic calculations, it would be nice to develop a general formalism to determine the expectation value of operators in the magnetic condensates. The trouble with this is that neither of the well-established calculational techniques work in this region of phase space: both the strong coupling and the weak coupling expansion fail. The former fails because the condensates

appear for large β, while the latter fails because it is not one configuration that contributes dominantly to the path integral, but a great many.

In the numerical corner, we would like to perform better Monte Carlo simulations on larger lattices. First we would like to obtain more accurate results for the confined dyons, since their behaviour is numerically difficult to handle. Since a dyonic operator's numerical value can roughly be seen as a product of an 't Hooft loop and a Wilson loop which have perimeter respectively area law behaviour in a phase where the dyon is confined, the numbers that are multiplied differ greatly in order of magnitude. This is the main source of this numerical difficulty.

The second objective is to perform good calculations of operators that are nontrivially linked with one another. Our present lattice sizes and computer power do not allow this. This would be very interesting nonetheless, since this would bring a full lattice picture of quantum symmetry breaking even closer.

Literature

Aharonov, Y. and D. Bohm; Significance of electromagnetic potentials in the quantum theory; *Phys. Rev.*, 115:485–491, 1959.

Alford, Mark G. and John March-Russell; New order parameters for nonabelian gauge theories; *Nucl. Phys.*, B369:276–298, 1992.

Bais, F. Alexander, Peter van Driel, and Mark de Wild Propitius; Quantum symmetries in discrete gauge theories; *Phys. Lett.*, B280:63–70, 1992.

Bais, F.A.; Topological excitations in gauge theories; an introduction from the physical point of view; *Geometric Techniques in Gauge Theories, Proceedings*, 1981.

Bais, F.A.; Flux metamorphosis; *Nucl. Phys.*, B170:32, 1980.

Bais, F.A. and C.J.M. Mathy; The breaking of quantum double symmetries by defect condensation; *Annals Phys.*, 322:552–598, 2007.

Bais, F.A. and J.K. Slingerland; Private communications; 2007.

Bais, F.A., B.J. Schroers, and J.K. Slingerland; Hopf symmetry breaking and confinement in (2+1)-dimensional gauge theory; *JHEP*, 05:068, 2003.

Balian, R., J. M. Drouffe, and C. Itzykson; Gauge fields on a lattice. 1. general outlook; *Phys. Rev.*, D10:3376, 1974.

Balian, R., J. M. Drouffe, and C. Itzykson; Gauge fields on a lattice. 2. gauge invariant ising model; *Phys. Rev.*, D11:2098, 1975a.

Balian, R., J. M. Drouffe, and C. Itzykson; Gauge fields on a lattice. 3. strong coupling expansions and transition points; *Phys. Rev.*, D11:2104, 1975b.

Coleman, Sidney R.; Quantum sine-gordon equation as the massive thirring model; *Phys. Rev.*, D11:2088, 1975.

Drinfeld, V.G.; Quantum groups; *J. Sov. Math.*, 41:898–915, 1988.

Einhorn, Martin B., Robert Savit, and Eliezer Rabinovici; A physical picture for the phase transitions in z(n) symmetric models; *Nucl. Phys.*, B170:16, 1980.

Elitzur, S.; Impossibility of spontaneously breaking local symmetries; *Phys. Rev.*, D12:3978–2982, 1975.

Forcand, Philippe de, Massimo D'Elia, and Michele Pepe; 't hooft loop in su(2) yang-mills theory; *Phys. Rev. Lett.*, 86(8):1438–1441, 2001.

Hooft, G. 't; Symmetry breaking through bell-jackiw anomalies; *Phys. Rev. Lett.*, 37(1):8, 1976.

Hooft, Gerard 't; On the phase transition towards permanent quark confinement; *Nucl. Phys.*, B138:1, 1978.

Itzykson, C. and J. M. Drouffe; Statistical field theory. vol. 1: From brownian motion to renormalization and lattice gauge theory; 1989; Cambridge, UK: Univ. Pr. (1989) 1-403.

Kramers, H. A. and G. H. Wannier; Statistics of the two-dimensional ferromagnet. part 1; *Phys. Rev.*, 60:252–262, 1941.

Lo, Hoi-Kwong; Aharonov-bohm order parameters for nonabelian gauge theories; *Phys. Rev.*, D52: 7247–7264, 1995.

Onsager, Lars; Crystal statistics. 1. a two-dimensional model with an order disorder transition; *Phys. Rev.*, 65:117–149, 1944.

Rebbi, C., (Ed.); Lattice gauge theories and monte carlo simulations; 1983; Singapore, Singapore: World Scientific (1983) 657p.

Roche, P., V. Pasquier, and R. Dijkgraaf; Quasihopf algebras, group cohomology and orbifold models; *Nucl. Phys. Proc. Suppl.*, 18B:60–72, 1990.

Smit, J.; Introduction to quantum fields on a lattice: A robust mate; *Cambridge Lect. Notes Phys.*, 15:1–271, 2002.

Thijssen, J.M.; *Computational Physics*; Cambridge University Press, second edition, 2007.

Wild Propitius, Mark de and F. Alexander Bais; Discrete gauge theories; 1995.

Wilson, Kenneth G.; Confinement of quarks; *Phys. Rev.*, D10:2445–2459, 1974.

Appendix A

Collection of results

In this section we will give all of our obtained results, for reference. Our results are presented in the form of graphs, plotting the expectation value of Wilson loops, 't Hooft loops and dyonic loops against their perimeter or enclosed area. We proceed phase by phase, starting with the trivial vacuum, and then enumerating the different magnetic condensates. Beneath each plot, we have given the particle sector corresponding to the operator.

We have chose to plot minus the logarithm of the expectation value of the operators as a function of area or perimeter, since we expect exponential falloff. This should then result in a straight line. We have not taken the logarithm of 't Hooft loops that have condensed in a certain phase, since we expect their value to be constant over all loop sizes. Therefore, for these loops, we have produced two graphs: one plotting the expectation value against perimeter, and one against area. This gives more compelling evidence for their constancy over all loop sizes.

Due to the large number of dyonic sectors in the theory, we have chosen not to plot all of them. In each of the three phases, we have chosen to give some typical plots, showing the difference between area and perimeter law falloff.

The graphs are a combination of Monte Carlo data and in some cases analytical expressions. We were able to find analytical expressions for the Wilson and 't Hooft loops in the trivial vacuum and the $\Pi_1^{\overline{e}}$ condensate.

The Monte Carlo measurements are represented by the little diamonds, whereas the analytical expressions are given by the dotted lines. The derivations for the analytical expressions are given in chapter 6.

The details on the Monte Carlo measurements (lattice size, number of sweeps and coupling constant values) are given beneath each graph. We have used the *C* code given in Appendix B, which implements a heat bath algorithm.

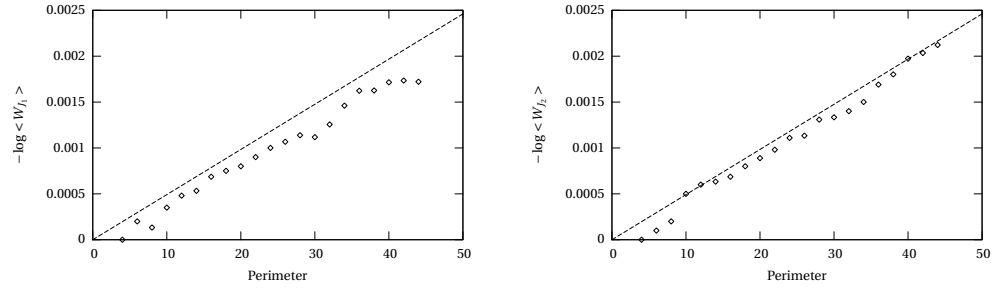

(a) $\Pi^{e}_{J_1}$

(b) $\Pi^{e}_{J_2}$

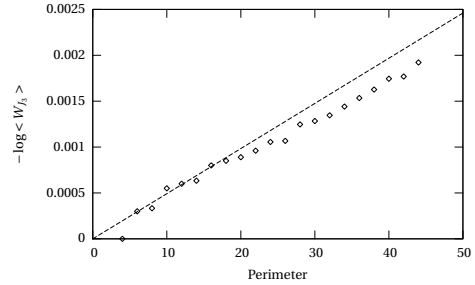

(c) $\Pi^{e}_{J_3}$

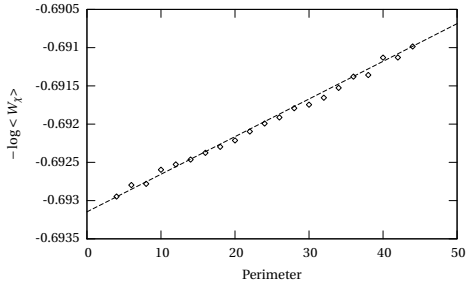

(d) Π^{e}_{χ}

Figure A.1: Wilson loop behaviour in the trivial vacuum as a function of perimeter. The Monte Carlo measurements were performed on a $16^2 \times 8$ lattice, $\beta_{[e]} = 3.0$, 10000 sweeps

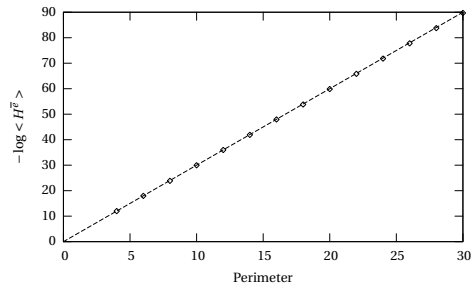

(a) $\Pi^{\overline{e}}_{1}$

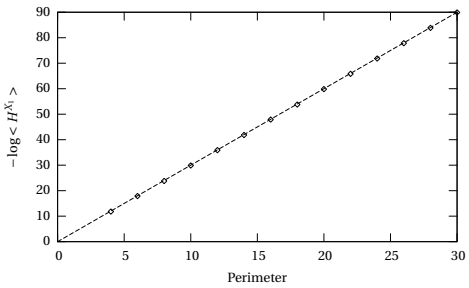

(b) $\Pi^{X_1}_{\Gamma^0}$

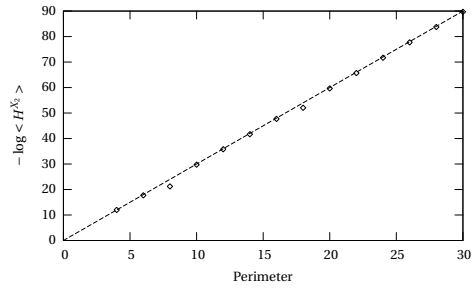

(c) $\Pi^{X_2}_{\Gamma^0}$

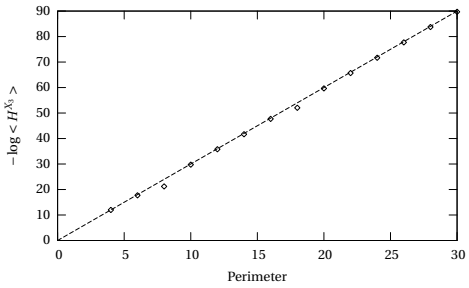

(d) $\Pi^{X_3}_{\Gamma^0}$

Figure A.2: 't Hooft loop behaviour in the trivial vacuum as a function of perimeter. The Monte Carlo measurements were performed on a $16^2 \times 8$ lattice, $\beta_{[e]} = 3.0$, 1000 sweeps

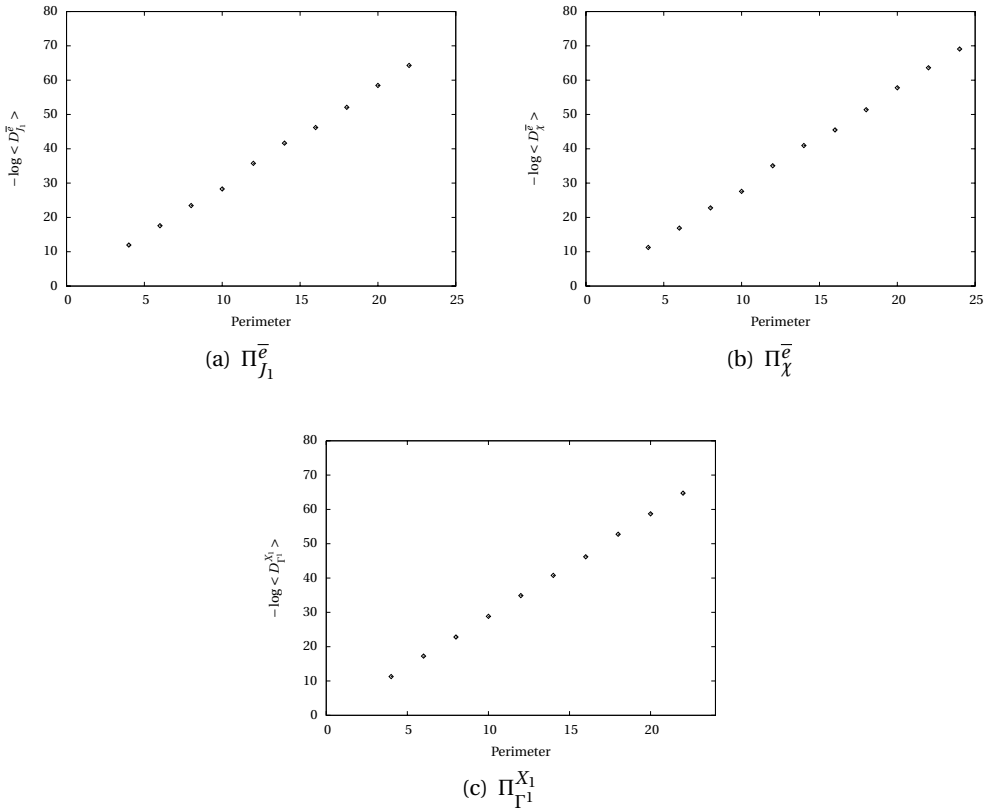

(a) $\Pi^{\bar{e}}_{J_1}$ (b) $\Pi^{\bar{e}}_{\chi}$

(c) $\Pi^{X_1}_{\Gamma^1}$

Figure A.3: Typical behaviour for some of the dyons in the trivial vacuum as a function of perimeter. The Monte Carlo measurements were performed on a $16^2 \times 8$ lattice, $\beta_{[e]} = 3.0$, 10000 sweeps

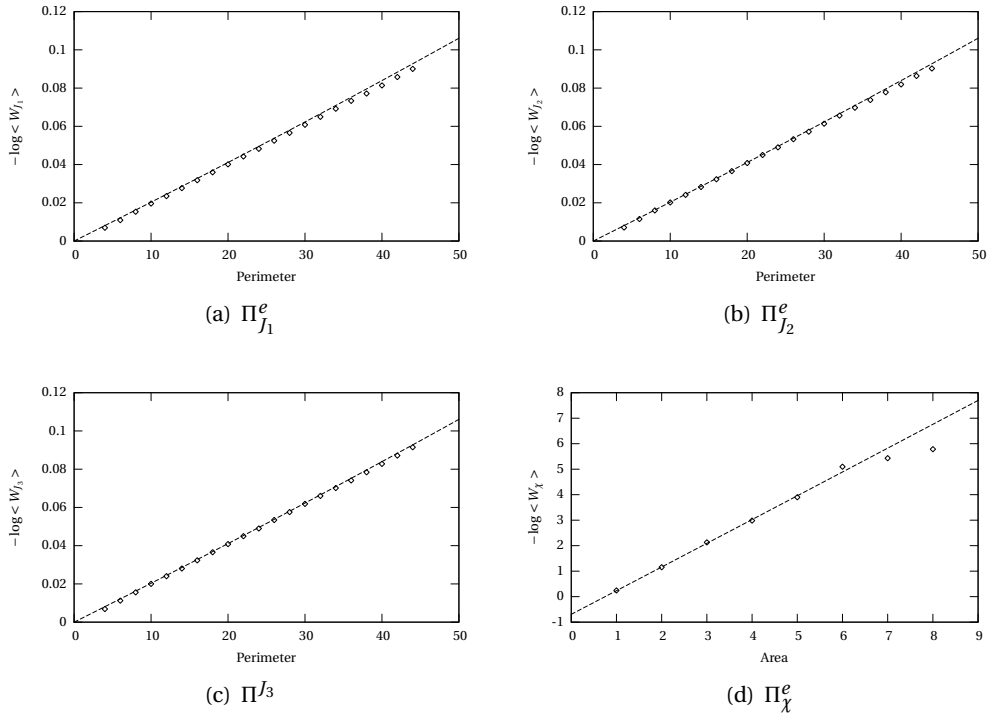

(a) $\Pi^e_{J_1}$ (b) $\Pi^e_{J_2}$

(c) Π^{J_3} (d) Π^e_χ

Figure A.4: Wilson loop behaviour in the $[\overline{e}]$ condensate as a function of perimeter or area. The Monte Carlo measurements were performed on a $16^2 \times 8$ lattice, $\beta_{[e]} = \beta_{[\overline{e}]} = 2.0$ for the plots showing W_{J_i} behaviour, $\beta_{[e]} = 3.2, \beta_{[\overline{e}]} = 2.4$ for plot showing W_χ behaviour, 10000 sweeps

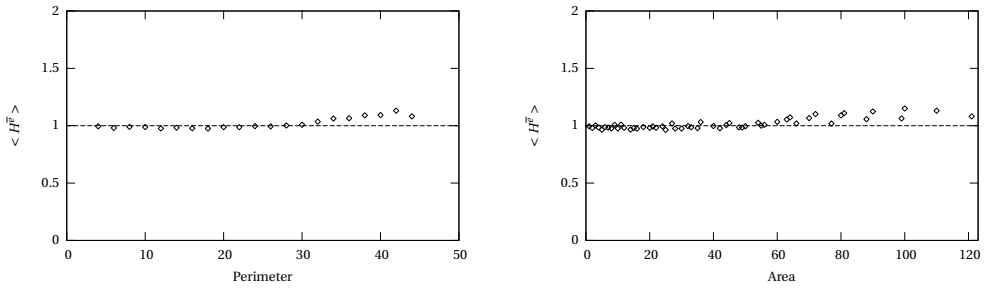

(a) $\Pi^{\overline{e}}_1$ vs perimeter (b) $\Pi^{\overline{e}}_1$ vs area

Figure A.5: 't Hooft loop behaviour in the $[\overline{e}]$ condensate for the $[\overline{e}]$ class as a function of perimeter and as a function of area. Please note that the scale is not logarithmic. The Monte Carlo measurements were performed on a $16^2 \times 8$ lattice, $\beta_{[e]} = 3.0$, $\beta_{[\overline{e}]} = 2.8$, 1000 sweeps

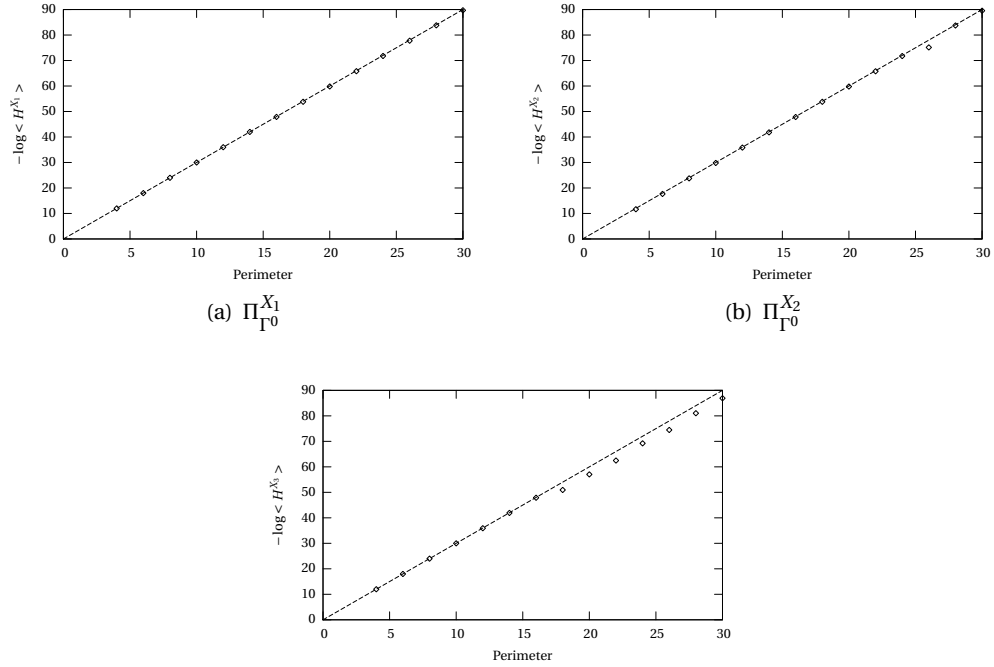

(a) $\Pi^{X_1}_{\Gamma^0}$ (b) $\Pi^{X_2}_{\Gamma^0}$

(c) $\Pi^{X_3}_{\Gamma^0}$

Figure A.6: 't Hooft loop behaviour in the $[\overline{e}]$ condensate for the $[X_i]$ classes as a function of perimeter. The Monte Carlo measurements were performed on a $16^2 \times 8$ lattice, $\beta_{[e]} = \beta_{[\overline{e}]} = 3.0$, 1000 sweeps

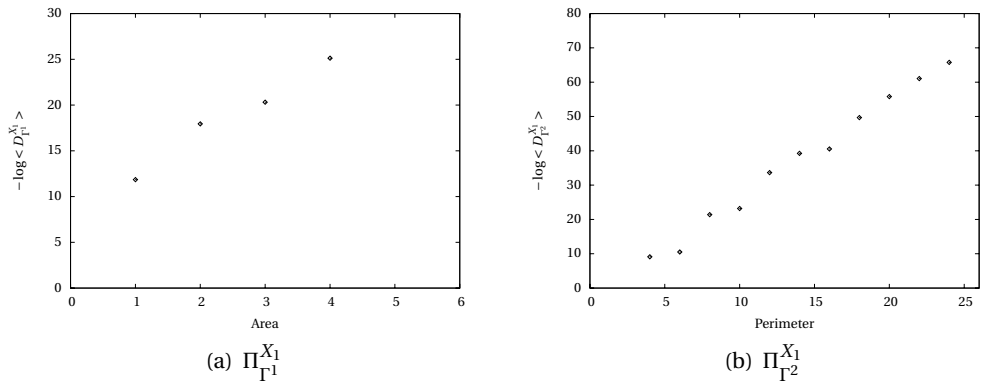

(a) $\Pi^{X_1}_{\Gamma^1}$ (b) $\Pi^{X_1}_{\Gamma^2}$

Figure A.7: Dyonic loop behaviour in the $[\overline{e}]$ condensate. The Monte Carlo measurements were performed on a $16^2 \times 8$ lattice, $\beta_{[e]} = \beta_{[\overline{e}]} = 3.0$, 1000 sweeps

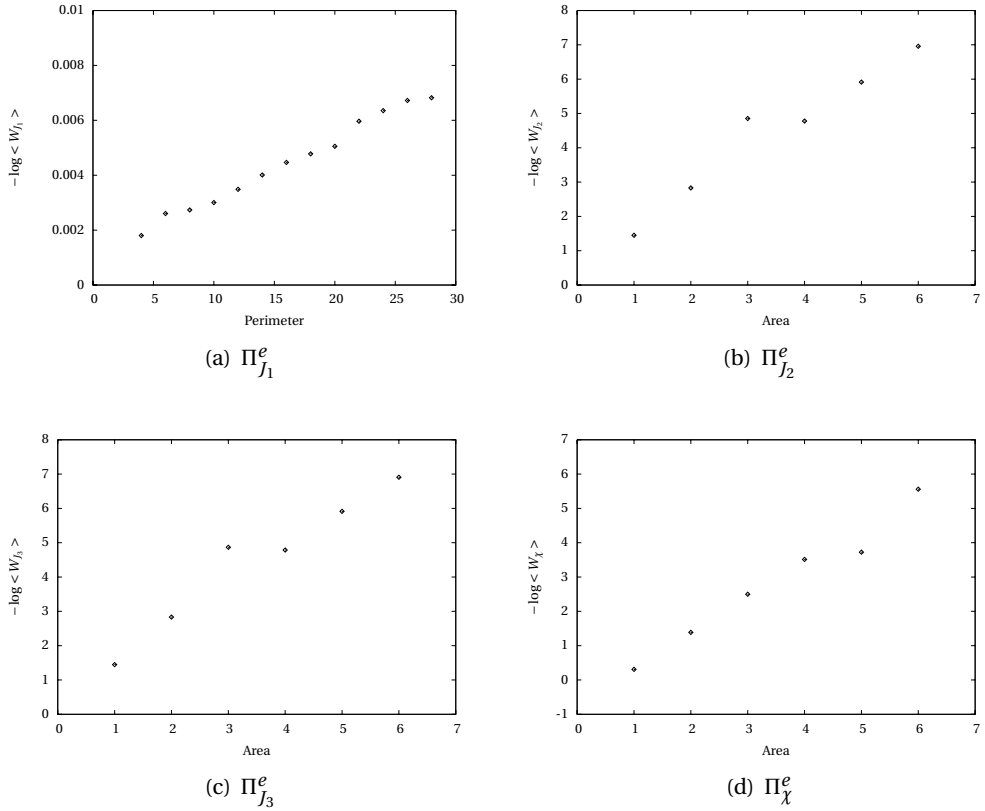

(a) $\Pi^e_{J_1}$ (b) $\Pi^e_{J_2}$

(c) $\Pi^e_{J_3}$ (d) Π^e_χ

Figure A.8: Wilson loop behaviour in the $[X_1]$ condensate as a function of perimeter or area. The Monte Carlo measurements were performed on a $16^2 \times 8$ lattice, $\beta_{[e]} = 2.4, \beta_{[X_1]} = \beta_{[\overline{e}]} = 2.3$ for the plot showing W_{J_1} behaviour, $\beta_{[e]} = 3.2, \beta_{[X_1]} = \beta_{[\overline{e}]} = 2.4$ for the other three plots, 10000 sweeps

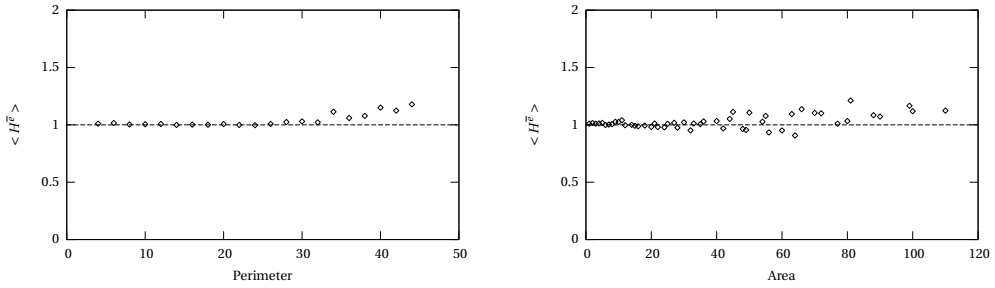

(a) $\Pi^{\overline{e}}_1$ vs perimeter (b) $\Pi^{\overline{e}}_1$ vs area

Figure A.9: 't Hooft loop behaviour in the $[X_1]$ condensate for the $[\overline{e}]$ class as a function of perimeter and of area. Please note that the scale is not logarithmic. The Monte Carlo measurements were performed on a $16^2 \times 8$ lattice, $\beta_{[e]} = 4.0$, $\beta_{[\overline{e}]} = \beta_{[X_1]} = 3.6$, 1000 sweeps

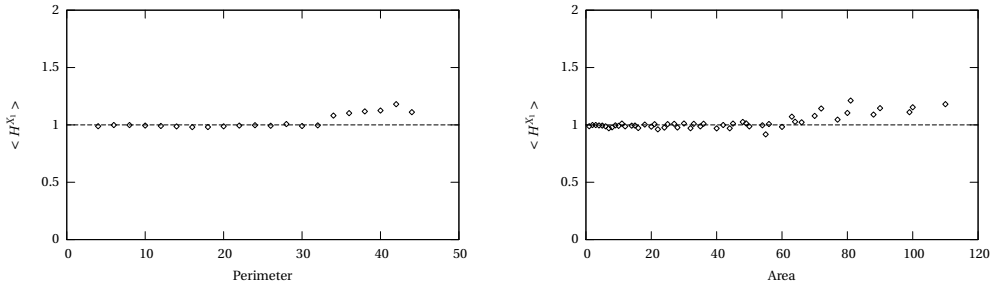

(a) $\Pi^{X_1}_{\Gamma^0}$ vs perimeter (b) $\Pi^{X_1}_{\Gamma^0}$ vs area

Figure A.10: 't Hooft loop behaviour in the $[X_1]$ condensate for the $[X_1]$ class as a function of perimeter and of area. Please note that the scale is not logarithmic. The Monte Carlo measurements were performed on a $16^2 \times 8$ lattice, $\beta_{[e]} = 4.0$, $\beta_{[\overline{e}]} = \beta_{[X_1]} = 3.6$, 1000 sweeps

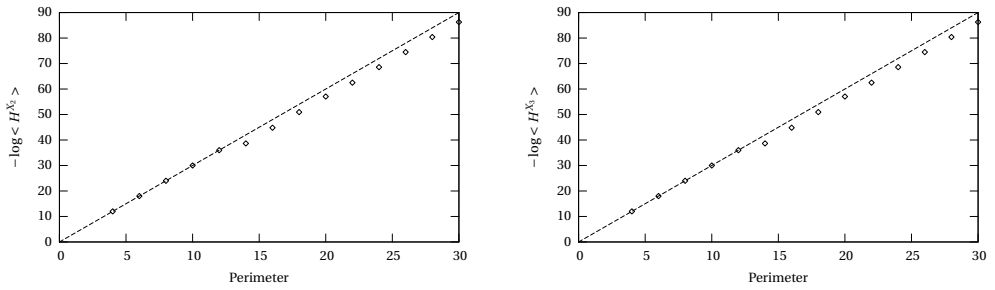

(a) $\Pi^{X_2}_{\Gamma^0}$ (b) $\Pi^{X_3}_{\Gamma^0}$

Figure A.11: 't Hooft loop behaviour in the $[X_1]$ condensate for the $[X_2]$ and $[X_3]$ classes as a function of perimeter. The Monte Carlo measurements were performed on a $16^2 \times 8$ lattice, $\beta_{[e]} = \beta_{[\overline{e}]} = \beta_{[X_1]} = 3.0$, 1000 sweeps

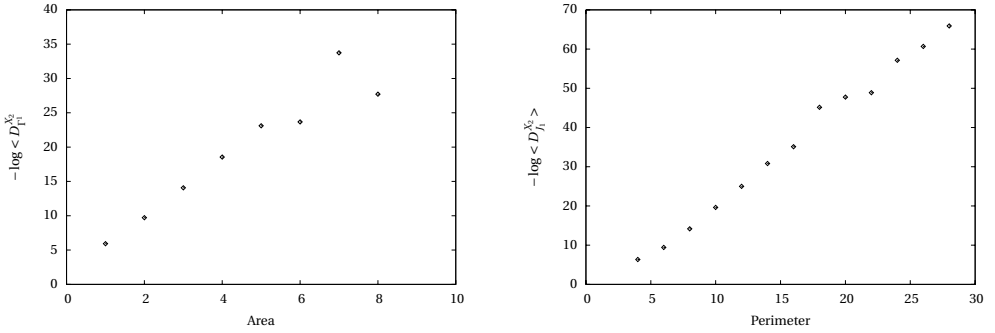

(a) $\Pi^{X_1}_{\Gamma^1}$ (b) $\Pi^{X_1}_{\Gamma^2}$

Figure A.12: Dyonic loop behaviour in the $[X_1]$ condensate. The Monte Carlo measurements were performed on a $16^2 \times 8$ lattice, $\beta_{[e]} = \beta_{[X_1]} = 2.5, \beta_{[\overline{e}]} = 2.0$, 10000 sweeps

Appendix B

Monte Carlo code

In this appendix we present the *C* code used to perform the Monte Carlo measurements. The code was compiled using the GNU compiler collection on an Apple iMac G5.

```
#include <stdio.h>
#include <stdlib.h>
#include <math.h>
#include <time.h>

/* the lattice is of dimensions SIZE**3 */
#define XSIZE 16
#define TSIZE 8
#define GPORD 8

/* link variables, coordinates t,x,y and direction, contain index for group element */
int link[TSIZE][XSIZE][XSIZE][3];

FILE *fp;

/* GROUP INFORMATION */
/* group elements are labelled by an integer:
   index 0   1   2   3   4   5   6   7
   elem  1   -1  X1  -X1 X2  -X2 X3  -X3 */
/* group multiplication table for D2bar */
int gpmul[GPORD][GPORD]={{0,1,2,3,4,5,6,7},
                         {1,0,3,2,5,4,7,6},
                         {2,3,1,0,7,6,4,5},
                         {3,2,0,1,6,7,5,4},
                         {4,5,6,7,1,0,3,2},
                         {5,4,7,6,0,1,2,3},
                         {6,7,5,4,2,3,1,0},
                         {7,6,4,5,3,2,0,1}};


/* table for group element inverses */
```

```
int gpinv[GPORD]={0,1,3,2,5,4,7,6};

/* gpchr[i][j] is character of group element i in irrep j */
int gpchr[GPORD][5]={{1,1,1,1,2},
                     {1,1,1,1,-2},
                     {1,1,-1,-1,0},
                     {1,1,-1,-1,0},
                     {1,-1,1,-1,0},
                     {1,-1,1,-1,0},
                     {1,-1,-1,1,0},
                     {1,-1,-1,1,0}};

/* utility functions */
void moveup(int x[],int d){
   int size;
   x[d]+=1;
   if(d==0) size=TSIZE;
   if(d!=0) size=XSIZE;
   if (x[d]>=size) x[d]-=size;
   return;
}

void movedown(int x[],int d){
   int size;
   x[d]-=1;
   if(d==0) size=TSIZE;
   if(d!=0) size=XSIZE;
   if (x[d]<0) x[d]+=size;
   return;
}

/* set all links to unity */
void coldlinks(){
   int x[3],d;
   for (x[0]=0;x[0]<TSIZE;x[0]++){
      for (x[1]=0;x[1]<XSIZE;x[1]++){
         for (x[2]=0;x[2]<XSIZE;x[2]++){
            for (d=0;d<3;d++){
               link[x[0]][x[1]][x[2]][d]=0;
            }
         }
      }
   }
   return;
}

/* calculate action corresponding to plaquette with group element plq
```

```
   two coupling constants for phase diagram. in this case
   beta0 is beta_e and beta1 is beta_ebar */

double gaugeact(int plq, double beta0, double beta1){
   double act0, act1, action;

   act0 = -0.125*(1.0 + (double)(gpchr[plq][1] + gpchr[plq][2] + gpchr[plq][3]
                      + 2.0 * gpchr[plq][4]));

   act1 = -0.125*(1.0 + (double)(gpchr[plq][1] + gpchr[plq][2] + gpchr[plq][3]
                      - 2.0 * gpchr[plq][4]));

   act0 += -0.250*(1.0 + (double)(gpchr[plq][1] - gpchr[plq][2] - gpchr[plq][3]));

   act0 *= beta0;
   act1 *= beta1;
   action = act0 + act1;

   return action;
}

/* give group element belonging to plaquette at (t,x,y)
   with orientation (orit,orix,oriy), which can be 1 or 0
   this function is called in the 't Hooft loop function */

int plqval(int t, int x, int y, int orit, int orix, int oriy){
   int g1=0, g2=0, g3=0, g4=0, plqtmp=0;
   int tx=0, ty=0, xy=0;
   int pos[3], dir[4];

   pos[0]=t; pos[1]=x; pos[2]=y;
   tx=orit*orix; ty=orit*oriy; xy=orix*oriy;

   if(tx==1){dir[0]=1; dir[1]=0; dir[2]=1; dir[3]=0;}
   if(ty==1){dir[0]=2; dir[1]=0; dir[2]=2; dir[3]=0;}
   if(xy==1){dir[0]=1; dir[1]=2; dir[2]=1; dir[3]=2;}

   g1 = link[pos[0]][pos[1]][pos[2]][dir[0]];
   moveup(pos,dir[0]);
   g2 = link[pos[0]][pos[1]][pos[2]][dir[1]];
   moveup(pos,dir[1]);
   movedown(pos,dir[2]);
   g3 = gpinv[link[pos[0]][pos[1]][pos[2]][dir[2]]];
   movedown(pos,dir[3]);
   g4 = gpinv[link[pos[0]][pos[1]][pos[2]][dir[3]]];

   plqtmp = gpmul[g1][g2];
```

```
   plqtmp = gpmul[plqtmp][g3];
   plqtmp = gpmul[plqtmp][g4];

   return plqtmp;
}


/* do a Monte Carlo sweep on the gauge field */
double updategauge(double beta_gauge0, double beta_gauge1, double beta_mat, int succ){
   int x[3],d,dperp,oldlink,newlink,newact,partplaq,plaq[GPORD],iter0=0,iter1=0,foundit;
   double act[GPORD],normact[GPORD],partsum,action=0.0;
   double cprob[GPORD],prob[GPORD],rndnum, success=0.0, successtot=0.0;

   for (x[0]=0; x[0]<TSIZE; x[0]++){
      for (x[1]=0; x[1]<XSIZE; x[1]++){
         for (x[2]=0; x[2]<XSIZE; x[2]++){
            for (d=0; d<3; d++){
               for(iter0=0;iter0<GPORD;iter0++){
                  act[iter0] = 0.0;
                  normact[iter0] = 0.0;
               }
               for (dperp=0;dperp<3;dperp++){
                  if (dperp!=d) {
                     /* move around thusly:
                        dperp    6--5
                        ^        |  |
                        |        1--4
                        |        |  |
                        -----> d 2--3 */

                     /* plaquette 1234 */
                     movedown(x,dperp);

                     partplaq=
                     gpmul[gpinv[link[x[0]][x[1]][x[2]][dperp]]][link[x[0]][x[1]][x[2]][d]]

                     moveup(x,d);
                     partplaq=gpmul[partplaq][link[x[0]][x[1]][x[2]][dperp]];
                     moveup(x,dperp); movedown(x,d);

                     //CREATE ARRAY OF PLQS
                     for(iter0=0;iter0<GPORD;iter0++){
                        plaq[iter0]=gpmul[partplaq][gpinv[iter0]];
                        act[iter0]+=gaugeact(plaq[iter0], beta_gauge0, beta_gauge1);
                        normact[iter0]+=-(1.0/2.0)*(gpchr[plaq[iter0]][4]);
                     }
                     moveup(x,d);
```

```
            /* plaquette 1456 */
            partplaq=link[x[0]][x[1]][x[2]][dperp];
            moveup(x,dperp); movedown(x,d);
            partplaq=gpmul[partplaq][gpinv[link[x[0]][x[1]][x[2]][d]]];
            movedown(x,dperp);
            partplaq=gpmul[partplaq][gpinv[link[x[0]][x[1]][x[2]][dperp]]];

            //CREATE ARRAY OF PLQS
            for(iter0=0;iter0<GPORD;iter0++){
               plaq[iter0]=gpmul[partplaq][gpinv[iter0]];
               act[iter0]+=gaugeact(plaq[iter0], beta_gauge0, beta_gauge1);
               normact[iter0]+=-(1.0/2.0)*(gpchr[plaq[iter0]][4]);
            }
         }
      }
      // right now, evaluated all plaquettes of given link

      // calculate small partition sum
      partsum = 0.0;
      for(iter0=0;iter0<GPORD;iter0++){
         partsum+=exp(-act[iter0]);
      }
      for(iter0=0;iter0<GPORD;iter0++){
         prob[iter0]=exp(-act[iter0])/partsum;
         cprob[iter0] = 0.0;
      }
      for(iter0=0;iter0<GPORD;iter0++){
         for(iter1=0;iter1<=iter0;iter1++){
            cprob[iter0]+=prob[iter1];
         }
      }
      rndnum = drand48();
      foundit = 0;
      for(iter0=0;iter0<GPORD;iter0++){
         if((rndnum<cprob[iter0])&&(foundit==0)){
            foundit=-1;
            successtot++;
            if(link[x[0]][x[1]][x[2]][d]!=iter0){
               success++;
            }
            link[x[0]][x[1]][x[2]][d]=iter0;
         }
      }
      action+=normact[link[x[0]][x[1]][x[2]][d]];
   }
}
```

```
      }
   }
   if(succ==1){
      printf("gauge success\t%3.2f%%\n",(double)success/successtot*100.0);
   }
   action /= (TSIZE*XSIZE*XSIZE*3*4);

   return action;
}

// Print a timeslice of plaquette values
void fluxtimeslice(int t){
   int x[3],plaq;

   x[0]=t;
   for (x[1]=0; x[1]<XSIZE; x[1]++){
      printf("\n");
      for (x[2]=0; x[2]<XSIZE; x[2]++){
         plaq=link[x[0]][x[1]][x[2]][1];
         moveup(x,1);
         plaq=gpmul[plaq][link[x[0]][x[1]][x[2]][2]];
         moveup(x,2);
         plaq=gpmul[plaq][gpinv[link[x[0]][x[1]][x[2]][1]]];
         movedown(x,1);
         movedown(x,2);
         plaq=gpmul[plaq][gpinv[link[x[0]][x[1]][x[2]][2]]];
         printf("%i ",plaq);
      }
   }
   printf("\n\n");
   return;
}

double wilson(int rep, int xlength, int ylength){
   // return Wilson loop value for current config in irrep "rep"
   // with width "xlength" and length "ylength"
   // this loop is a rectangular loop in the x-y plane,
   // stretching from x=0 to x=xlength and from y=0 to y=ylength
   int i=0,j=0,xpos=0,ypos=0,wil=0;
   double tr=0.0, wilavg=0.0;

   // x,t are the running coordinates, wil is the group element of the wilson loop
   wil=0; xpos=0; ypos=0;
   for(xpos=0; xpos<xlength; xpos++){
      wil = gpmul[wil][link[0][xpos][ypos][1]];
   }
```

```
   for(ypos=0; ypos<ylength; ypos++){
      wil = gpmul[wil][link[0][xpos][ypos][2]];
   }
   for(xpos=xlength-1; xpos>=0; xpos--){
      wil = gpmul[wil][gpinv[link[0][xpos][ypos][1]]];
   }
   xpos++;
   for(ypos=ylength-1; ypos>=0 ; ypos--){
      wil = gpmul[wil][gpinv[link[0][xpos][ypos][2]]];
   }
   wilavg = (double)gpchr[wil][rep];

   return wilavg;
}


/* make timelike t hooft loop for class class, in tx plane, start at (t,x,y)
   size tlength*xlength at coupling b0, b1 */

double hooft(int class, int t, int x, int y,
   int xlength, int tlength, double b0, double b1){
   int g1, g2, plq, plq1, plq2;
   int pos[3], i0, i1;
   double twistactsum1=1.0, twistactsum2=1.0, tmpval;

   pos[0]=t; pos[1]=x; pos[2]=y;
   switch(class){
      case 0:
         g1=0; g2=0; break;
      case 1:
         g1=1; g2=1; break;
      case 2:
         g1=2; g2=3; break;
      case 3:
         g1=4; g2=5; break;
      case 4:
         g1=6; g2=7; break;
      default:
         g1=0; g2=0; break;
   }

   for(i0=0;i0<tlength;i0++){
      plq = plqval(pos[0],pos[1],pos[2],0,1,1);
      plq1 = gpmul[g1][plq];
      plq2 = gpmul[g2][plq];
      twistactsum1 *= exp(gaugeact(plq,b0,b1)-gaugeact(plq1, b0, b1));
      twistactsum2 *= exp(gaugeact(plq,b0,b1)-gaugeact(plq2, b0, b1));
```

```
      moveup(pos,0);
   }

   movedown(pos,0); moveup(pos,1);
   for(i0=0;i0<xlength;i0++){
      plq = plqval(pos[0],pos[1],pos[2],1,0,1);
      plq1 = gpmul[g1][plq];
      plq2 = gpmul[g2][plq];
      twistactsum1 *= exp(gaugeact(plq,b0,b1)-gaugeact(plq1, b0, b1));
      twistactsum2 *= exp(gaugeact(plq,b0,b1)-gaugeact(plq2, b0, b1));
      moveup(pos,1);
   }
   movedown(pos,1);
   for(i0=0;i0<tlength;i0++){
      plq = gpinv[plqval(pos[0],pos[1],pos[2],0,1,1)];
      plq1 = gpmul[g1][plq];
      plq2 = gpmul[g2][plq];
      twistactsum1 *= exp(gaugeact(plq,b0,b1)-gaugeact(plq1, b0, b1));
      twistactsum2 *= exp(gaugeact(plq,b0,b1)-gaugeact(plq2, b0, b1));
      movedown(pos,0);
   }
   for(i0=0;i0<xlength;i0++){
      plq = gpinv[plqval(pos[0],pos[1],pos[2],1,0,1)];
      plq1 = gpmul[g1][plq];
      plq2 = gpmul[g2][plq];
      twistactsum1 *= exp(gaugeact(plq,b0,b1)-gaugeact(plq1, b0, b1));
      twistactsum2 *= exp(gaugeact(plq,b0,b1)-gaugeact(plq2, b0, b1));
      movedown(pos,0);
   }

   tmpval = 0.5*(twistactsum1 + twistactsum2);

   return tmpval;
}

/*****************************/
int main(){
   double betag0,betag1,betam, action, actionsum=0.0;
   double hooftsum=0.0;
   double wilarea[400][5],wilperi[400][5];
   double wilcntarea[400];
   double wilcntperi[400];
   double wiltemp = 0.0;
   int i0,i1,i2,i3;
   time_t seed=(time_t)0;

   // open file
```

```
fp = fopen("d2.dat","w");
coldlinks();

// initialize random numbers
time(&seed);
srand48((long)seed);
betag0 = 3.00;
betag1 = 3.00;

// initialize variables for storing wilson loop values
for(i1=1;i1<400;i1++){
   wilcntarea[i1] = -100.0;
   wilcntperi[i1] = -100.0;
   for(i2=0;i2<5;i2++){
      wilarea[i1][i2] = 0.0;
      wilperi[i1][i2] = 0.0;
   }
}

// thermalize
for(i0=0;i0<100;i0++){
   updategauge(betag0, betag1, 0.0, 0);
}

// calculate expectation value of Wilson loop
for(i0=0;i0<20000;i0++){
   updategauge(betag0, betag1, 0.0, 0);

   if(i0==2000){
      printf("10 percent sweeps\n");
   }
   if(i0==5000){
      printf("25 percent sweeps\n");
   }
   if(i0==8000){
      printf("40 percent sweeps\n");
   }
   if(i0==10000){
      printf("50 percent sweeps\n");
   }
   if(i0==12000){
      printf("60 percent sweeps\n");
   }
   if(i0==15000){
      printf("75 percent sweeps\n");
   }
   if(i0==18000){
```

```
      printf("90 percent sweeps\n");
   }

   // for given configuration, calculate Wilson loops in all irreps
   // and store them in the appropriate variable
   for(i1=1;i1<5;i1++){
      for(i2=1;i2<5;i2++){
         if(wilcntarea[i1*i2]<-99.0){
            wilcntarea[i1*i2] = 0.0;
         }
         if(wilcntperi[2*i1+2*i2]<-99.0){
            wilcntperi[2*i1+2*i2] = 0.0;
         }
         wilcntarea[i1*i2] = wilcntarea[i1*i2] + 1.0;
         wilcntperi[2*i1+2*i2] = wilcntperi[2*i1+2*i2] + 1.0;
         for(i3=0;i3<5;i3++){
            wiltemp = (wilson(i3,i1,i2)+wilson(i3,i2,i1))/2.0;
            wilarea[i1*i2][i3] += wiltemp;
            wilperi[2*i1+2*i2][i3] += wiltemp;
         }
      }
   }
   updategauge(betag0, betag1, 0.0, 0);
}

// Output to screen and file

printf("couplings\t%f\t%f\n",betag0,betag1);
fprintf(fp,"couplings\t%f\t%f\n",betag0,betag1);

for(i0=0;i0<5;i0++){
   printf("irrep\t%i\n",i0);
   fprintf(fp,"irrep\t%i\n",i0);
   printf("area behaviour\n");
   fprintf(fp,"area behaviour\n");
   for(i1=1;i1<200;i1++){
      if(wilcntarea[i1] > -99.0){
         printf("%i\t\t%f\n",i1,wilarea[i1][i0]/(wilcntarea[i1]));
         fprintf(fp,"%i\t\t%f\n",i1,wilarea[i1][i0]/(wilcntarea[i1]));
      }
   }
}

for(i0=0;i0<5;i0++){
   printf("irrep\t%i\n",i0);
   fprintf(fp,"irrep\t%i\n",i0);
   printf("perimeter behaviour\n");
```

```
      fprintf(fp,"perimeter behaviour\n");

      for(i1=1;i1<200;i1++){
         if(wilcntperi[i1] > -99.0){
            printf("%i\t\t%f\n",i1,wilperi[i1][i0]/(wilcntperi[i1]));
            fprintf(fp,"%i\t\t%f\n",i1,wilperi[i1][i0]/(wilcntperi[i1]));
         }
      }
   }
   fclose(fp);
   exit(0);
}
```